MEMBRANE EXTRACTION WITH A SORBENT INTERFACE

By

Yuzhong Luo

A thesis

presented to the University of Waterloo

in fulfillment of the

thesis requirement for the degree of

Doctor of Philosophy

Chemistry

Waterloo, Ontario, Canada, 1999

The University of Waterloo requires the signatures of all persons using or photocopying this thesis. Please sign below, and give address and date.

ABSTRACT

Membrane extraction with a sorbent interface (MESI) is a new technique for the analysis of volatile or semi-volatile organic compounds. The method has been developed to enable rapid routine analysis and short- or long-term on-site continuous monitoring. A MESI system comprises a membrane extraction module, a sorbent interface, a gas chromatograph (GC), and a computer. This study employed a silicone hollow fiber membrane, which can selectively extract some organic compounds and exclude water from the GC system. The sorbent interface enables on-line preconcentration and injection and the computer-controlled system enables the automatic operation of trapping and injection, which makes the technique flexible in extraction time and sensitivity. MESI has many advantages including no use of solvent, ease of automation, simplicity, efficiency, low cost, the possibility of on-line and on-site monitoring, and good selectivity and sensitivity.

Two mathematical models have been developed to describe the processes of extraction from air and water. The models have been found to be in good agreement with experimental results. Some important parameters which effect the extraction efficiency have been theoretically discussed and experimentally investigated. These include membrane length, membrane wall thickness, stripping gas flow rate, temperature, pressure, humidity, sample size, and agitation. The partition coefficient and the diffusion coefficient of the analyte are the most important parameters in membrane extraction. Their influence on extraction rate and response time have been extensively investigated and are discussed. The partition coefficients and diffusion coefficients of some analytes (in the membrane) were experimentally determined.

Estimation of air concentration without additional external calibration, on the basis of the mathematical model for air extraction, was investigated. The experiment showed that the method has advantages of simplicity, speed, and reasonable accuracy. Quantitation based on different extraction processes was studied and the steady-state extraction process is highly recommended for this application. To increase the limit of detection, various approaches were used, including microwave heating, stop-flow extraction, membrane probe cooling, and heating.

For on-site headspace monitoring a practical field sampling device was designed and coupled to MESI. The extraction was assisted by use of a microfan and by magnetic stirring, and improved extraction efficiency was observed. Headspace monitoring was also performed by placing the extraction module under water. Real-time headspace monitoring of a fermentation process demonstrates the potential use of MESI.

ACKNOWLEDGEMENT

I wish especially to thank Professor Janusz Pawliszyn for his guidance and encouragement throughout my Ph. D. program. I also thank him for giving me the opportunity to work on this exciting and challenging research project.

I would like to thank Marc Adams for his help for the derivation of the mathematical models.

I would like to thank the members of Professor Pawliszyn's research group, past and present, Marc Adams, Meng Chai, Jian Chen, Zhiping Deng, Gaoyuan Liu, Tadeusz Gorecki, Yanni Gou, Xiaozhong Han, Minyan Huang, Chongrong Jia, Heather Lord, Perry Martos, Maureen Orton, Lin Pan, Jiaqi Wu, Jingcun Wu, Rongrong Xu, Min Yang, Haodan Yuan, and Zhouyao Zhang for their help in aspects of my work.

Financial support from the University of Waterloo, the Waterloo Center for Groundwater Research, the Dow Chemical Company, and the Natural Sciences and Engineering Research Council of Canada is gratefully acknowledged.

To

Xiaomei, David and Ray

TABLE OF CONTENTS

LIST OF TABLES

LIST OF FIGURES

CHAPTER 1

INTRODUCTION

CHAPTER 1

INTRODUCTION

1.1 Sampling and Sample Preparation

Sampling and sample preparation play important roles in modern analysis. Although many dedicated analytical instruments have been developed to reduce analysis time and to make the analysis more sensitive and accurate, sampling and sample preparation are still the bottleneck of modern analysis, because these steps determine not only the analysis time but also the final results and cost. Generally, an analytical process involves several steps including sampling, sample preparation, separation, quantitation, and statistical evaluation. The steps involved are critical for obtaining accurate and precise results. Sampling and sample preparation are the most important steps and much effort remains focused on the study of the two areas.

In a sampling step, deciding where and how to obtain representative samples in the right amounts can have major influence on the final results. Frequently, the accuracy of an analysis is predetermined by this step. Errors or faults in the sampling protocol and preparation process cannot be corrected at any later point in the analysis, even with the most advanced methods and instrumentation.[1] Most traditional sampling methods need special containers or sorbent for sample loading, and the samples have to be shipped to a laboratory for analysis. Because of the time between sampling and analysis, the sample needs special treatment, such as low-temperature storage, addition of anti-bacterial agent, etc. These steps are the most common reasons for sample loss, degradation, and contamination. On the other hand, traditional sampling and laboratory analysis methods cannot provide immediate information about environmental contamination, release of toxic materials by industry, and danger forecasting. Therefore, recent

approaches to on-line and on-site analysis have attracted increasing attention. For example, different sensors, for example CO sensors, are used industrially and domestically. Most of these sensors, however, respond to one chemical component only. Obviously, a method enabling on-site multi-component analysis is needed in analytical chemistry and environmental science.

Sample preparation, on the other hand, is the most critical stage of instrumental analysis. This is because of the limited tolerance of analytical instruments of complicated sample matrices. Most samples obtained from biological and environmental sources are too dilute or too complex for analysis by direct sample introduction; others are incompatible with most instrumental systems. Therefore, sample preparation is often necessary to separate the analytes of interest from the sample matrix and to provide a sample of concentration and purity amenable to instrumental analysis. Traditional sample preparation includes liquid–liquid or solid–liquid extraction, phase isolation, and concentration steps. These steps are time consuming, employ toxic and expensive organic solvents, and are laborious and of low efficiency. These problems frequently make sample preparation the major source of error in an analysis and prohibit the use of a particular analytical process. As a consequence of restrictions aimed at environmental protection, these traditional methods of sample preparation will be phased out.[2] Therefore, a method for on-site field analysis or monitoring with solvent-free sample preparation, or without any sample preparation, that is simple, low cost, efficient, and selective has obvious advantages for future applications.

1.2 On-Site Real-Time Monitoring

As we approach the 21st century, the Environment Protection Agency (EPA) is moving to a policy of environmental compliance at the source. Any industry that discharges anything

into the environment will have to demonstrate, on site, that their emissions are within the allowable limits. This will create an entirely new market for on-site monitoring instrumentation designed to enable individual industries to inexpensively record compliance with environmental waste stream and small stack emission limit policies. The challenge faced by analytical instrumentation manufacturers and government regulators is to move away from slow and inefficient conventional analytical methodology and create a new breed of instrumentation designed to meet the requirements of the new regulations. In recent years, the need for real time trace analysis of air and water streams has increased. Methods are being sought for the in situ analysis of process streams for process optimization and control. The challenge of environmental monitoring of air and wastewater emissions grows with increasingly stringent regulations. As opposed to off-line analysis, on-line analysis can provide more efficient use of information about a process in terms of the amount of data, the quality of data, and the ability to respond to changes in the process as revealed by the data.[3] Currently, on-line process measurements are often obtained by chromatographic, spectroscopic, or solid-state chemical sensor techniques, as dictated by the nature of the analyte and the matrix. Often the extraction, concentration, desorption, and analysis of organic compounds from air or water can be accomplished in a single step by using a membrane sampling device. Membrane extraction with a sorbent interface (MESI) is emerging as a prime candidate to satisfy requirements for the direct analysis of volatile organic compounds (VOCs) in water and air. At present, no other direct analysis method can improve on the speed, cost, and trace level detection capabilities of MESI.

Sampling in general provides the greatest difficulty associated with the on-line analysis of process streams, irrespective of the analytical technique used. Many gas and liquid process

streams are chemically and physically complex and require pretreatment before analysis. Many sampling problems can be circumvented by utilizing membrane extraction techniques. Advantages of sampling with silicone hollow-fiber membranes include the simplicity of the membrane extractor device, the high surface area-to-volume ratio in the hollow fiber, the ability to obtain high linear flows at relatively low-volume flows, low cost, and the suitability of the membrane for efficient extraction for VOCs.[4] In addition, the inertness of the silicone membrane material makes it suitable for use in many biological and chemically reactive systems.

1.3 Background of MESI

Membrane separation has been developing rapidly in recent years. Because different types of membranes are commercially available, membrane separation can be widely used for microporous filtration, reverse osmosis, electrodialysis, ultra-filtration, dialysis, and gas separation.[5] In the field of organic component separation, various membrane separation techniques have attracted increasing attention and been widely applied in trace organic monitoring and analysis. Many applications of membrane separation techniques are reported yearly. The supported liquid membrane (SLM) technique has been coupled with gas chromatography (GC) and liquid chromatography (LC) for the analysis of ionizable and charged species[6–8] The supported liquid membrane enrichment technique involves the use of a porous PTFE membrane, which is impregnated with an organic solvent, separating two aqueous solutions. Target analytes then can be transferred from the solution on one side to that on the other by the supported liquid membrane. Because the transfer is not reversible, the analytes can be separated and enriched. Membrane introduction mass spectrometry (MIMS) has been widely applied in air, water and biological analysis. [9–13] In this technique, one side of the membrane is

exposed to an aqueous or gaseous sample while the other side of the membrane is directly exposed to the vacuum of the ion-source chamber of the instrument. Analytes penetrate the membrane wall, move directly to the ion source to be ionized and then can be analyzed. Because of the selectivity of the membrane and the sensitivity of MS, analyte concentrations in the sub-ppt or ppq concentration levels in the original matrix can be detected.

Blanchard and Hardy[14,15] were among the first to couple membrane extraction with gas chromatography. They used a flat sheet membrane to isolate the analytes from the sample and nitrogen to strip the analytes from the membrane surface to a bed of activated charcoal, followed by desorption of the analytes for GC analysis. Melcher and co-workers described the use of hollow fiber membranes and organic solvents as the stripping phase for introducing analytes into a liquid chromatograph.[16]

Membrane extraction with a sorbent interface coupled to gas chromatograph is conceived as an exceptionally simple method for the sampling and analysis of trace volatile organic compounds in the environment. The MESI approach was introduced in 1992 by Pratt and Pawliszyn.[17,18] The original concept entails pumping an aqueous sample through a single hollow fiber membrane while an inert gas flows countercurrently around the exterior of the fiber. The volatile organic compounds permeate from the liquid phase through the membrane and into the gas phase where they are collected by cryofocusing and then thermally desorbed for GC analysis. MESI was developed to enable rapid routine analysis and long term, on-line continuous monitoring of VOCs at different environmental and industrial sites. In the MESI process, the sampling and sample preparation steps are integrated within the analytical instrument. An attractive feature of MESI is the capability to perform VOC analysis without sample pretreatment.

In VOCs separations, the membrane material can be nonporous silicone rubber, polyethylene, or microporous polypropylene. The advantage of using silicone is that the volatile organic analytes can selectively permeate the membrane. Silicone membrane is elastic and reliable. Two kinds of membrane have been used most often, flat sheet and hollow fiber membranes. Although flat sheet membranes have been used in different separation techniques for several years, the geometry of the hollow fiber membrane is more useful for analytical applications, because of its large surface area per unit volume—this results in more efficient extraction and easy installation. The hollow fibers can also be a useful probe for field analysis.

1.4 Construction of MESI

The MESI system consists of four major sections:[19,20] (1) the membrane extraction module, (2) the cryofocusing trap and thermal desorption sorbent interface, (3) the GC, and (4) the computer control and data acquisition center. **Figure 1-1** depicts the MESI system. The membrane extraction module is the sampling device. During sampling the membrane probe is exposed to the sample and analytes which can penetrate the membrane wall pass through the membrane. A stripping gas flowing through the inside of the hollow fiber membrane strips the analytes from the inner surface of the membrane and carries them to the sorbent. **Figure 1-2** illustrates the permeation of analyte through the membrane wall with stripping gas flowing inside. At the sorbent interface the analytes are trapped and accumulated and then injected on to the GC column. Separation and detection are performed by a chromatograph. The computer controls the trapping time and injection, and simultaneously performs data acquisition.

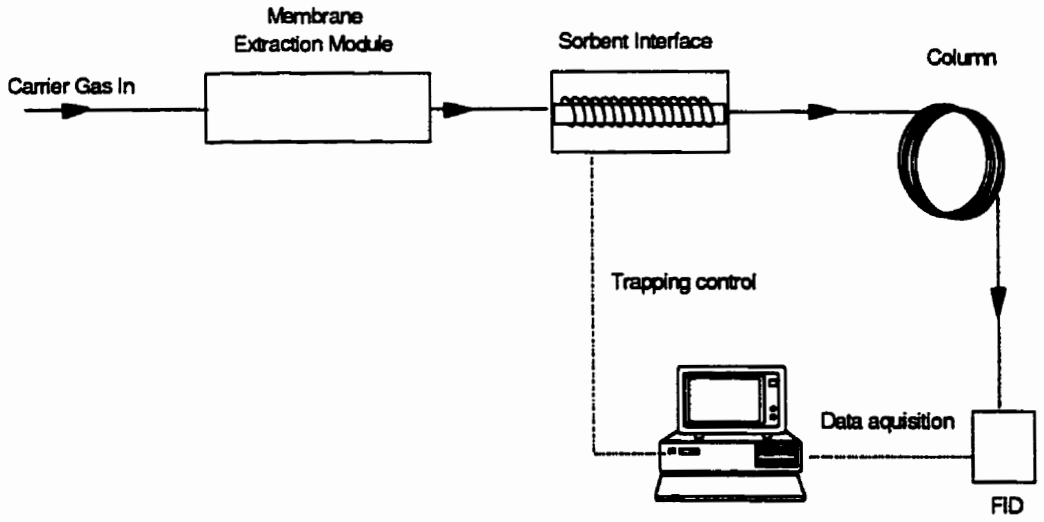

Figure 1-1. Schematic diagram of the MESI system

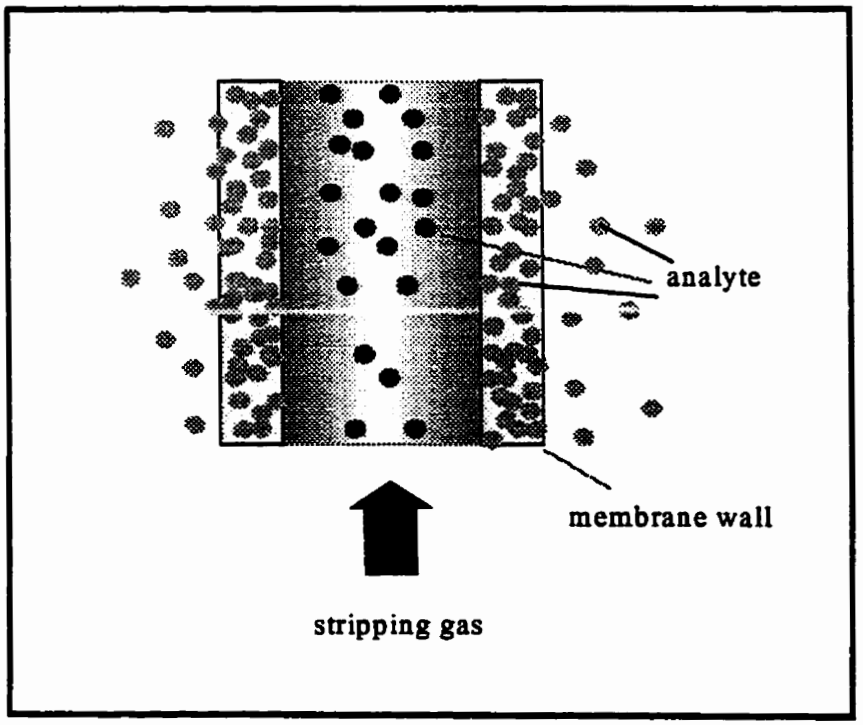

Figure 1-2. Schematic diagram of analyte permeation through the membrane

Figure 1-3 depicts the MESI system in trapping and desorption modes. In trapping mode analytes are continuously delivered to the sorbent interface; they are then accumulated by trapping for a period of time. In desorption mode the analytes are thermally desorbed from the sorbent interface to the gas stream, which carries the desorbed analytes to the GC system for analysis. After desorption the system switches to trapping mode. The two modes are alternately on and off to perform trapping and injection.

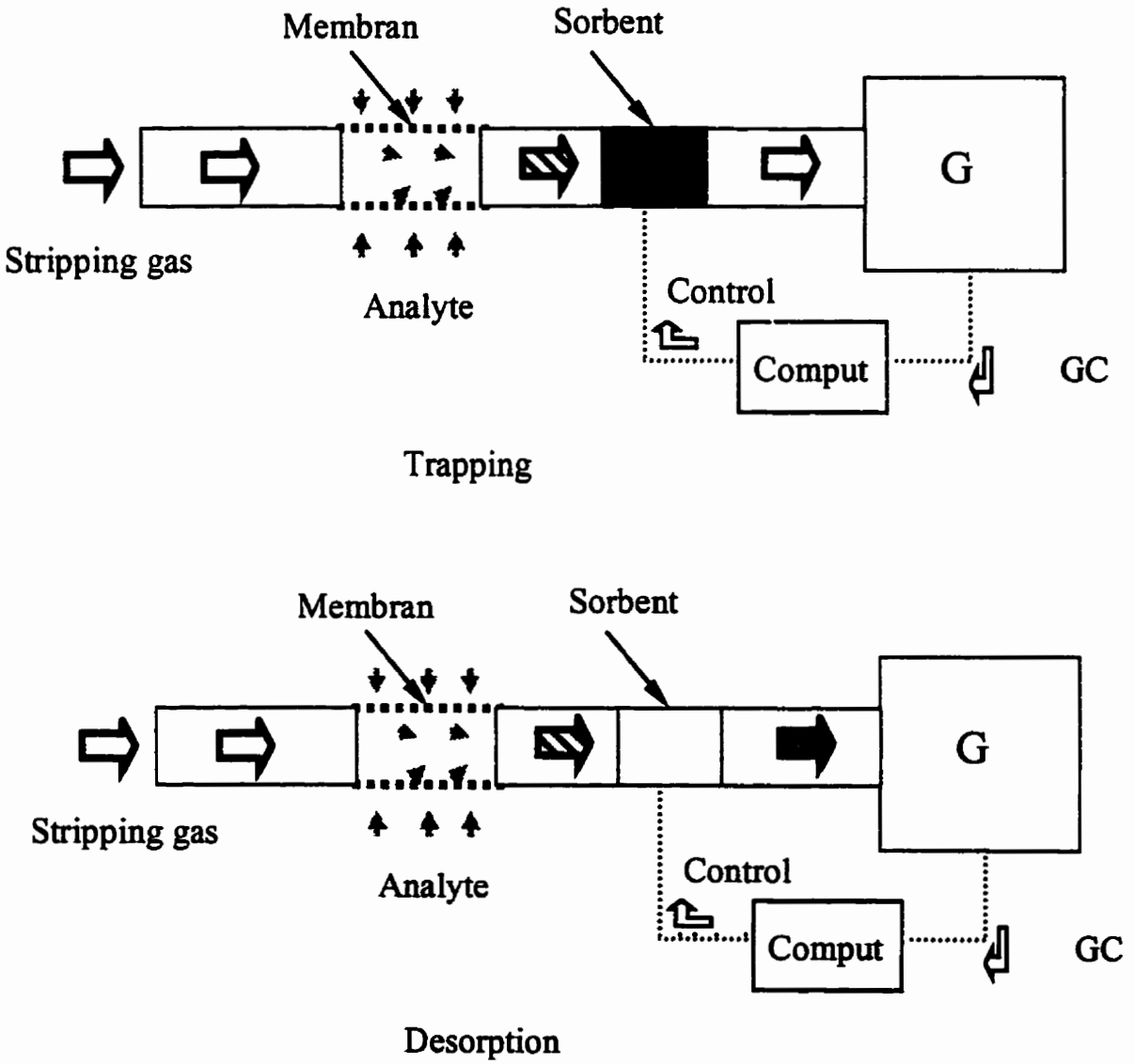

Figure 1-3. Schematic diagram of MESI processes in trapping and desorption

1.5 Thesis Objective

The major objective of the research described in this thesis is to acquire an understanding of the membrane extraction process and to optimize the extraction conditions by applying the results from theoretical and experimental investigations. For better description of the membrane extraction process in air and water matrices, two mathematics models will be derived. On the basis of theoretical studies, a number of parameters that govern the extraction efficiency will be investigated. These parameters include the dimensions of the membrane, the flow rate of stripping gas, temperature, sample size, humidity, pressure, agitation, breakthrough, response, and carry-over. Detailed aspects of quantitation in MESI will be studied on the basis of the various extraction processes. A method without external calibration for air analysis will be discussed. A field monitoring module will be designed and its application will be investigated. Some applications will also be studied to show the advantages and disadvantages of the method for the future applications. The strengths and weaknesses of the MESI technique will be extensively discussed.

CHAPTER 2

MEMBRANE PROBE AND SORBENT TRAP

CHAPTER 2

MEMBRANE PROBE AND SORBENT TRAP

2.1 Material of Membrane

With the development of membrane industry, numerous membranes have been developed for diverse uses in many applications. Membranes can be made from a large number of materials. Biological membranes are essential for life on earth. Every living cell is surrounded by a membrane, but these membranes differ completely in structure, functionality, etc., from synthetic organic and inorganic membranes. Synthetic polymer membranes are the most important members of the membrane family. Membrane types can be divided into porous and nonporous according to the structure, or can be divided into hydrophobic and hydrophilic. Different membrane characteristics result in different separation mechanisms. The membranes used successfully for the monitoring of organic and inorganic compounds in aqueous solutions are all hydrophobic; they include silicone rubber, Teflon, polyethylene, and polypropylene polymers.[21] Such membranes have the great advantage that they discriminate against passage of water, resulting in enrichment of the compounds of interest. It is therefore appropriate to use a hydrophilic membrane for the monitoring of polar compounds in a nonpolar matrix, and indeed such membranes have been used successfully for the measurement of water activity in organic solvents.[22] Hydrophilic membranes, however, have drawbacks—for example, transport properties are strongly modified by water and occasionally water can permeate the membrane and condense at the sorbent interface in MESI, and then extinguish the FID flame after thermal desorption. Water should be excluded from the MESI system. In MESI, the use of a porous membrane not only enables passage of the stripping gas from the inside to the outside of the

membrane, resulting in fluctuations of the flow rate, but also transfers water into the system causing the FID flame to be extinguished. A nonporous and hydrophobic membrane should, therefore, be used for MESI. In this study, a poly(dimethylsiloxane) (PDMS) hollow fiber membrane is used for the investigation. A silicone membrane is preferred because of its high permeability to VOCs.

PDMS membrane has a low glass transition temperature of –123°C. At ambient temperature, it is an elastomer. Its structure is written as:

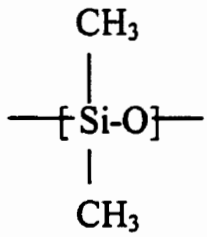

Poly(dimethylsiloxanes) are widely used as GC column stationary phases. Some of the most essential advantages of silicones are chemical inertness, thermal stability, and good solubility for numerous solutes.[23] The high thermal and oxidative stability, compared with those of organic polymers, is a consequence of the high energy of the Si–O bond. Poly(dimethylsiloxanes) have been shown to be thermally stable up to 400°C. [24]

2.2 Membrane Probe with Hollow Fiber Geometry

Two types of silicone membrane can be chosen. Flat-sheets are available in a wider variety of materials and thickness, but are not easy to implement in a small probe. Hollow fibers can be used in small probes for many applications. The hollow fiber membrane used in this study has inner diameter of 305 μm and an outer diameter of 635 μm.

The hollow fiber membrane probe can be easily installed. Normally, a piece of membrane, typically 4 cm for example, is attached to two pieces of deactivated silica tubing. To attach the membrane on to the tubing, the membrane is first submerged for 30 s in an organic solvent such as toluene—the membrane swells and the silica tubing is easily slipped into the membrane. After installation of the membrane the probe is exposed to air to evaporate the organic solvent. On evaporation of the solvent the membrane shrinks to its original size and a tight seal is formed. This tight connection ensures no leak at the junctions. **Figure 2-1** shows a schematic diagram of the membrane probe. The small dimensions of the membrane probe enable extraction to be easily performed in different monitoring locations, such as industrial pipework, chimney, exhaust gas vent, lake, river, bio-broth, etc.

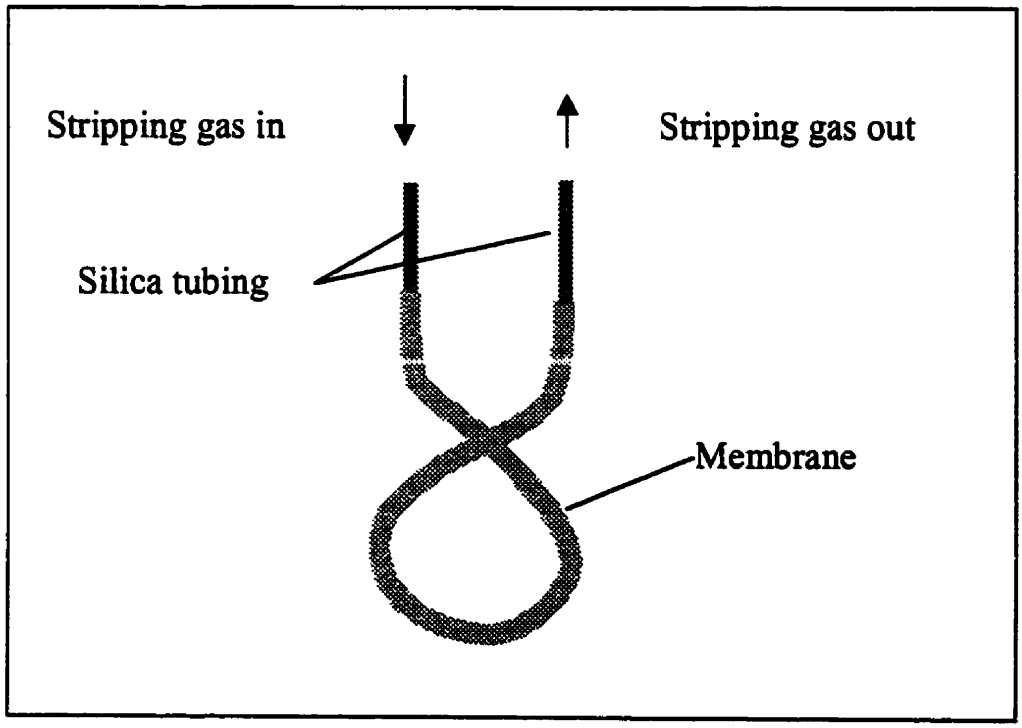

Figure 2-1. Schematic diagram of the membrane probe

2.3 Extraction Modules

The design of a membrane module depends on its applications; **Figure 2-2** shows some extraction modules. Each membrane module consists of a piece of hollow silicone fiber (Dow Corning Canada Inc., Mississauga, ON) encased in a sample container. The headspace extraction module has the advantage of no matrix contamination, which leads to a good membrane performance in long-term monitoring, even for analysis of dirty environmental samples. For air monitoring, the membrane is simply exposed in air or in a chamber though which the air sample flows continuously, or the chamber is sealed after air sampling. The cap module is typically suitable for field analysis. In air analysis the cap functions as a probe supporter; in water monitoring the cap can conveniently float on the water surface to enable headspace extraction. The cap can be even positioned in deep water to enable headspace extraction. The details will be discussed in **Chapter 7**. The cap extraction module can also be applied for soil monitoring.

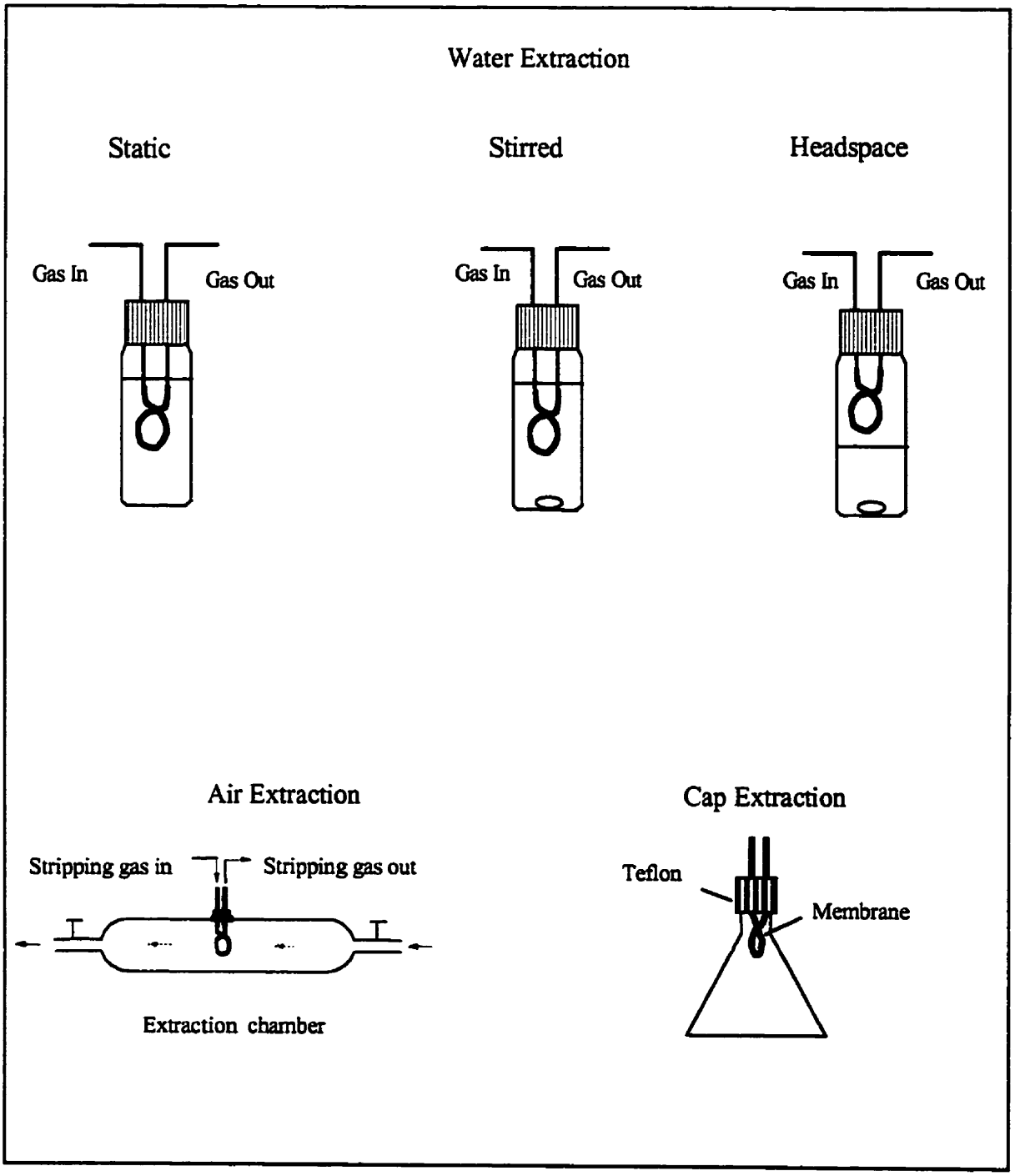

Figure 2-2. The membrane extraction modules

2.4 Sorbent Trap

Sorbent trap is one of the most important components of the MESI, because it controls the sensitivity of the method. Normally, the sorbent material is a polymer and the size is small. The sorbent can be a piece of a GC column or a PDMS- or PDMS/DVB (divinylbenzene)-coated fused silica fiber, or another material. In this research, a 1-cm PDMS fiber with a 100-μm coating is used. The fiber is located inside deactivated fused-silica capillary tubing and supported by a bent stainless steel needle, shown in **Figure 2-3**. The fiber is suspended to expose its surface to the stripping gas to trap analytes. The left end of the tubing is connected to the GC column while the other end is connected to the membrane probe.

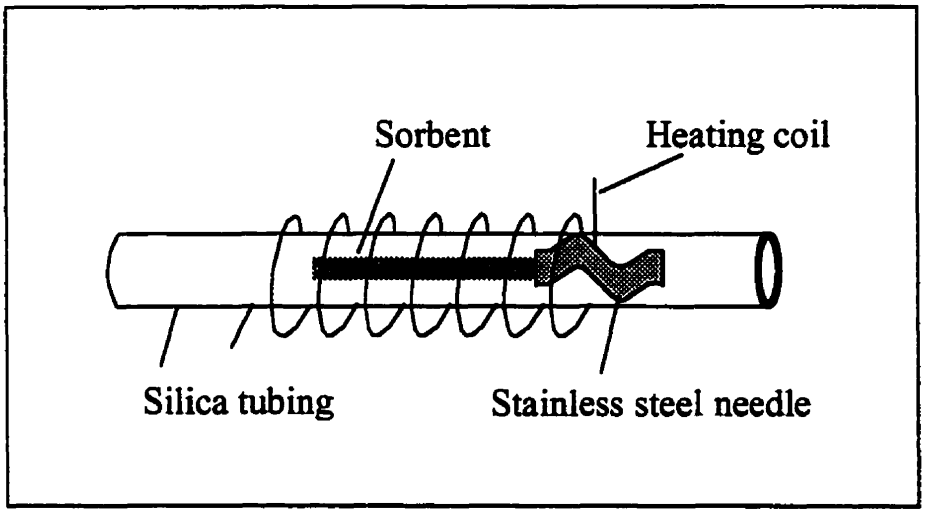

Figure 2-3. Schematic diagram of the sorbent setup

It can be seen from **Figure 2-3** that on the outside of the silica tubing, a heating coil (Ni–Cr wire, 20% Cr, 0.1 mm diameter, Johnson Mathew Metals Ltd. USA) is wrapped tightly round the tubing, covering the entire region where the sorbent is located. In this study, a 40-cm long, 47 Ω

heating coil is used. The heating coil is employed to generate the heat needed for thermal desorption.

2.5 Cryofocusing Trap

Because the sorbent material is PDMS, nonpolar VOCs have high affinity for the polymer. When the stripping gas flows by, the analytes are trapped by the sorbent. At room temperature, the absorption is an equilibrium process, which means the sorbent simultaneously absorbs and desorbs analytes and so the analytes cannot be completely trapped by the sorbent from the stripping gas. At low temperatures, however, typically below 0°C, the analyte partition coefficients between the sorbent and the gas are very large, generally several orders of magnitude higher than at room temperature.[25] Analytes can be completely trapped on to the sorbent under the cryofocusing conditions.

Obviously more analytes are retained by the sorbent for longer at low temperatures. To reach low temperature, different coolants can be used, **Table 2-1** lists the coolants and the corresponding temperatures.[26] At the temperature of liquid nitrogen, –197°C, most VOCs can be trapped for long periods of time. It is, however, is not practical to use this coolant in field analysis. In practice the sorbent in MESI is kept at temperatures within the range –10°C to –80°C, depending on the application. When dry ice (CO_2) is used, the temperature can go down to –80°C, but the inconvenience of this coolant is that dry ice evaporates quickly under ambient conditions and must be added frequently to maintain the trap temperature. Another inconvenience is that dry ice is not easy to obtain and apply in field analysis. Thus the practical use of coolants in MESI is inconvenient, even though they can create very low temperatures. As an alternative, semiconductor-based cooling has the advantages of ease of operation, maintenance of constant temperature, small geometry, and reliability. Typically, three-stage

semiconductor-based cooling can be used to maintain a constant temperature of –40°C by use of a constant voltage (13 V).

Table 2-1. Coolants and temperatures

Coolant	CO_2	CH_4	O_2	Ar	N_2	He
Temperature (°C)	–78.5	–161.4	–183.0	–185.7	–195.8	–269.9

The MESI sorbent interface is used to perform on-line cryogenic preconcentration and injection. The preconcentration step enables high sample throughput and high sensitivity. The use of cryogenic conditions can greatly increase trapping capacity. Normally, the heat pulse is short, 1 s for example, a sharp injection band is generated at the inlet of the GC column, and good chromatographic resolution can be achieved. It can be seen that the sensitivity of MESI is directly related to the trapping time. Obviously, a longer trapping time results in greater analyte accumulation, hence higher sensitivity.

2.6 Trapping Efficiency

One important effort in MESI is to improve the trapping efficiency. A low trapping efficiency means that only a small fraction of the analytes can be accumulated by the sorbent. Poor trapping efficiency results in low sensitivity and serious GC baseline shifting, which makes quantitation difficult. There are several practical means of improving the trapping efficiency. As mentioned above, a lower trapping temperature can directly result in larger trapping capacity. Use of a lower stripping gas flow rate provides analytes with a longer time in contact with the sorbent and reduces removal of the analytes by stripping. A larger volume of sorbent can also be used to increase the trapping capacity, and changing the sorbent material can also greatly

improve the trapping efficiency. In MESI, the trapping time is limited by breakthrough, i.e. elution of the analytes from the sorbent by the stripping gas. Increasing the trapping time in the sorbent trap is, therefore, essential for high sensitivity. **Table 2-2** lists the breakthrough time of 500 ppb trichloroethylene (TCE) (solution) for different sorbents and trap temperatures. The sample size was 25 mL and the sample was stirred at 1200 rpm by magnetic stirring. The extraction temperature was 25 °C. In this investigation, a 4 cm membrane was used as extraction probe and a 1cm long with 100 μm outer diameter PDMS fiber was employed as sorbent. It was observed that because of the larger coating capacity of the coated PDMS fiber, its trapping efficiency was higher.

Table 2-2. Comparison of the breakthrough time of trichloroethylene (TCE) in different sorbent traps at different temperatures. The flow rate of stripping gas was 1.5 mL min^{-1}.

Sorbent trap	Breakthrough time (s)				
	24°C	–10°C	–32°C	–40°C	–78°C
DB-5 column, 1.5 μm coating thickness, 2 cm by 0.53 mm i.d.	3	6	13	22	1500 *
Optical fiber (95 μm coating PDMS)	45	180	900	1020	1680

*4-cm column

2.7 The Feature of Pulse Heating

In MESI the sorbent interface is connected to the membrane extraction module and GC column without the use of a sampling valve or injector. The injection is performed by on-line thermal desorption from the sorbent. A typical design of such an interface consists of a sorbent trap surrounded by a heating coil, and a solid relay. The electric current can be supplied by a

capacitor or a regulated electrical source. A solid relay switches the electrical power supply to the heating coil on and off, according to the computer signal. The sorbent in the trap should have low thermal capacity to enable rapid desorption. The desorbed analyte forms a narrow band of sample at the inlet of the separation column. When the electrical power is turned off the temperature of the sorbent drops again (to –40°C) and the interface begins to trap the analytes for the next cycle of the analysis.

Both pulse voltage and pulse duration affect chromatographic peak shape and intensity. Short but efficient reproducible pulse heating is desired. A reproducible heating pulse ensures reproducible injection, which is critical for quantitation. **Figure 2-4** shows a set of temperature–time profiles for of a series of 1-s hating pulses at a voltage of 24 V. In the temperature measurement, a piece of E-type precision fine wire thermocouple (0.01-in diameter and 12-in long, Omega Engineering, Inc. CT. USA) was used. This thermocouple was coiled around the outside of the sorbent trap. The ends of the wire were connected to an amplifier which in turn was connected to a computer. It is apparent that the pulses were reproducible. A short heating pulse generates a narrow injection band, which results in sharp chromatographic peaks and thus high sensitivity. Because the sorbent trap has a very low thermal mass, the temperature of the trap can be changed very rapidly and effectively. **Figure 2-5** shows the temperature–time profile of 1-s pulse heating at a voltage of 38.6 V. The profile indicates that a pulse of only 1 s increased the sorbent temperature from –40 to 260°C, and that 4 s was needed to cool down to –40°C again. The duration of the temperature cycle was only 5 s. The rapid change of temperature from below zero to 263°C is essential for producing sharp injection bands. The quick decline of the trap temperature ensures that the next cycle of trapping can be resumed immediately.

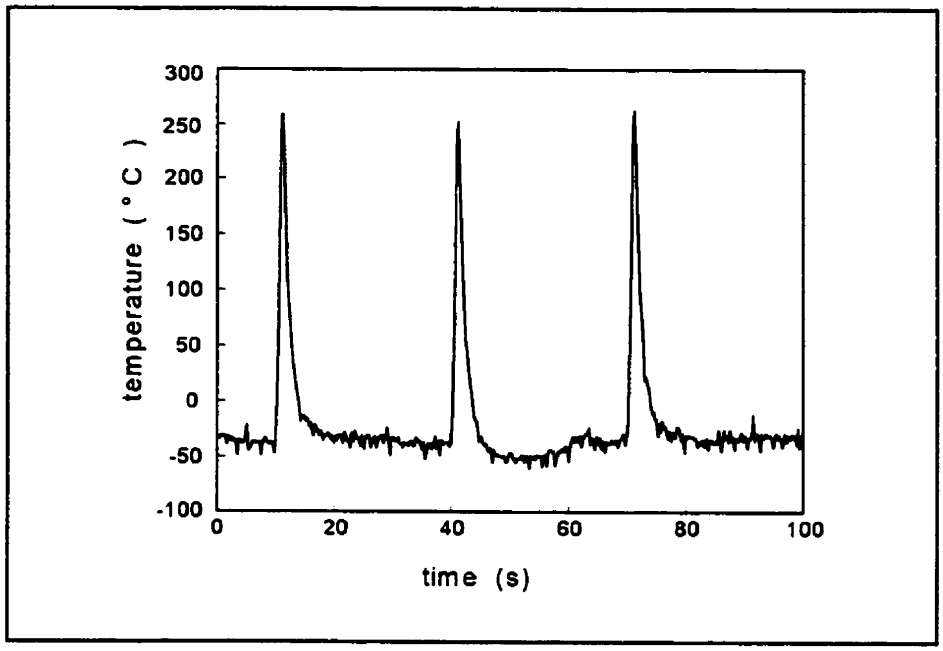

Figure 2-4. Temperature–time profiles for a set of heating pulses

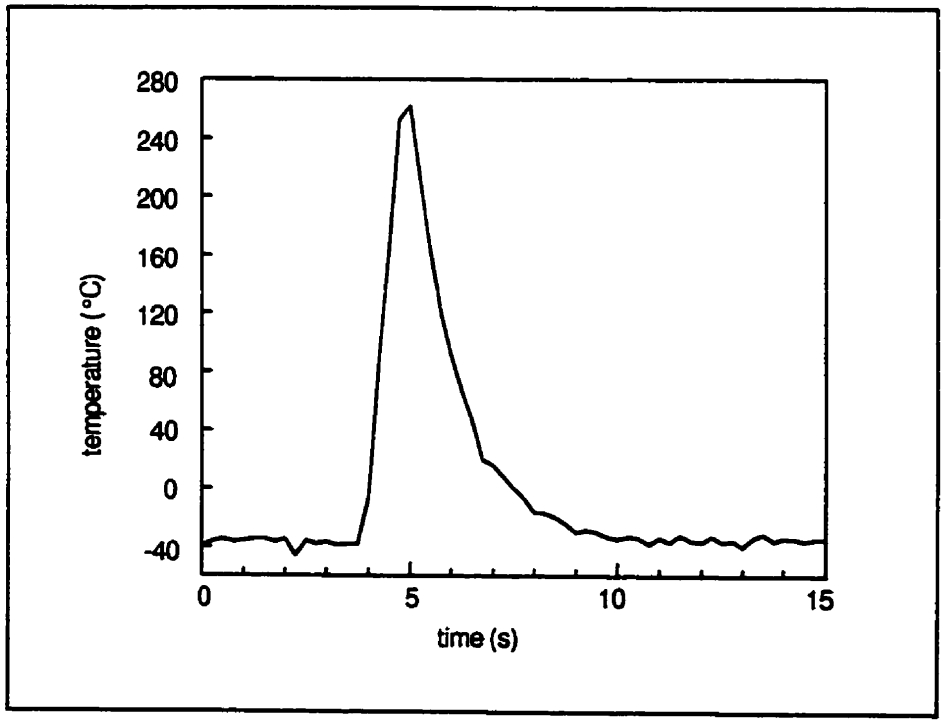

Figure 2-5. Temperature–time profile in pulse heating. Pulse width 1 s.

During thermal desorption from the sorbent the pulse voltage cannot be too high, otherwise excess heating would damage the sorbent coating; this reduces trapping capacity and generates extra peaks. The pulse voltage cannot, on the other hand, be too low, because insufficient heating would lead to incomplete desorption and serious carry-over. Experimentally, the pulse voltage and pulse duration can be adjusted to control the heating intensity. **Figure 2-6** shows chromatograms of TCE obtained after desorption at different pulse voltages. In the experiment, a 500 ppb solution was tested. The sample size was 25 mL and the sample was stirred at 1200 rpm by magnetic stirring. At low pulse voltage the peaks of TCE were small, which indicates that heating was insufficient. At high voltage, 41.0 V for example, two peaks were obtained. The extra small peak was attributed to decomposition of the sorbent at the high desorption temperature. After testing a series of pulse widths and pulse voltages, a 1-s pulse with at 38.6 V was chosen as optimum for this study.

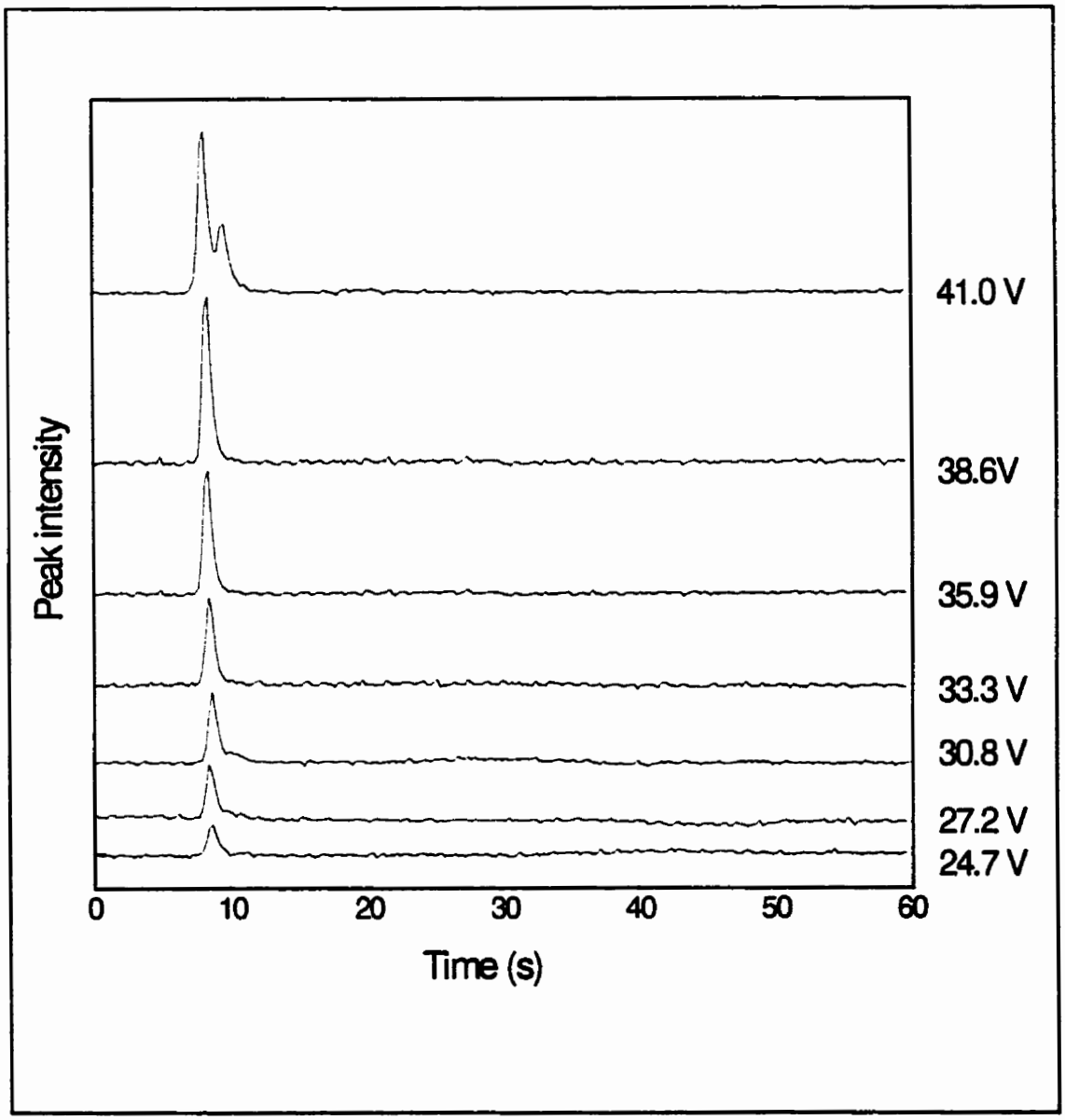

Figure 2-6. TCE peak and pulse voltage.

2.8 Injection Band and Carry Over

To obtain high sensitivity, a narrow injection band is necessary. In MESI the injection band is controlled by the pulse width or pulse duration. In **Figure 2-5** it has been seen that for a 1 s

pulse width, the temperature change from –40 to 263°C and back to –40°C takes approximately 5 s. The actual injection band should be much shorter than 5 s, because the temperature increased from –40°C to 263°C in approximately 1 s, i.e. all the analytes trapped by the sorbent should have been desorbed within the first second. Therefore, the effective injection band is approximately 1 s. The injection band of MESI is reasonable compared with conventional syringe injection. **Table 2-3** lists peak base widths obtained for the components of BTEX (benzene, toluene, ethylbenzene, *o*-xylene) by use of conventional syringe injection (regular GC method) and MESI heating-pulse injection. The injector temperature used for syringe injection was 120°C; 0.5 μL of 1 ppm BTEX mixture (in methanol) was injected. In MESI the membrane was placed 20 mL of 500 ppb aqueous BTEX solution for extraction and the pulse width was 1 s. It is apparent that there was no large difference between the results obtained from these two modes of injection.

Table 2-3. Peak base widths of the components of BTEX. The measurement based on three replicate injections.

Injection mode	Benzene (RSD%)	Toluene (RSD%)	Ethylbenzene (RSD%)	*o*-xylene (RSD%)
Syringe (s)	0.8 (0.1)	1.0 (0.2)	2.2 (0.2)	2.5 (0.3)
MESI (s)	0.8 (0.3)	1.1 (0.2)	2.7 (0.2)	3.0 (0.3)

A shorter pulse width should generate a sharper injection. **Figure 2-7** shows the chromatograms of TCE obtained by use of different pulse widths for desorption. In this experiment, a 500 ppb solution was tested. The sample size was 25 mL and the sample was stirred at 1200 rpm by magnetic stirring. The extraction was at room temperature. The pulse

width was controlled by a computer. It is apparent from this figure that when the pulse width was 0.25 s, the peak width was sharper than for a 1 s injection. The peak intensity was, however, lower after the 0.25 s pulse desorption, indicating that the desorption temperature was insufficient to desorb the analytes completely from the sorbent; a carry over was the consequence.

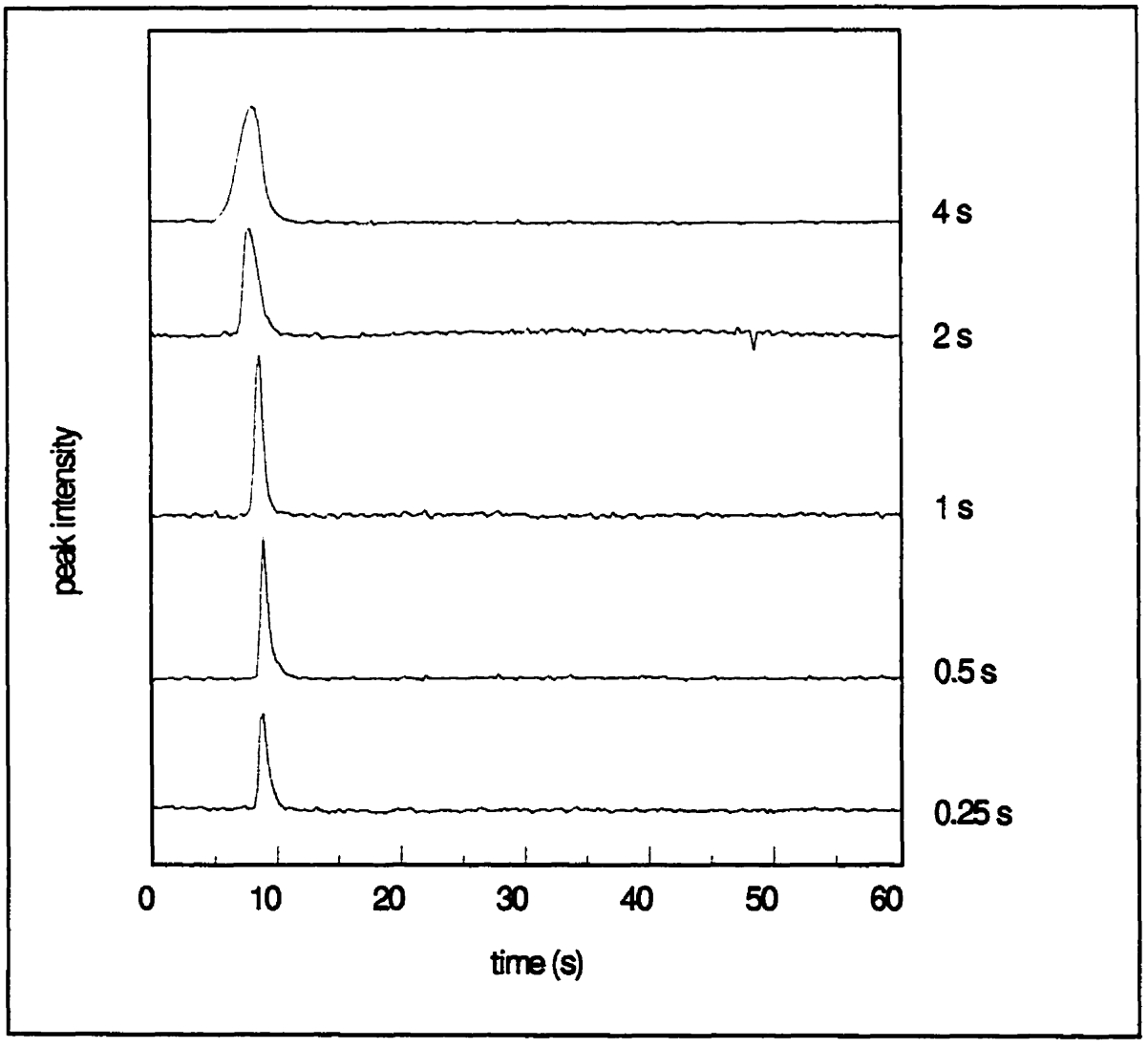

Figure 2-7. TCE peak width and pulse duration. The corresponding pulse voltage: 0.25 s–45 V, 0.5 s–40 V, 1 s–38 V, 2 s–31 V, 4 s–20 V.

Obviously, increasing the heating temperature by increasing the pulse voltage is a solution. Care must be taken when using a very high temperature, because of the degradation of sorbent and a burning of the sorbent tubing. A capacitance charge method can be used for the thermal desorption. In that method, the heating rate can be as high as 1000° s^{-1}.[27] Another way of dealing with the carry over is to extend the pulse width and simultaneously reduce the pulse voltage. In **Figure 2-7** it is apparent that when a longer pulse width, e.g. 4 s, was used, the pulse peaks became broader. This is attributed to the slow increase of the desorption temperature which leads to slow release of analytes from the sorbent because of the use of a lower pulse voltage (to avoid the damage of the sorbent coating). It is easy to conclude that this kind of pulse mode should be avoided because it results in a wide injection band, and affects the second cycle of trapping in continuous monitoring. On the basis of this discussion it is clear that after trapping at –40°C a 1 s pulse width at 38 V is suitable, and results in a short injection band and sufficient desorption.

When the trapping temperature is changed, the pulse heating profile is changed. For example, at room temperature a 1 s pulse resulted in a wide injection peak, **Figure 2-8** shows the temperature-time profile. The profile was obtained by the same operation which was described in Figure 2-5. It is apparent that the temperature increase from 23°C to 263°C was very fast, but the temperature decrease was very slow, taking approximately 30 s. Such a lengthy temperature decline after the pulse can significantly affect the second cycle of trapping in continuous monitoring; for short term trapping the effect can be serious. This slow temperature decrease occurred because cooling by the ambient air was not efficient and heat release was slow.

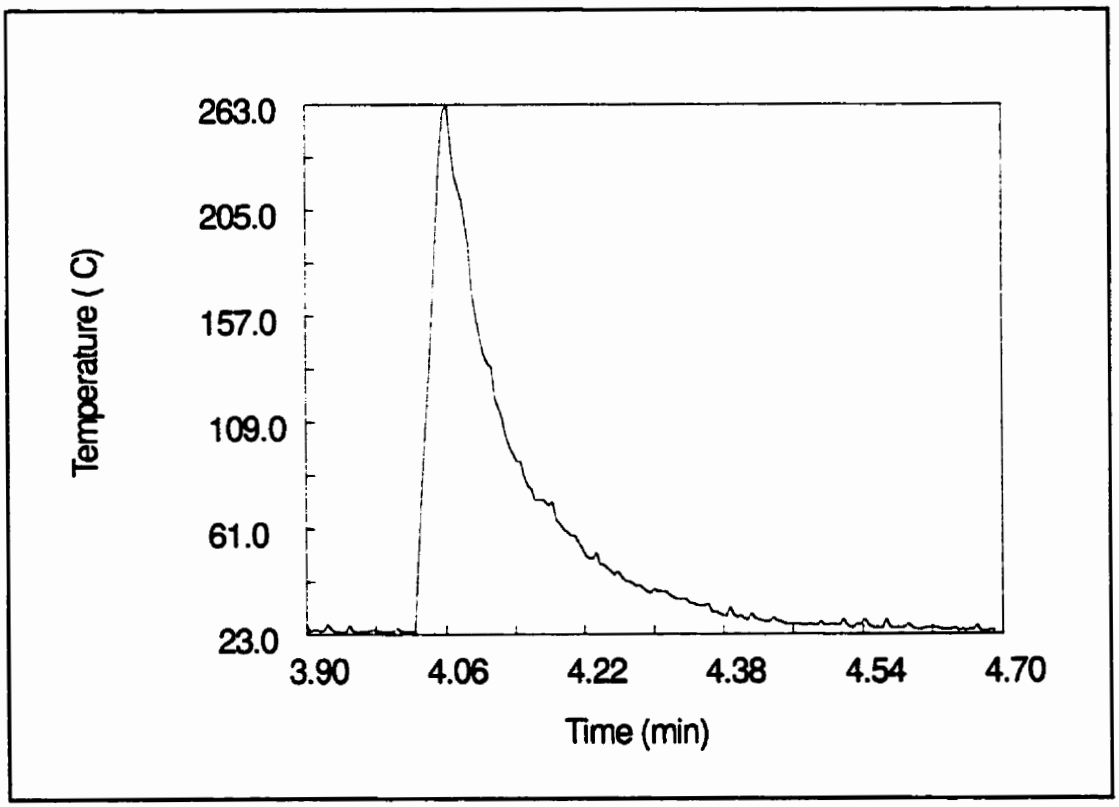

Figure 2-8. Pulse temperature profile when the sorbent was at room temperature

Optimization of thermal desorption is a step-by-step process. Ideal thermal desorption should be without carry over; the injection band should be short and there should be no sorbent damage. The injection band can be controlled by choosing an appropriate trapping temperature and pulse width. Usually a short pulse width is expected.

Carry over should be carefully monitored by inspection of the chromatogram from a second pulse desorption in which the membrane probe is disconnected from the sorbent interface. The aim of disconnection is to avoid the effect of the membrane memory. Experimentally, the trapping time is set relatively long to ensure that a sufficient amount of analytes is accumulated

in the sorbent; the probe is then disconnected from sorbent, but continuous flow of stripping gas through the sorbent is maintained. Two consecutive heating pulses are sent to the sorbent to desorb the analytes. If there are no peaks after the second pulse, there is no carry over. Otherwise, carry over is present. **Figure 2-9** shows the chromatograms obtained from BTEX by use of different pulse temperatures. In the experiment, a 500 ppb BTEX solution was used. The sample size was 25 mL and the sample was stirred at 1200 rpm by magnetic stirring. The trapping time was 2 minutes. In chromatogram A, three peaks were observed after the second injection, i.e. carry over was present. Carry over was prevented by increasing the pulse voltage, as is shown in chromatogram B. Carry over is related to the physical properties of the analyte, for example its partition coefficient. In general, analytes with large partition coefficients are readily be trapped but difficult to desorb. In **Figure 2-9** chromatogram A, there is no carry over for benzene, because benzene has the smallest partition coefficient of these compounds. Close examination of chromatogram A shows that for BTEX the carry over is 0, 1.3, 7.3 and 12%, respectively. It is apparent that different analytes require different minimum pulse voltages. Obviously, for multi-component analysis the pulse voltage level should be set to completely desorb the analyte which has the largest partition coefficient. If the required desorption temperature is higher than the degradation temperature of the sorbent, a sorbent with a higher degradation temperature should be used.

2.6 Conclusion

In this thesis study, a 4 cm long membrane was employed as extraction probe. The small size of the probe allowed the application of MESI in different areas such as air, water and headspace extraction. In the sorbent interface, a 1 cm of PDMS fiber and a three-stage semiconductive

cooler were used to trap analytes at the temperature below 0. A pulse voltage of 38.6 V with 1 s pulse width was used to thermally desorb the analytes from the sorbent onto the GC column. Two parameters of breakthrough and carrier over should be carefully inspected in the MESI setup.

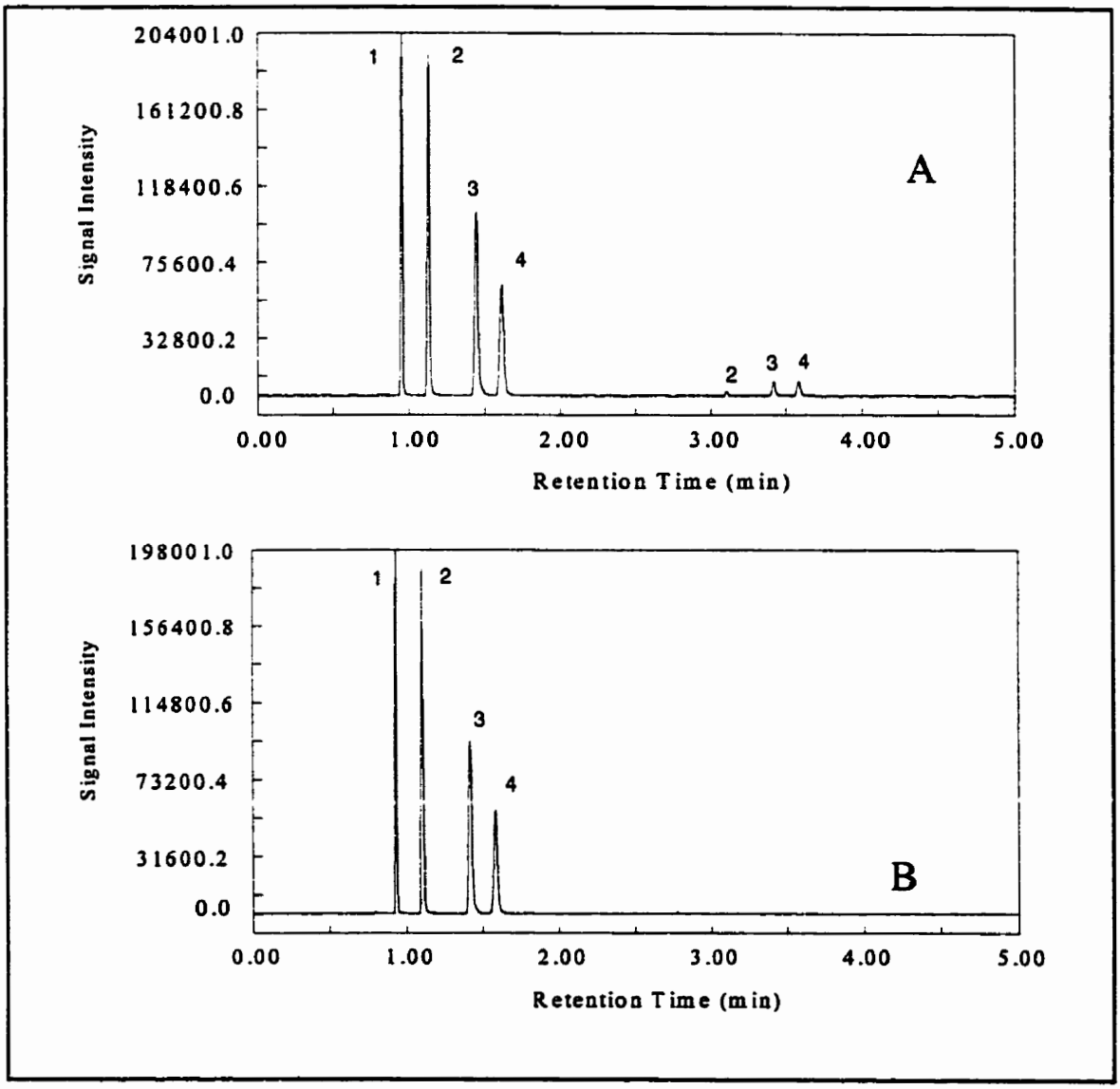

Figure 2-9. Chromatograms obtained from the components of BTEX by use of two desorption temperatures. A. 250°C, B, 275°C. The peaks are: 1. Benzene, 2. Toluene, 3. Ethylbenzene, 4. *o*-Xylene.

CHAPTER 3

MESI FOR AIR SAMPLE EXTRACTION

CHAPTER 3

MESI FOR AIR SAMPLE EXTRACTION

3.1 Mass Transfer

To understand the membrane extraction process better, a mathematical model was derived to describe the behavior of extraction. The primary concern in the discussion is mass transfer. The permeation of volatile organic compounds through a nonporous polymer membrane is generally described in terms of a 'solution–diffusion' mechanism.[28–31] The membrane used in this study is hollow fiber. The extraction processes consist of several steps and they are described as follows:

1. mass flux of analyte from the air to the boundary layer outside the membrane surface;
2. diffusion of analyte through the boundary layer to the membrane outer surface, a diffusion process;
3. partition of analyte between air and membrane at the membrane outer surface, a partitioning process;
4. random movement of the analyte in and through the membrane, a diffusion process;
5. release and stripping of analyte by stripping gas at the inner surface of the membrane, a partitioning process;
6. diffusion of analyte through the gas boundary layer which is close to the inner membrane surface, a diffusion process; and
7. mass transfer of analyte to the sorbent interface by stripping gas.

Because most volatile organic compounds have large diffusion coefficients in air, mass transfer through air can be considered fast. Typically when the membrane is exposed in a fast

flowing gas stream, steps 1 and 2 are fast. Because stripping gas flows through the inside of the hollow fiber membrane, steps 6 and 7 are fast. Steps 3 and 5 are partitioning processes, which are relatively fast. Because of the slow diffusion process in the membrane, step 4 is the rate-determining step in the whole extraction process. This chapter describes studies focused on extraction in a fast flowing gas stream. To simplify the model, perfect mixing is assumed in the gas stream, hence the boundary layers are not considered in the calculations.[32]

The theoretical analysis treats the membrane as having hollow cylinder geometry (**Figure 3-1**). The inner radius is '*a*' and outer radius is '*b*'. The membrane length is '*L*'. The stripping gas is on the inside at the flow rate '*Q*'.

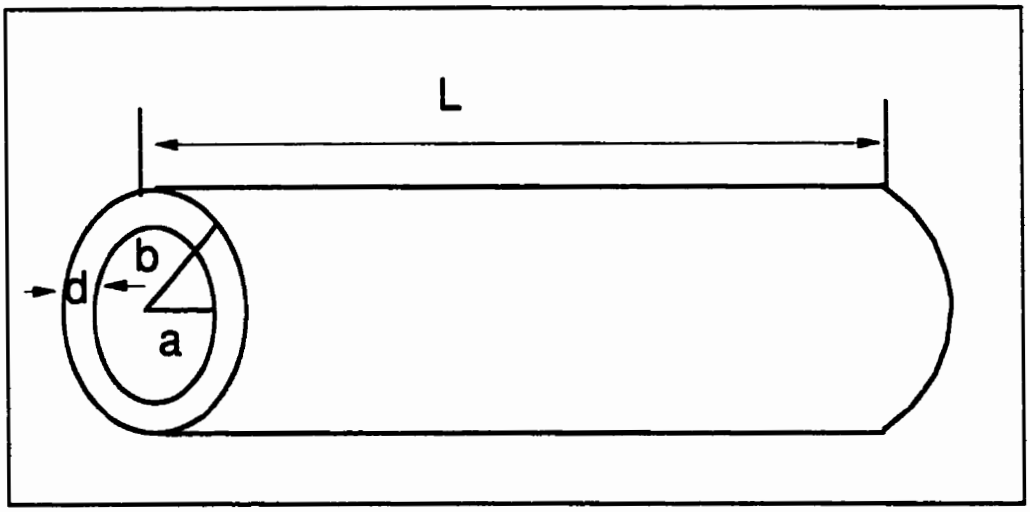

Figure 3-1. Geometry of the hollow fiber membrane.

The concentration distribution is an important aspect in this study. **Figure 3-2** shows the expected concentration profile of analyte across the membrane. A high concentration accumulates near the outer surface of the membrane, because of the partitioning. Most non-polar or weakly polar organic compounds have a large partition coefficient between the PDMS

membrane and air. The concentration on the outer membrane surface can be one to several orders magnitude higher than in the air, depending on the analytes. A concentration gradient is formed in the membrane, and again the gradient is related to properties of the analyte and to other conditions which will be discussed later in this chapter. The concentration in the stripping gas is lower than the concentration in air, because of the concentration gradient. At steady-state, the concentration gradient in the membrane is logarithmic, but the gradient at the inner surface is proportional to the concentration in the stripping gas. Therefore, the average diffusion flux will correspond to the average concentration in the stripping gas, assuming proportionality also holds during non-steady-state conditions. This assumption is assumed to be an adequate approximation.

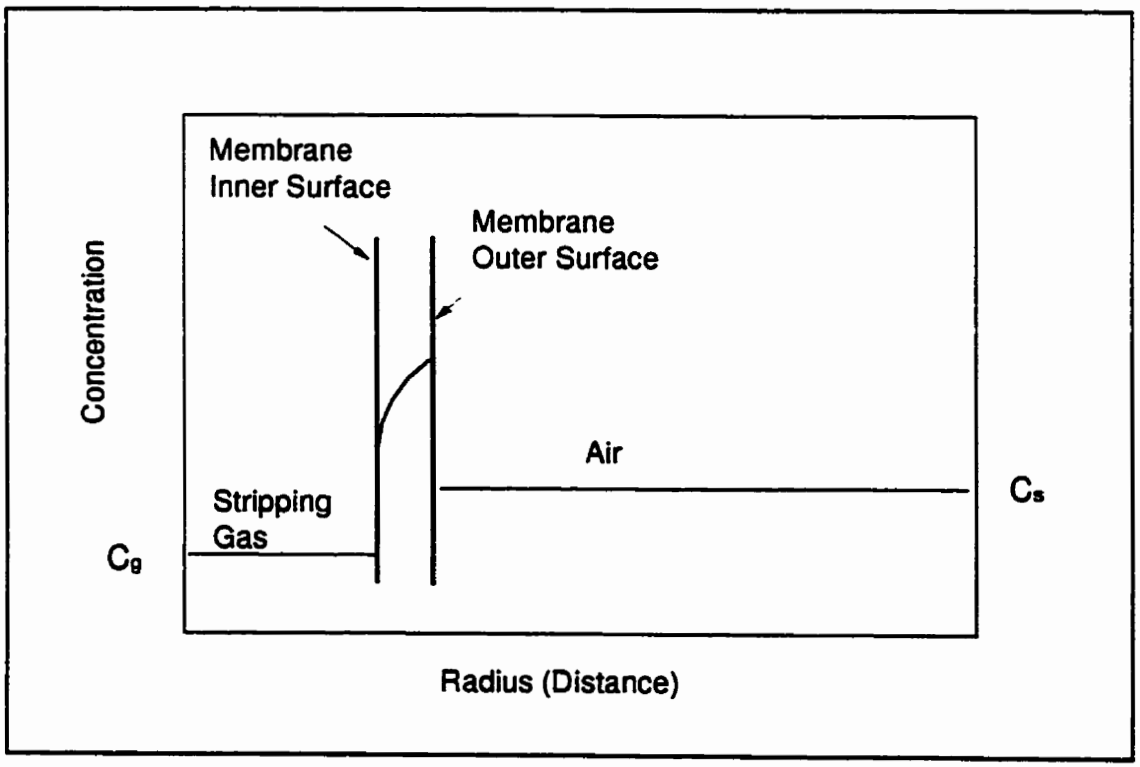

Figure 3-2. Concentration distribution in membrane air extraction.

3.2 Assumption

To simplify the model, the following assumptions are made in the study.

1. The air temperature is assumed constant during the extraction. C_s represents the analyte concentration in the air stream flowing outside the membrane.

2. The pressure inside and outside the membrane is constant during the extraction.

3. The air is assumed to be perfectly mixed and the concentration of analyte in the air is assumed to be constant. $C(r, t)$ is the analyte concentration in the membrane at position r and time t, and D is the diffusion coefficient of the analyte in the membrane. The initial analyte concentration in the membrane is assumed to be zero.

4. Only perpendicular diffusion to the membrane wall is counted, the flux is considered equal everywhere along the length of the membrane.

The extraction rate of the MESI process can be predicted by solving the diffusion equation for the membrane geometry and boundary conditions. Details of the derivation of the equations are given in Appendix II.

The total amount extracted at time t can be expressed as

$$Z(t) = AC_s DK_s \{\frac{t}{\theta + a\ln b/a} + \frac{2}{aD}\sum_{n=1}^{\infty}(1 - e^{-D\alpha_n^2 t})\frac{J_0(b\alpha_n)[\theta\alpha_n J_1(a\alpha_n) + J_0(a\alpha_n)}{F(\alpha_n)\alpha_n^2}\} \quad (1)$$

and the extraction rate is

$$G(t) = \frac{\partial}{\partial t}Z(t) = AC_s DK_s \{\frac{1}{\theta + a\ln b/a} - \frac{2}{a}\sum_{n=1}^{\infty} e^{-D\alpha_n t})\frac{J_0(b\alpha_n)[\theta\alpha_n J_1(a\alpha_n) + J_0(a\alpha_n)}{F(\alpha_n)}\} \quad (2)$$

where $\theta = ADfK_s / Q$, A is the membrane surface area, K_s is the partition coefficient between the air and the membrane, $f = \overline{C_g}/C_g$ and $\overline{C_g}$ is the average lengthwise concentration in the

stripping gas, $F(\alpha_n) = [\theta\alpha_n J_1(a\alpha_n) + J_0(a\alpha_n)]^2 - (\theta^2\alpha_n^2 + 1)[J_0(b\alpha_n)]^2$ and α_n are the positive roots of

$$-[\theta\alpha J_1(a\alpha) + J_0(a\alpha)]Y_0(b\alpha) + [\theta\alpha Y_1(a\alpha) + Y_0(a\alpha)]J_0(b\alpha) = 0 \qquad (3)$$

where J_0, (J_1) and Y_0 are Bessel functions of the first and second kind, of order *i*.

The above formula can be used to calculate the time to reach steady-state extraction. A computer program must be used to find the roots of Eq. 3 and then calculate extraction rate or extraction amount. At steady-state, the formula for $C(r, t)$ simplifies to

$$C(r) = K_s C_s \frac{\theta + a\ln r/a}{\theta + a\ln b/a} \qquad (4)$$

the extraction rate at steady-state is

$$G_{ss} = AC_s DK_s \frac{1}{\theta + a\ln b/a} \qquad (5)$$

3.3 Theoretical Predication and Experimental Agreement

Understanding the extraction process is important in an MESI study, because the membrane extraction dominates the whole analytical process. Membrane extraction determines the selectivity and sensitivity of the method, and the extraction is also affected by other parameters which can be optimized to improve the extraction efficiency.

3.3.1 Experimental Setup

The setup of the membrane probe and the sorbent interface have been described in Chapter 2. A Varian model 3500 GC (Varian Canada Inc., Mississauga, ON) equipped with a flame ionization detector (FID) was operated isothermally with a column temperature of 40ºC. The FID was maintained at 250°C, at range 12. An SPB-5 column, 5 m × 0.32 mm i.d., with a

stationary phase thickness of 1.0 μm, (Supelco Canada, Mississauga, ON) was used. Nitrogen was the carrier gas and the flow rate was 2.2 mL min^{-1}.

A computer was used to control the pulse heating of the sorbent interface and for data acquisition. For pulse heating, the computer sent a series of electric pulses of preset duration to the solid-state relay which converted the pulses to more powerful electrical current pulses through the heating coil around the trap. The first pulse at time 0 cleared the trap. Subsequent pulses, each after an equal trapping period, were sent to desorb all analytes into the carrier stream for GC analysis. The second pulse also started a computer program for real-time GC detector signal collection and display on the computer monitor. The cycle of trapping and desorption was repeated automatically for continuous monitoring.

Benzene, toluene, ethylbenzene, *n*-hexane, and trichloroethylene, were purchased from Sigma–Aldrich (Mississauga, On, Canada). Nitrogen, compressed air and hydrogen gases for flame ionization detection were purchased from Praxair (Waterloo, ON, Canada). The certified permeation tubes of benzene, toluene, ethylbenzene, hexane, and trichloroethylene were purchased from KIN-TEK Company (La Marque, Texas, USA).

Standard gas mixture generation The standard analyte–N_2 mixture gas was generated by the permeation method.[33,34] The permeation chamber was made of aluminum and the shape was similar to that of the extraction chamber (20 cm long, 4.5 cm i.d.). The permeation tube was located inside the permeation chamber and the chamber was wrapped with heating tape. **Figure 3-3** illustrates the setup for generation of the standard gas mixture. When a constant voltage was applied to the heating tape, a constant temperature of 60°C was obtained for generation of the standard gas mixture. The temperature was monitored by means of a digital temperature indicator (Cole-Palmer Instrument Company, Chicago, Illinois). Nitrogen gas flowed through the

permeation chamber; the flow rate was controlled by means of a compressed gas regulator and was monitored by use of a calibrated flow meter (Brooks Instrument Division, Emerson Electric Canada, Markham, On). The gas mixture then flowed through a glass extraction chamber (Supelco Canada, Mississauga, ON, Canada). In the experiment, 125 mL and 1000 mL glass globes were used as extraction chambers. Like the permeation chamber, the extraction chamber was also wrapped with a heating tape for temperature control. The concentration of the standard gas mixture generated can be expressed as:

$$C_{mix} = \frac{K_0 \times ng/\min}{F} \qquad (6)$$

Where F is dilution gas flow in mL min^{-1} at STP, C_{mix} is the concentration at 60ºC, K_0 is the reciprocal vapor density of the permeating component at temperature 25°C, ng min^{-1} is the certified permeation rate. To convert C_{mix} to the concentration C_s at room temperature (25°C), the equation can be written as:

$$C_s = \frac{333K_0 \times ng/\min}{298F} \qquad (7)$$

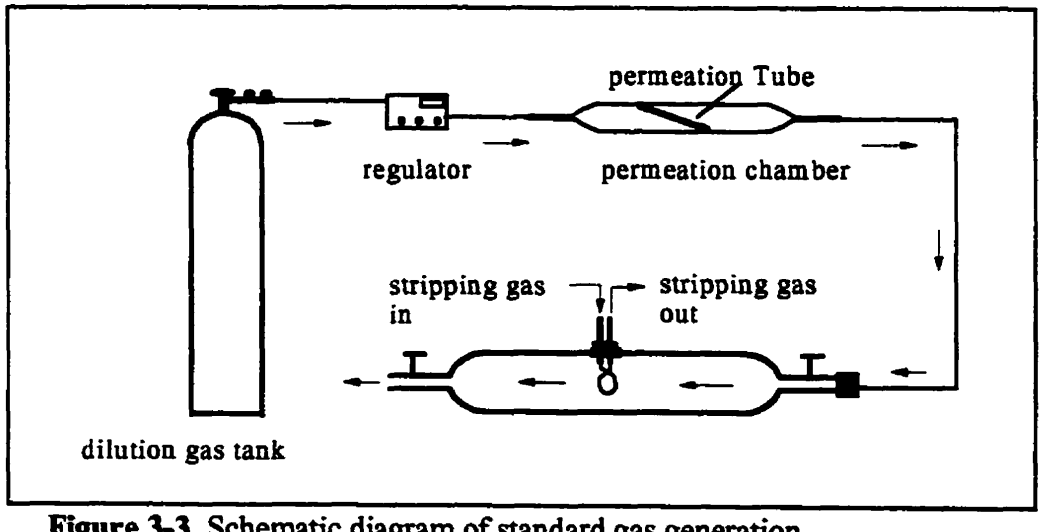

Figure 3-3. Schematic diagram of standard gas generation.

Investigation of the factors affecting extraction In the studies, a 12.7 μg L^{-1} benzene–N_2 or BTEX-N_2 gas mixture (benzene 12.7 μg L^{-1}, toluene15.2 μg L^{-1}, ethylbenzene 15.7 μg L^{-1}, o-xylene 12.5 μg L^{-1}) was used as the air sample and the extraction temperature was 25 °C. The stripping gas flow rate was 2.2 mL min^{-1}. A 1-min trapping time and 10 or 20 min monitoring time were chosen. In the studies of the stripping-gas flow rate, the flow rate was measured down stream of the membrane by use of a soap bubble meter.

In the investigation of the membrane response to changes of concentration, the membrane probe was initially exposed in the glass extraction chamber for 20 min, with a 12.7 μg L^{-1} benzene–N_2 gas mixture flowing through the chamber. The probe was then removed from this chamber and exposed in front of a fan. The air speed was 5 m s^{-1}. This resulted in the concentration on the outside of the membrane suddenly changing to zero. During this time period, the computer recorded the permeation time profile.

3.3.2 The Extraction Process and Response Time

At the moment the membrane is exposed to the sample, the concentration in the membrane is 0; the concentration then increases with time. Some analytes reach the inside membrane surface and are removed by the stripping gas. The concentration in the membrane increases until a constant concentration gradient is formed. These processes can be expressed by the extraction time profile. **Figure 3-4** shows the theoretical prediction and the experimental results for the extraction time profile of benzene on the basis of conditions: room temperature, membrane length 4cm, membrane inner radius 152.5 μm, outer radius 317.5 μm, membrane wall thickness 165 μm, flow rate of stripping gas 2.2 mL L^{-1}. This profile indicates that the extraction comprises two permeation processes—non-steady-state permeation and steady-state permeation.

The term 'non-steady-state permeation' refers to the process that leads to the formation of the constant concentration gradient in the membrane. The term 'steady-state permeation' refers to the process occurring when the constant concentration gradient has been formed; under these conditions permeation through the membrane wall is constant. In **Figure 3-4**, the increasing signal corresponds to the non-steady-state permeation process and the stable signal corresponds to the steady-state permeation process. The experimental extraction time profile obtained is shown as profile b. When profiles a and b are compared it is apparent that the theoretical predication and the experimental result are close. The time from the beginning of the extraction to a signal intensity 90% of that at the steady-state is denoted the non-steady-state time. The experimental results showed the non-steady-state time was 66 s; the theoretical prediction was 62 s.

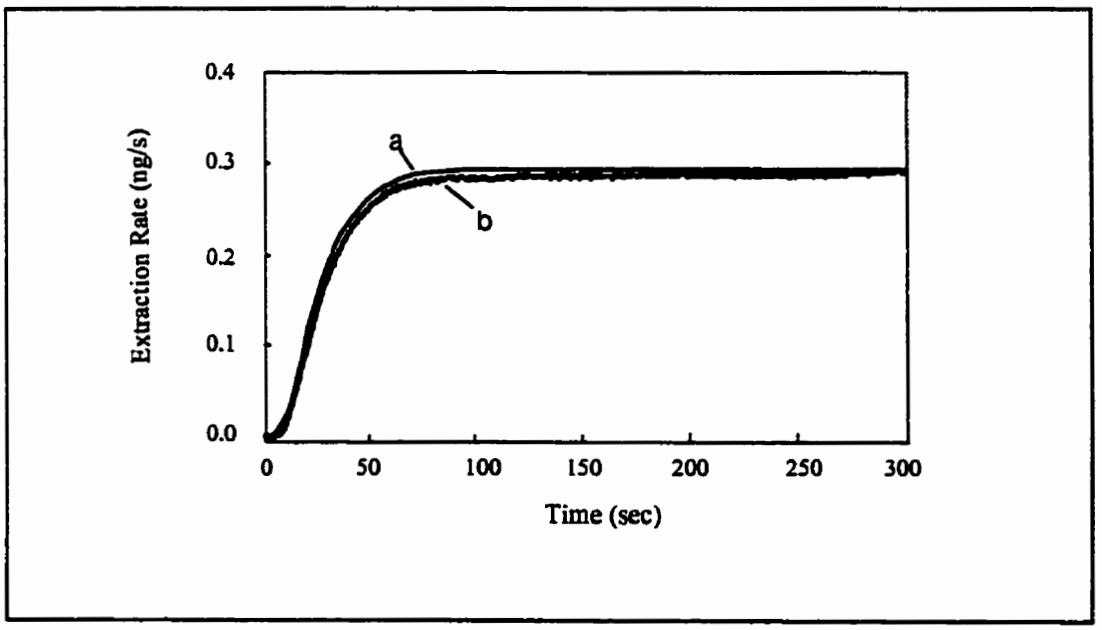

Figure 3-4. Agreement of model and experimental extraction rate and extraction process of benzene. Profile a: model prediction, profile b: experimental result.

3.3.3 The Effect of Membrane Length

As the model predicts, a large membrane surface results in a high extraction rate. A longer membrane length means a larger surface area, hence a higher extraction rate. Experimentally, to simplify the analysis, only the extraction rate under steady-state permeation conditions was investigated. **Figure 3-5** shows the theoretical prediction of the relationship between membrane length and extraction time profile. **Table 3-1** lists theoretical and experimental results for comparison. The parameters for modeling and experiment are described in section 3.3.2. The membrane length is variable in this section. Agreement was obtained for 2- and 4-cm membrane extraction but not for the 8-cm membrane. When the stripping-gas flow rate was increased from 2.2 mL min^{-1} to 5.0 mL min^{-1}, however, the extraction rate was increased to 0.49 ng s^{-1}; the theoretical prediction was 0.60 ng s^{-1} at this flow rate, so an improvement in agreement was observed. It is apparent from this improvement that the stripping-gas flow rate affects the extraction rate.

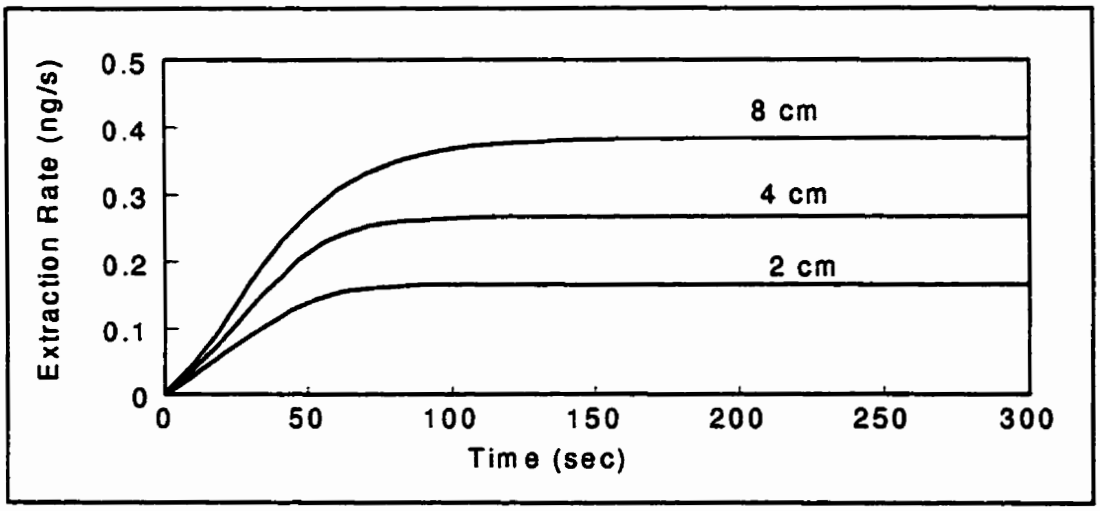

Figure 3-5. Theoretical prediction of the relationship between membrane length and extraction time profile.

Table 3-1. Relationship between membrane length and rate of extraction of benzene. Measurement was based on three replicates.

Membrane length (cm)	$2^{(1)}$	$4^{(1)}$	$8^{(1)}$	$8^{(2)}$
Extraction rate (ng s^{-1})				
Theory	0.18	0.29	0.41	0.60
Experiment	0.19	0.28	0.31	0.49
	(±0.02)	(±0.02)	(±0.03)	(±0.03)

The stripping-gas flow rate was (1) 2.2, (2) 5.0 mL min^{-1}

3.3.4 The Effect of Membrane Wall Thickness

According to the theory, the extraction rate should increase with the decreasing membrane wall thickness. The reason for this increase is apparent from consideration of the concentration gradient across the membrane. **Figure 3-2** shows the model prediction for benzene extraction. A higher concentration at the inner surface of the membrane leads to a greater flux of analyte into the stripping gas, and a higher overall extraction rate. **Figure 3-6** illustrates the theoretical relationship. The parameters for modeling are described in section 3.3.2. The membrane wall thickness is variable in this section. From this figure we can see that when the thickness is reduced to 82.5 μm, half the original thickness, the extraction rate under steady-state diffusion conditions is increased from 0.27 ng s^{-1} to 0.36 ng s^{-1}. If the thickness is doubled, to 330 μm, the extraction rate is reduced to 0.19 ng s^{-1}. It is apparent that when the membrane wall thickness is halved, the time to reach the steady-state is much shorter. Obviously, a longer time is

needed to reach the steady-state point when the thickness is doubled. No data were obtained to prove this prediction because membranes of different thickness but with the same i.d. and material of construction were not commercially available.

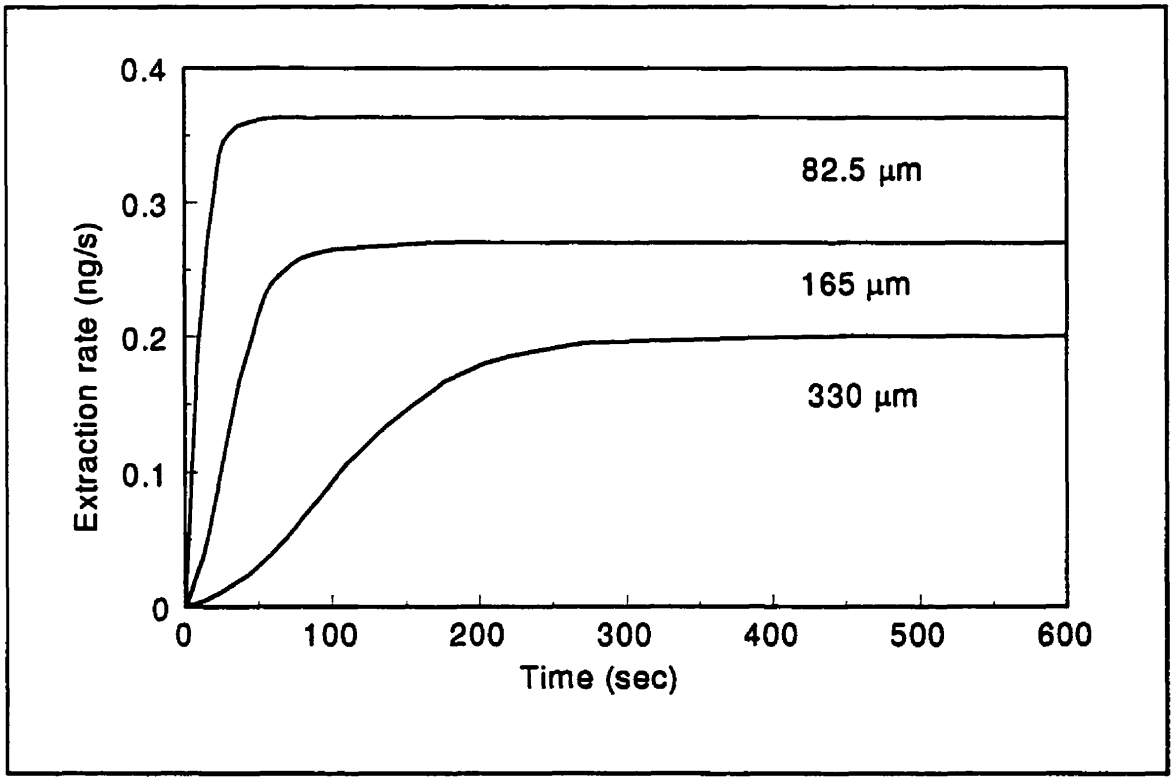

Figure 3-6. Relationship between membrane wall thickness and extraction rate.

3.3.5 The Effect of Stripping-gas flow rate

As already mentioned, the stripping-gas flow rate affects the extraction rate. The theory predicts this effect. **Figure 3-7** shows the model prediction and **Table 3-2** shows the relationship between flow rate and extraction rate for benzene. The parameters for modeling and experiment are described in section 3.3.2. The membrane length is variable in this section. This table indicates that a high flow rate leads to a high extraction rate and a low flow rate results in a low

extraction rate. Because the stripping gas is in contact with the inner membrane surface for a relatively long time, at a low flow rate the analyte easily reaches partition equilibrium between the gas and the inner surface. Although the stripping gas can obtain a relatively high concentration, only a small amount of analyte can be stripped from the inner surface per time unit, thus the overall extraction rate is low. At higher flow rates, the stripping gas either does not reach partition equilibrium, or reaches partition equilibrium near the membrane exit; although the concentration in the stripping gas is lower than when a lower flow rate is used, the overall extraction rate is higher because of the higher flow rate.

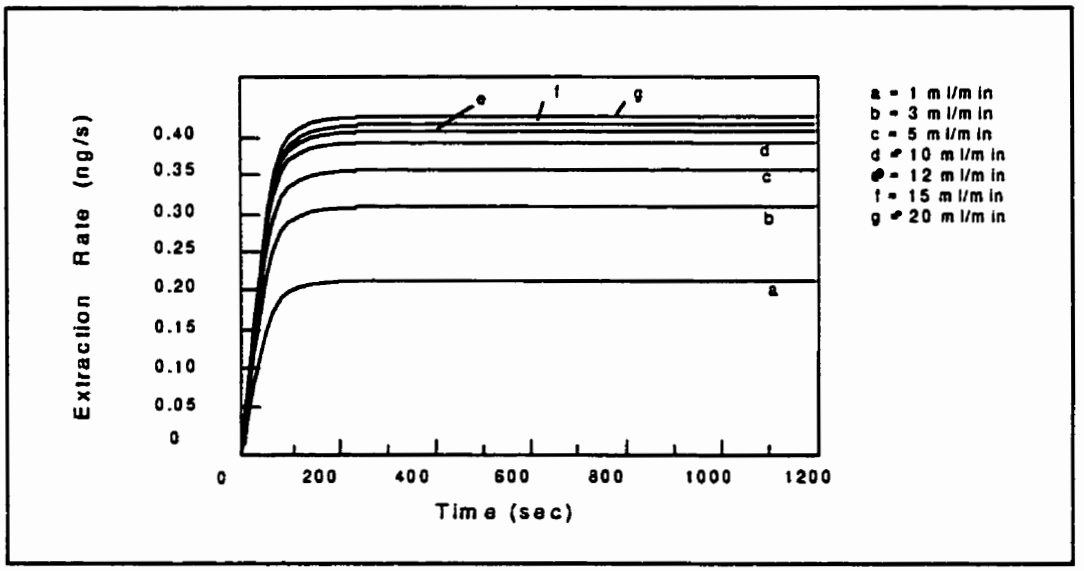

Figure 3-7. Relationship between stripping-gas flow rate and extraction rate.

Table 3-2 suggests that good agreement is obtained between experiment and theory when the flow rate is between 1 and 5 mL min^{-1}. At higher flow rate, 10 mL min^{-1} for example, the experimental extraction rate was significantly reduced. This was attributed to breakthrough at the sorbent interface. Experimentally, the extraction rate at high flow rate is partially represented by

the amount trapped in unit time. Because of the breakthrough, the detected rate was lower than the real permeation rate. Breakthrough can be reduced by reducing the linear flow rate at the sorbent interface; in this way the detected extraction rate will be higher. Experimentally, the linear flow rate can be increased at the membrane probe and reduced at the sorbent interface; this significantly enhances the extraction rate but without breakthrough.

Table 3-2. Relationship between stripping-gas flow rate and rate of extraction of benzene. Measurement was based on three replicates.

Flow rate ($mL\ min^{-1}$)	1	3	5	10	12	15	20	25	30
Extraction rate ($ng\ s^{-1}$)									
Theory	0.19	0.32	0.36	0.39	0.4	0.41	0.42	0.43	0.43
Experiment	0.19 (± 0.02)	0.29 (± 0.03)	0.33 (± 0.05)	0.32 (± 0.04)	0.31 (± 0.06)	0.28 (± 0.06)	0.249 (± 0.05)	0.21 (± 0.05)	0.15 (± 0.06)

3.3.6 The Effect of Temperature

Extraction temperature changes the K and D values. The effect on K can be expressed as[35]:

$$K = K_0 \exp[\frac{\Delta H}{R}(\frac{1}{T} - \frac{1}{T_0})] \qquad (8)$$

where K is the distribution constant at temperature T in degrees Kelvin, K_0 is the distribution constant at temperature T_0, ΔH is the change in enthalpy when analyte goes from the membrane into air , and R is the gas constant. ΔH is considered constant for the ambient temperature range, and is close to the value of ΔH_v, the enthalpy change for vaporization of the pure analyte. From this equation we can see that the value of K decreases with increasing temperature. A low K

value results in a low concentration at the membrane outer surface, hence a lower permeation driving force in the membrane and a low extraction rate.

An increase in extraction temperature, on the other hand, accelerates molecular motion in both air and the membrane, and so the diffusion coefficients are increased. The diffusion coefficients of many penetrating gases in polymers are exponentially dependent on temperature over a limited range of temperatures[35]. Equation 9 shows the relationship.

$$D = D_0 \exp(-E_d / RT) \qquad (9)$$

In this equation D_0 is a pre-exponential factor and E_d is the apparent activation energy for diffusion. Over a certain range of temperatures, E_d is constant, and a plot of the logarithm of D against $1/T$ is linear.[36] When the diffusion coefficient is increased, the diffusion rates in both air and the membrane are increased, and the extraction rate should be increased.

The extraction temperature has opposite effects on the partition and diffusion coefficients. The total effect depends on which factor is most affected by the temperature change. Experimentally, temperatures between 0 and 100ºC were investigated for BTEX extraction. It was found that the rates of extraction of BTEX decreased significantly as the temperature was increased, **Figure 3-8** shows the results. The experimental conditions are described in the experimental section of this chapter. The results indicate that in this extraction the effect of temperature on the partition coefficient was more important than that on the diffusion coefficient.

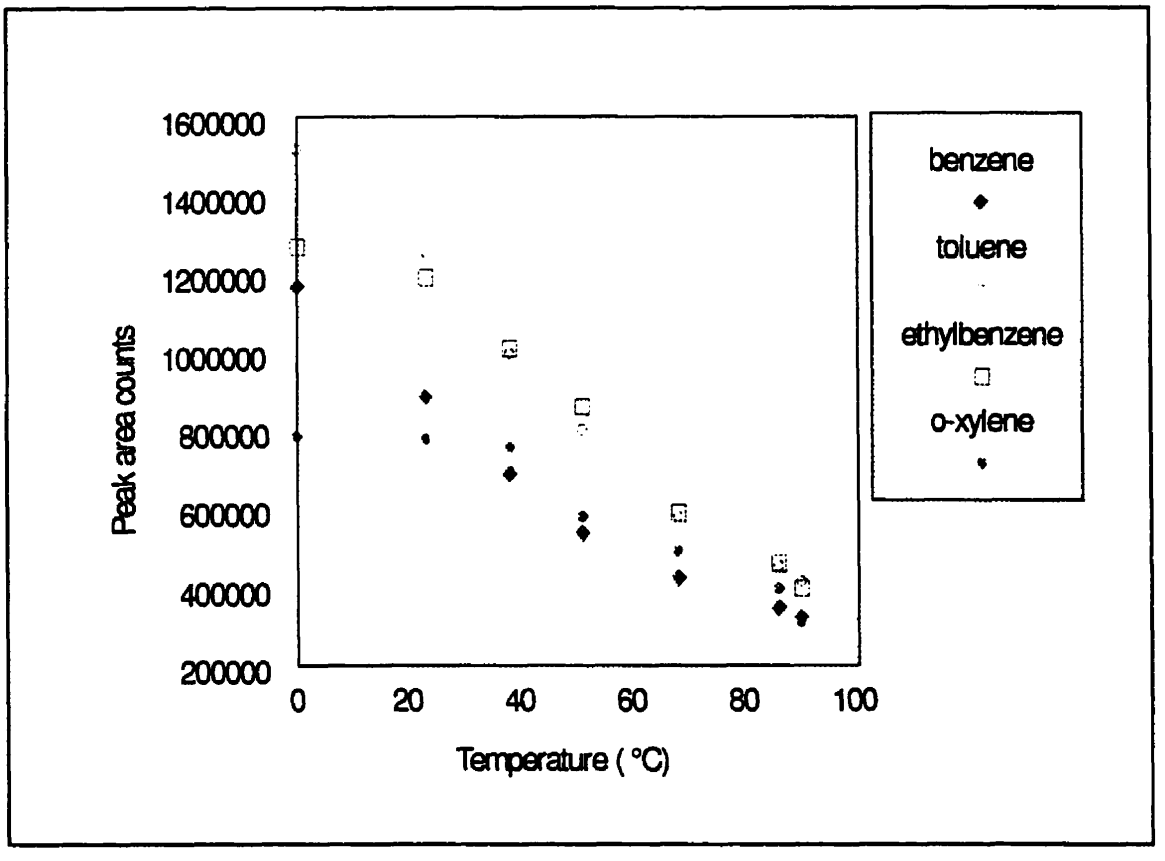

Figure 3-8. Effect of extraction temperature on extraction rate.

3.3.7 Amount Extracted—Agreement between Experiment and Theory

There is excellent agreement between the amount extracted as predicted by the model and that measured experimentally in both non-steady-state and steady-state extraction. **Figure 3-9** shows the agreement for benzene monitoring. The experimental conditions are described in the experimental section of this chapter. The parameters for modeling are described in section 3.3.2. To test the model, other compounds were also investigated at the same experimental conditions. It was found that the model was in good agreement with experimental results for toluene, ethylbenzene, hexane, and trichloroethylene; **Table 3-3** summarizes the results.

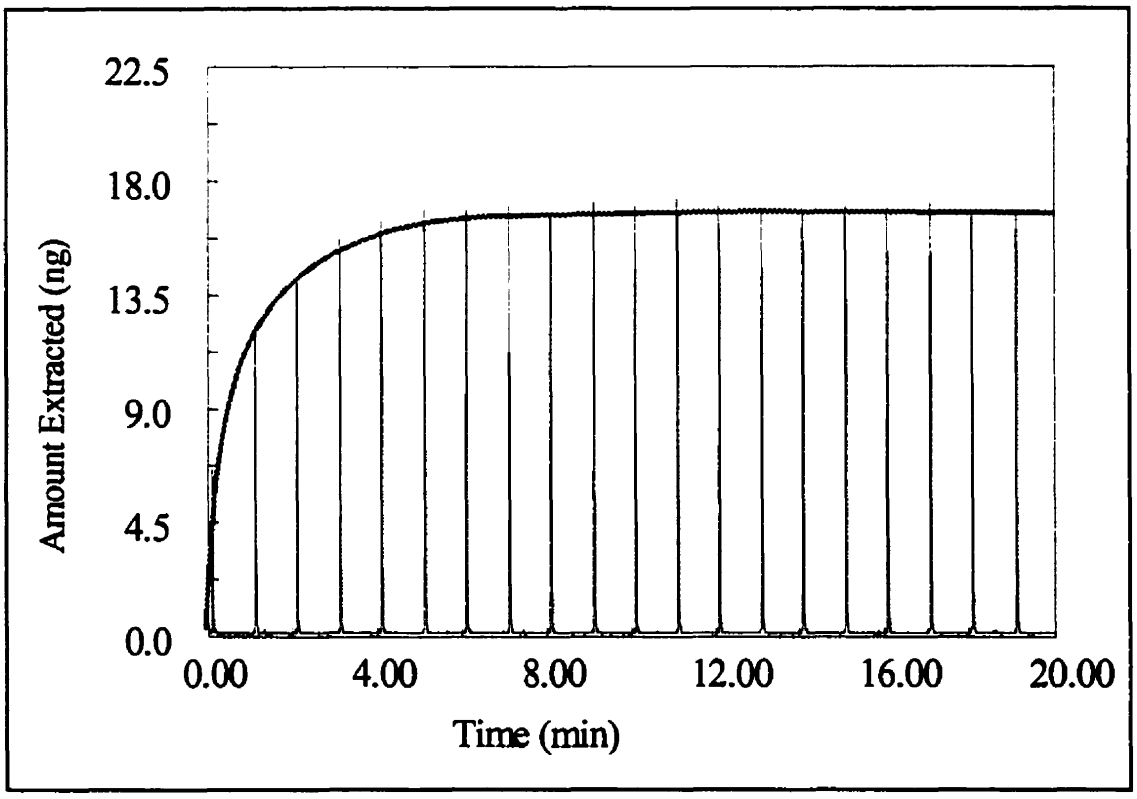

Figure 3-9. Agreement of theoretical prediction and experimental result for the amount of benzene extracted. The line represents the model prediction.

Table 3-3. Agreement between model and experiment for the amount extracted.

	Partition coefficient K	Diffusion coefficient (10^{-6} cm^2 s^{-1})	C_g (μg L^{-1})	Amount extracted (ng)		%RSD (5 replicates)
				Theory	Experiment	
TCE	443	1.81	21	0.41	0.42	6.2
Toluene	1,872	1.59	1.4	0.05	0.04	3.4
Hexane	224	2.27	8.2	0.11	0.12	2.8
Ethylbenzene	3,379	1.09	1.2	0.04	0.04	3.6

3.4 The Factors Affecting Extraction Efficiency

Some effects on extraction efficiency of the membrane probe and of the stripping-gas flow rate have been discussed in the above sections. In this section, other extraction conditions will be discussed including sample volume, pressure, humidity, and response. Because most VOCs have large diffusion coefficients in air, the diffusion of analyte is fast and the boundary layer between the air and the membrane outer surface is not significant. Mixing, therefore, has little effect either on extraction rate or on reducing the time to steady-state. This conclusion is supported both by model prediction and by experimental investigation. The effect of mixing will, therefore, not be discussed in this section.

3.4.1 The Effect of Sample Volume

In a sealed extraction chamber, because the extraction process continuously removes analyte via the membrane probe, the amount of analyte is reduced with time. As the amount of analyte decreases, the concentration in the air also decreases and so the extraction rate is reduced, because the rate of extraction is proportional to the sample concentration. Obviously, larger sample volumes can buffer the concentration change, because the fraction extracted is relatively small. It was found experimentally that in a 20 min continuous extraction, there was no decrease in peak size for a sample size of 1000 mL. When, however, the sample size was 125 mL peak size started to drop after 7 min extraction. **Figure 3-10** shows the chromatograms obtained for benzene during continuous monitoring from two sealed extraction chambers. The other experimental conditions are can be found in the experimental section of this chapter.

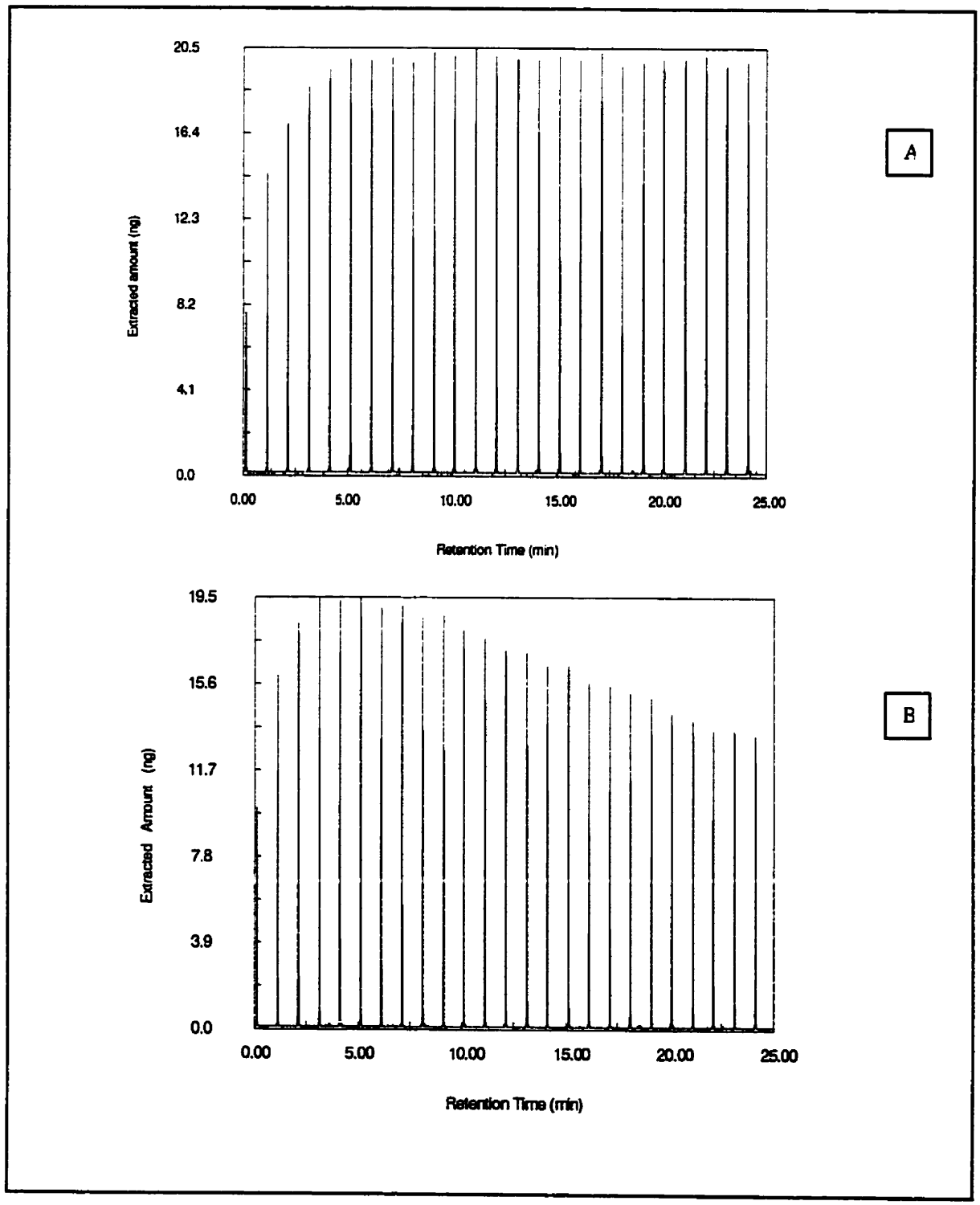

Figure 3-10. Effect of sample volume on extraction: (A) 1000 mL; (B) 125 mL.

3.4.2 The Effect of Pressure

The extraction rate is pressure-dependent. Changing the pressure difference between the outside and the inside of the membrane changes the diffusion coefficient of the analyte in the membrane,[35] causing the extraction rate to change. As the pressure increases downstream (inside the membrane), the extraction rate is reduced.[37] When, however, the pressure is increased, the extraction rate is increased slightly.[38] This is because the membrane is non-porous and the solution–diffusion process is relatively independent of air pressure. Experimental investigation showed that when the pressure on the outside of the membrane was changed from 1 to 2 atm, the extraction rate was increased by less than 8%. Normally, air extraction with MESI is performed under atmospheric pressure, so changes in extraction rate caused by pressure changes can be assumed to be minimal.

3.4.3 The Effect of Humidity

The effect of humidity on the extraction rate is an important factor. Although the membrane used in the experiment is hydrophobic, a small amount of water can still penetrate the membrane wall, even under ambient conditions.[39] It is suggested that the formation of hydrophilic sites during manufacture of the membrane is the reason for water permeation.[40] During the absorption and permeation of water, the diffusion of VOCs is obstructed and hence the extraction rate is reduced. When, moreover, the humidity increases, the partition coefficient of the analyte between the membrane and air will be reduced, because the partition coefficient of an analyte between the membrane and air is usually greater than that between the membrane and water. Experimentally, when the humidity was increased to 80%, no effect on extraction rate was

observed. When the humidity was higher, 100% for example, the extraction rate was 5% lower. Thus, the effect of humidity on extraction from air is not significant, as expected.

3.4.4 The Memory Effect

In air monitoring, the membrane probe is required to respond to a concentration change as rapidly as possible, so a short memory time is essential. Experimentally, to simplify the investigation, the concentration of the benzene–nitrogen mixture was suddenly changed from 12.7 $\mu g\ L^{-1}$ to zero, **Figure 3-11** shows the response time profile. The ideal response should exactly follow the air concentration change, which is indicated by the dotted line in the figure. Because of the small diffusion coefficient of the analyte in the membrane, however, and the effect of membrane thickness, benzene partitions continuously from the membrane for a while after the change of the concentration to zero. In this figure, the time taken for the signal to change from 100% to 10% was 36 s. A membrane with a thinner wall might lead to a faster response.

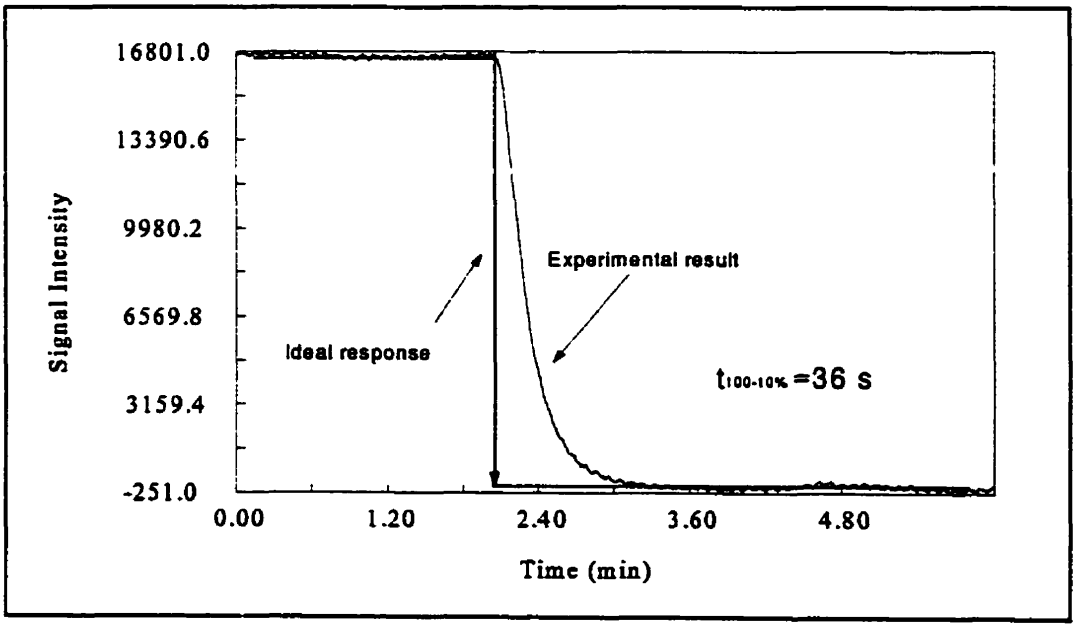

Figure 3-11. Response of the extraction to a change of the sample concentration.

3.4.5 Membrane Probe Cooling and Heating

As known for air extraction (**Figure 3.8**), the extraction rate decreases with increasing extraction temperature. In many applications, however, for example the monitoring of exhaust gases, chemical reactions, industrial pipes, chimney vents, etc., the extraction environment is at high temperature. Under these conditions, the extraction rate is low.

Extraction efficiency can be improved by creating a temperature gradient between the air and the membrane probe. Experimentally, a gas sample was heated to above room temperature, 95ºC for example, while the membrane probe was kept at a relatively low temperature by cooling the stripping gas which was passing through the membrane, **Figure 3-12** illustrates the setup. In the experiment, the stripping gas was cooled by dry ice, the temperature at the inner surface of the membrane was 12 °C while the temperature of gas sample was 95 °C. The temperature was measured by using a fine thermocouple which was described in Chapter 2. A heating coil was employed to conduct pulse heating to desorb the analytes from the membrane into the stripping gas. We have learnt that a high extraction temperature is good for mass transfer in both air and membrane, but a high temperature results in low partitioning of analyte into the membrane. When the temperature gradient is created, the rate of mass transfer from air to the membrane is increased and the partition coefficient between air and the membrane is greatly increased.[21] Although the diffusion coefficient of analyte in the membrane is reduced, because of the reduced of membrane temperature, the reduction can be offset by the increased partition coefficient. At a low extraction temperature, the membrane probe can absorb a large amount of analyte in the membrane wall. When this amount of analyte is thermally desorbed to the stripping gas, the extraction efficiency is increased. Overall, the extraction rate is increased. **Table 3-4** lists the

increases in the amounts of the BTEX components extracted as a result of membrane cooling and heating compared with the amounts extracted by conventional MESI extraction.

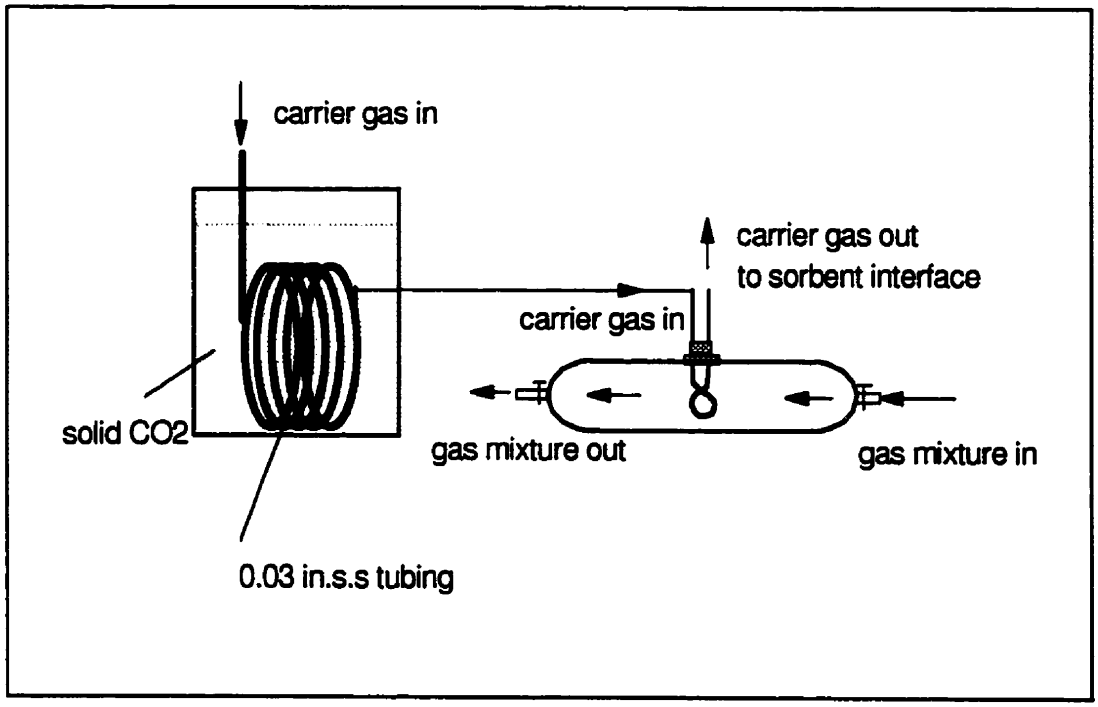

Figure 3-12. Schematic diagram of the experimental setup for membrane probe cooling and heating in air extraction.

Table 3-4. Increased amounts of the BTEX components extracted as a result of membrane probe cooling and heating. (Gas mixture was maintained at 95ºC, the stripping gas temperature at the membrane inner surface was 12ºC). RSD% was based on five replicate measurements.

	Benzene	Toluene	Ethylbenzene	*o*-Xylene
Amount increased (%)	30.1	44.5	59.7	100.6
RSD (%)	2.1	3.2	2.8	2.5

3.5 Summary

The model derived in this paper has successfully predicted the extraction processes. Good agreement with experimental results was obtained. In MESI air analysis several parameters affect the extraction efficiency. A longer membrane probe leads to a higher rate of extraction if the stripping-gas flow rate is sufficiently enough, although a higher stripping-gas flow rate results in breakthrough at the sorbent interface. If an optimized high stripping-gas flow rate can be applied at the membrane probe, a high extraction rate without breakthrough will be achieved. Membrane thickness is a factor affecting extraction rate and the membrane response time for an analyte. A thinner membrane would be beneficial for the applications. Temperature is an important factor in the extraction, it affects both the partition coefficient and the diffusion coefficient of an analyte, but in opposite directions. A relatively low extraction temperature results in a high extraction rate. Membrane cooling and heating can significantly increase the rate of extraction. Optimization of these factors results in a substantial improvement in extraction efficiency.

CHAPTER 4

MESI FOR AQUEOUS SAMPLE EXTRACTION

CHAPTER 4

MODEL OF AQUEOUS SAMPLE EXTRACTION

The MESI technique is adaptable to continuous monitoring or field analysis. Some applications have been published recently.[50–54] Understanding the mechanisms of MESI in terms of well established basic scientific theory will enable the rapid development of MESI for reliable, effective analysis in different applications. This chapter develops a theory to examine the processes in MESI extraction directly from stirred water. The theory includes the fluid dynamics around the membrane because diffusion through water is a significant part of the extraction process. Unlike air extraction, direct membrane extraction of water is affected by the boundary layer which is present between the aqueous phase and the membrane outer surface. The boundary layer between the stripping gas and inner membrane surface is also considered in this discussion.

4.1 Boundary Layers and Boundary Condition

The hollow fiber membrane was exactly the same as that used in the air extraction. (**Figure 3-1** shows the geometry) The theory analyses MESI by use of a diffusion model according to Fick's law, through a hollow cylinder with mass-transfer resistance at the boundaries and a stripping gas flowing inside. **Figure 4-1** illustrates the influence of the boundary layers on membrane extraction and the concentration gradients. The basic equations are from established theory and will apply to any liquid sample, and any membrane with Fickian diffusion. Analyte transport in the MESI system is divided into seven major steps:

1. convection and diffusion of analyte through the sample to the boundary layer outside the membrane surface;

2. diffusion of analyte though the boundary layer to the membrane outer surface;

3. partitioning between sample and membrane at the membrane outer surface;

4. diffusion through the membrane;

5. partitioning between membrane and stripping gas at the membrane inner surface;

6. diffusion of analyte through the boundary layer which is close to the inner membrane surface; and

7. diffusion and convection of analyte into the stripping gas which flows out of the membrane.

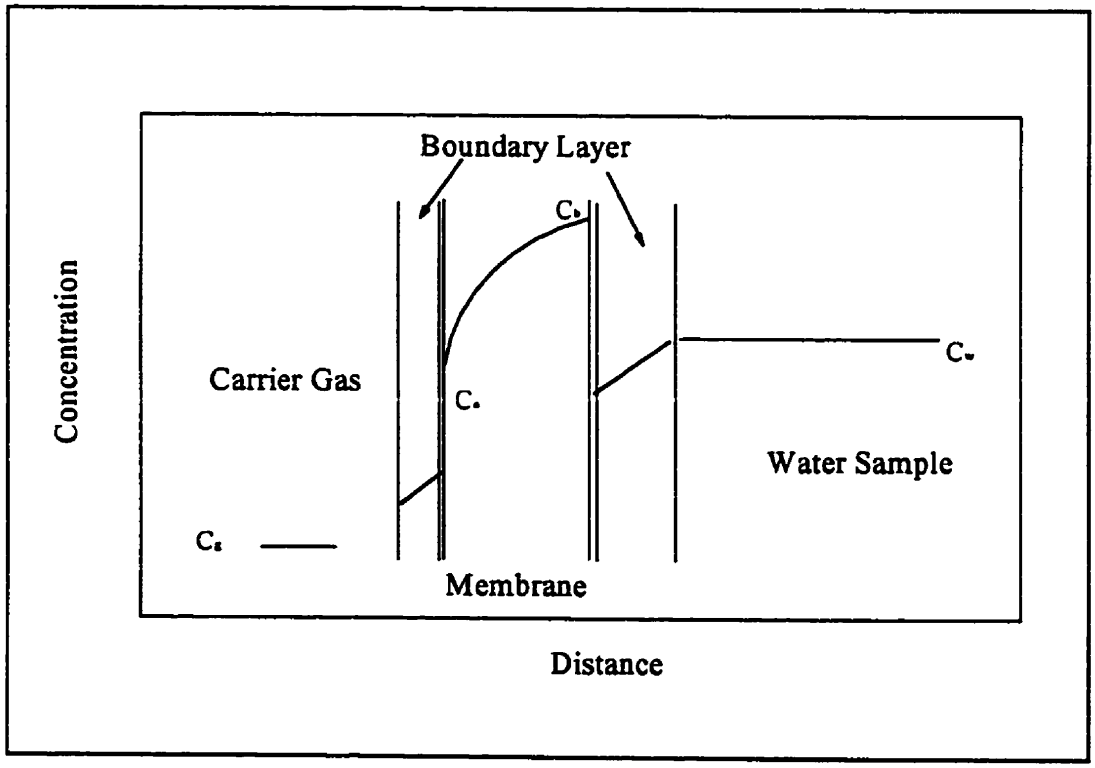

Figure 4-1. Concentration distribution in aqueous phase membrane extraction.

4.2 Equations

Details of the derivatization of the model can be found in Appendix III. A formula for response time, the time when the rate of extraction reaches 90% of its steady state value, accurate to ±15% for $1.3 < \phi < 5$ was derived as explained elsewhere[32] by use of a symbolic algebra program:[57]

$$t_{90\%} = \frac{a^2}{2D_m} \frac{(1+\phi^2)\ln\phi - \phi^2 + 1 + (\phi^2 - 1 - 2\ln\phi)k_1 - (\phi^2 - 1 - 2\phi^2\ln\phi)k_1' + 2(\phi^2 - 1)k_1 k_1'}{k_1' + k_1 + \ln\phi} \tag{1}$$

where $\phi = b/a$, k_1 is a measure of resistance to mass transfer at the membrane inner surface; k_1' is of similar significance at the outer surface.

If k_1' and k_1 are not significant, the response time is:

$$t_{90\%} = \frac{a^2}{2D_m}(\phi^2 + 1 - \frac{\phi^2 - 1}{\ln\phi}) \cong 0.32\frac{(b-a)^2}{D_m} \tag{2}$$

The formula for the steady-state extraction rate is:

$$G_e = \frac{2\pi L D_m K_{ms} C_s}{k_1' + k_1 + \ln\phi} = \frac{\pi L C_s}{\frac{1}{Nu_0 D_s} + \frac{K_{mg}}{K_{ms}}(\frac{1}{3.65 D_g} + \frac{\pi f L}{Q}) + \frac{\ln\phi}{2D_m K_{ms}}} \tag{3}$$

Where Q is the stripping gas flow rate, K_{ms} and K_{mg} is the partition coefficient for membrane/sample and membrane/gas, respectively. The extraction rate G_e is:

$$G_e = 0.9 C_s Q K_{ms} / K_{mg} \qquad \pm 10\% \tag{4}$$

4.3 Factors Affecting Extraction Rates

In aqueous extraction, the extraction rates are affected by several parameters. Some including membrane length, membrane wall thickness, and the stripping gas flow rate are the same as for air extraction, which has already been discussed in Chapter 3. The effects of these

parameters will not be further discussed in this chapter. Additional effects such as mixing, headspace, and headspace volume will be investigated. Although the effect of temperature on extraction rate was investigated in Chapter 3, the effect on gaseous and aqueous phases is different; it will therefore be explored. The effect of pressure on extraction rate in air extraction has been discussed, and found to be insignificant. This conclusion is assumed to apply to aqueous sample extraction also, because extraction is not normally performed in deep water and the pressure change is small.

4.3.1 Effect of Agitation

The migration of an analyte in water is usually much slower than in air. The value of the diffusion coefficient in water is 4 to 5 orders of magnitude lower than in air.[58] This indicates that in water extraction, mass transfer from bulk solution to the membrane outer surface is one of the major rate-controlling steps of the extraction. To speed up mass transfer in an aqueous sample, good mixing is needed. On the other hand, the boundary layer between the aqueous phase and the membrane outer surface has a significant effect on an extraction. To improve extraction efficiency, the boundary layer must be reduced by mixing. Magnetic stirring is the most commonly used method of mixing in MESI for both direct aqueous sample and headspace extraction. Magnetic stirring is efficient when a fast stirring speed is used. Care must be taken when using this technique to ensure the temperature is not changed. **Figures 4-2A** and **4-2B** show chromatograms obtained from benzene by liquid sample extraction with and without stirring, respectively. The figures show the reduced response time and the increased extraction rate which result when the sample was stirred. In **Figure 4-2B**, the reduced peak heights after 12 min extraction was attributed to depletion of the analyte in the sample. Obviously, a higher stirring rate results in better mixing, hence a higher extraction rate

and rapid response. **Figures 4-3A** and **B** show the extraction time profiles for benzene at stirring speeds of 400 and 1200 rpm. The profiles were obtained by direct connecting the membrane probe to the FID through a silica tubing. As expected, sample stirring enhanced the extraction rate and reduced the response time. Note that at high stirring rates, imbalance of the stirrer bar can result in poor mixing.

Use of ultrasound another means of mixing; experiments have revealed, however, that this approach is inefficient compared with magnetic stirring. Although ultrasound can stimulate molecular motion, the migration of molecules in the bulk solution is limited.

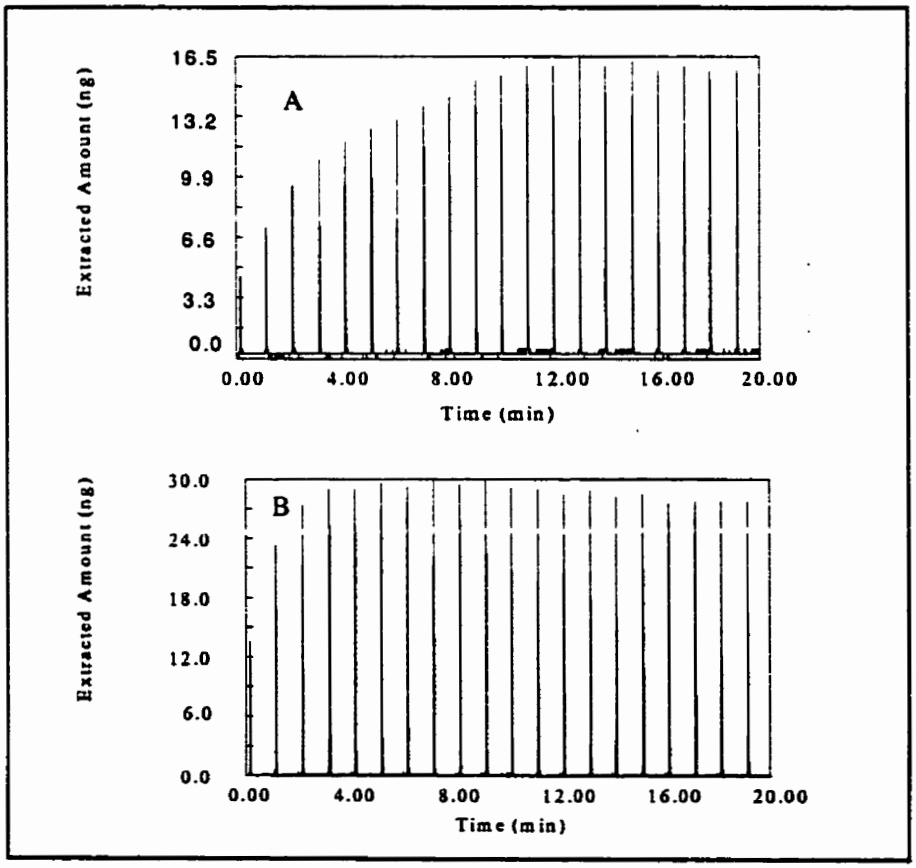

Figure 4-2. Chromatograms obtained from benzene after continuous extraction. Sample concentration 123 ppb. Extraction temperature: 23°C. Membrane length: 4 cm. Flow rate of stripping gas: 2.2 mL L^{-1}. Trapping time: 1 minute. A. Extraction under relatively static conditions; B. Extraction with stirring (800 rpm).

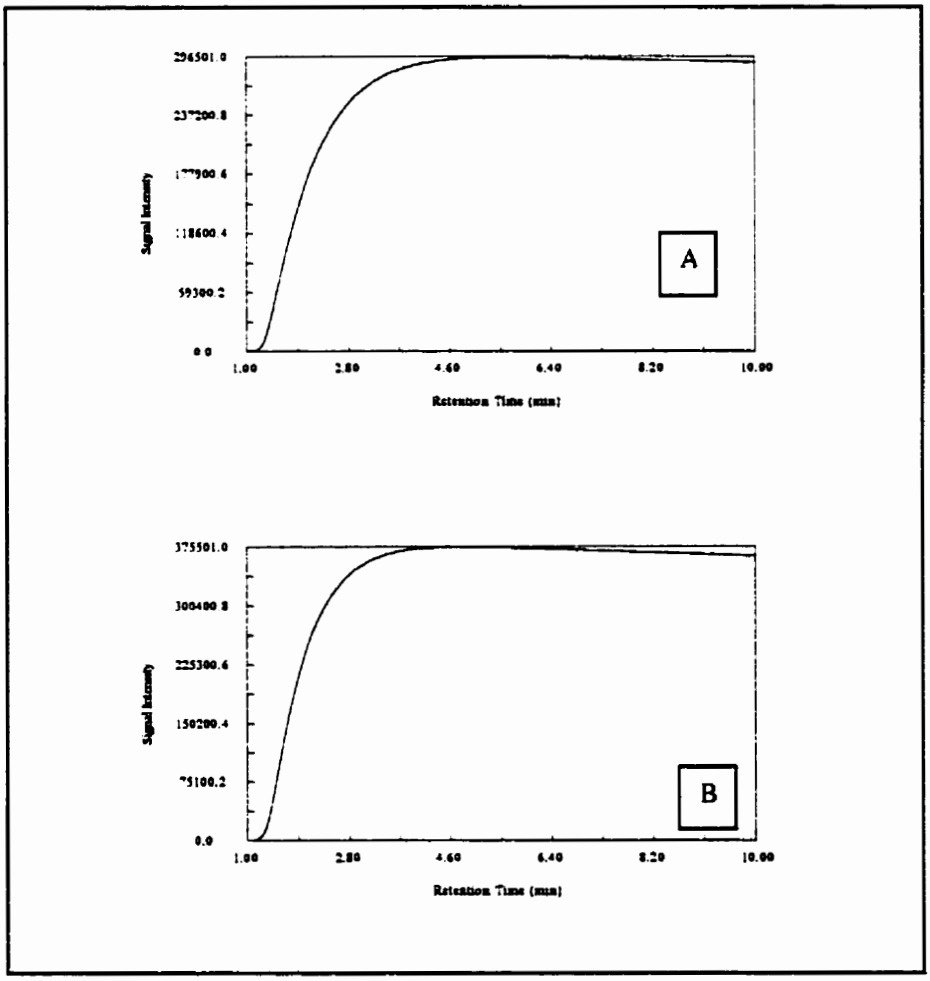

Figure 4-3. Extraction time profiles for benzene solution at different stirring speeds. A: 400 rpm, B: 1200 rpm. (The other experimental conditions are described in Figure 4-2).

4.3.2 Headspace Effects

Experiments also revealed that a small headspace can increase the rate of extraction from aqueous samples, **Table 4-1** lists results from experiments on benzene extraction. It is apparent that with 0.5mL headspace the amounts of BTEX components extracted were higher than with no headspace. The total amount extracted in the first 20 min was increased by 10% to 20% depending on the compound (toluene 20.3%, trichloroethylene 23.1%, ethylbenzene

17.7% and hexane 13.7%). When headspace was present many small gas bubbles were observed adhering to the membrane surface. A compressible headspace enabled the stripping gas to penetrate the membrane wall and form bubbles on the membrane's outer surface. Although the analyte still needed to diffuse through the water to the gas bubbles, mass transfer was enhanced because small gas bubbles have a large surface area, and the molecules of analyte could easily diffuse through the gas bubbles and, in general, compounds have larger distribution constants between the membrane and air than between membrane and water. With headspace present the concentration of aqueous solution dropped somewhat because analytes became distributed into the headspace, but overall the extraction rate was increased if the volume of headspace was small. The amount extracted decreased when the volume of headspace was further increased. This reduction was because more molecules of analyte became distributed into the headspace, which resulted in significant reductions in the concentrations in the solution. Therefore, when a headspace is used to aid direct aqueous sample extraction, it should be kept as small as possible. It can be seen that an appropriate headspace is beneficial to extraction efficiency in the direct extraction of water. For high repeatability the volume of headspace should be maintained constant.

Table 4-1. Effect of headspace on the rate of extraction of benzene in the direct extraction of water. Benzene concentration: 100 ppb, vial size 40 mL, stirring speed 1200 rpm, membrane length 4cm, flow rate of stripping gas 2.2 mL L^{-1}, trapping time 1 minute, temperature 24 °C.

Headspace (mL)	0	0.5	1	2	5	20
Extraction rate change (%)		9.1 (±0.2)	7.4 (±0.3)	2.9 (±0.2)	2.8 (±0.2)	-0.5 (±0.2)

4.3.3 Temperature Effects

The extraction temperature has a substantial effect on the rate of extraction. As discussed in Chapter 3, temperature affects both the diffusion coefficient and distribution constant. As the temperature is increased, the diffusion coefficient is increased but the distribution constant is reduced. It is known that the rate of extraction depends on these two parameters—large K and D values are required for a high extraction rate. The rate of extraction can be expressed in terms of permeability the P, which is the product of K and D.[30] The relationship between temperature and permeability can be described by Arrhenius equation:

$$P = P_0 \exp[-E_p(\frac{1}{RT} - \frac{1}{RT_0})] \qquad (5)$$

where the initial permeability, P_0, is given by the initial temperature, T_0; the activation energy for permeation, E_p is the sum of the activation energy for diffusion, E_d; and the difference between the heats of solution in the membrane and in the sample matrix, $\Delta H_s = H_s$(membrane) $- H_s$(water). Therefore Equation (5) can be rewritten:

$$DK = D_0K_0 \exp[-(E_d + \Delta H_s)(\frac{1}{RT} - \frac{1}{RT_0})] \qquad (6)$$

The activation energy E_d is greater than 0 and for most VOCs ΔH_s is less than 0. The direction for the change in permeability with temperature depends on whether the change in the diffusivity or the distribution ratio dominates, as determined by the relative magnitudes of E_d and ΔH_s. Increases in organic permeation rates from water can also be because the Reynolds number increases with temperature according to the relation $N_{Re} = dv(0.00538T^2 + 2.38T + 48.7)$, and so boundary layers are reduced at higher temperatures. This relationship was determined from curve fitting a plot of water density/viscosity ratios against temperature.[59]

Experiments showed that the extraction rate increased with increasing temperature. **Figure 4-4** shows the results.

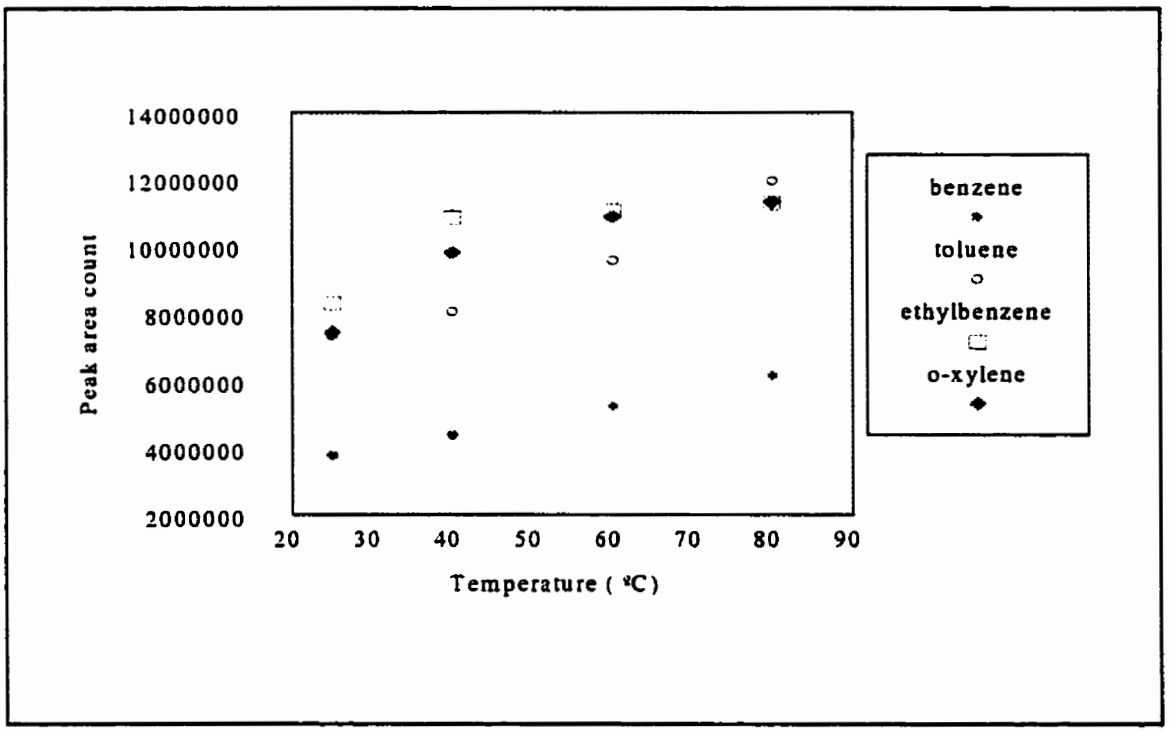

Figure 4-4. Effect of temperature on extraction rate of BTEX aqueous sample. Concentration: benzene 200 ppb, toluene 300 ppb, ethylbenzene 250 ppb, o-xylene 260 ppb; sample size 40 mL; membrane length 4 cm, flow rate of stripping gas 2.2 mL L^{-1}; trapping time 1 minute; sample stirring speed 1200 rpm; extraction temperature 25 °C.

Microwave heating is an efficient method in MESI water extraction. Because water, but not the membrane, can efficiently absorb microwaves, microwave heating is perfect for coupling to MESI water extraction. Microwave energy is a non-ionizing radiation that causes molecular motion by inducing migration of ions and rotation of dipoles; it does not promote changes in molecular structure.[60] The frequencies 300–300000 MHz are used for industrial and scientific purposes, the most common being 2450 MHz which is used in all domestic

microwave units.[61] At 2450 MHz, the alignment of the molecules followed by their return to disorder occurs 4.9×10^9 times per second; this results in rapid heating.[62] **Figure 4-5** compares the effects of two heating methods, microwave heating and hot-plate heating. The extraction time profile for microwave heating is indicative of a rapid change in the amount extracted; the change is slow for hot-plate heating. Note that the amount extracted decreases in microwave heating, because of concentration depletion.

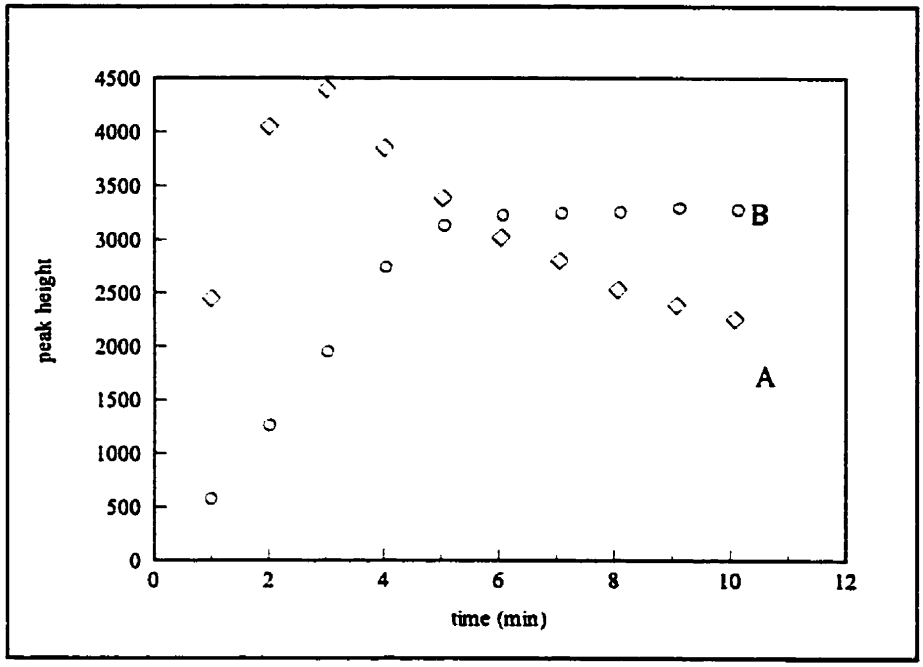

Figure 4-5. Extraction time profile of TCE. A. microwave heating, B. hot-plate heating at 100°C. Sample concentration 5 ppb, sample size 2 mL, membrane length 2 cm, flow rate of stripping gas 2.2 mL L^{-1}, trapping time 1 minute.

4.4 Membrane Response

Membrane response to the concentration change is an important parameter. The response can be represented by the response time which is defined as the time taken for rate of permeation to increase from 0 to 90% of steady state. To determine the response time

experimentally the membrane was connected directly to the FID, and the permeation process was monitored by the detector and recorded as the time sequence. By analyzing the time profile, the response time can be obtained. **Figure 4-6** shows a plot of FID signal against time for benzene. The time profile was obtained by directly connecting the membrane probe to the FID detector through a piece of silica tubing. The benzene concentration was 500 ppb, sample size 40 mL, and the flow rate of stripping gas was 5.3 mL L^{-1}. The sample was stirred at 1200 rpm by magnetic stirring at room temperature. From this figure it is apparent that the response time for benzene is 113 s. In MESI a short response time is required, because it indicative of steady-state extraction being reached rapidly, which is required for quantitative analysis. Memory effect, on the other hand, affects the response of the membrane to changes the concentration from a given concentration level to zero. Memory effect can be also represented by the response time, but here the response time is defined as the time for the rate of permeation to decline from 100% to 10%. In **Figure 4-6**, the decline curve represents the memory effect. Theoretically, for a selected membrane and analyte, $t_{0-90\%}$ and $t_{100-10\%}$ should be identical. Experimental observation, however, revealed a difference (**Table 4-2**). The difference can be small, as for benzene, or large, as for hexane. This phenomenon might be attributed to different rates of stripping of the analytes from the inside and outside of the membrane. For fast responses to concentration changes during monitoring, low values are required for $t_{0-90\%}$ and $t_{100-10\%}$. Obviously, a membrane with a thinner wall thickness can result in a shorter response time.

Table 4-2. Physicochemical parameter values at 25°C.

	K_{ms} water (determined experimentally)	K_{ms} air	D_{water} [10^{-5} cm^2 s^{-1}] [Ref. 77]	D_{air} [cm^2 s^{-1}] [Ref. 78]	D_m [10^{-6} cm^2 s^{-1}] (determined experimentally)	D_{N2} [Ref. 67]
Benzene	136	485	1.09	0.093	2.12	0.38
Toluene	346	1872	0.95	0.085	1.59	–
Ethylbenzene	847	3380	0.9	0.0755	1.09	–
TCE	182	443	0.96	0.0875	1.81	–
Hexane	126	224	0.9	0.0732	2.27	–
Methanol	29	–	1.66	0.152	–	–
i-Butanol	52	–	0.93	0.088	–	–

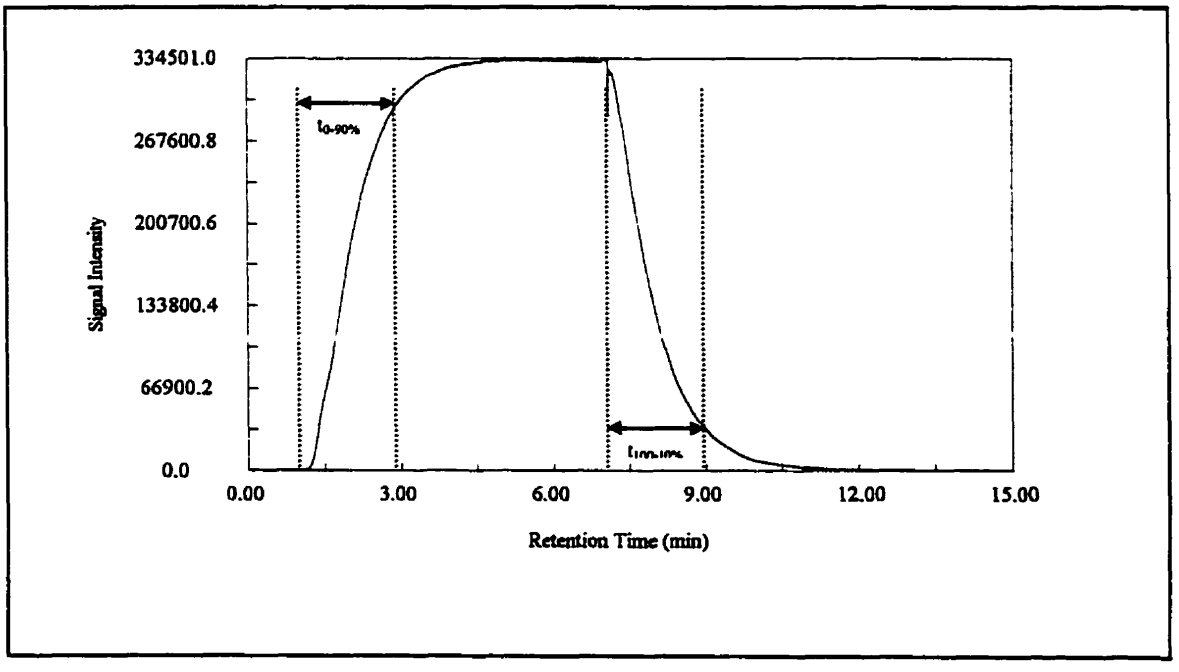

Figure 4-6. Response time profile of the membrane for benzene.

4.5 Agreement Between Model Prediction and Experiment

Agreement between model and experiment has been investigated by comparison of extraction rate and response time. **Figure 4-7** shows a comparison of extraction time profiles for benzene on the basis of conditions: membrane length 4 cm, membrane inner radius 152.5 μm, outer radius 317.5 μm, membrane wall thickness 165 μm, flow rate of stripping gas 2.2 mL L^{-1}, benzene concentration 200 ppb, extraction temperature 23 °C, sample stirring speed 1200rpm. It is apparent that agreement is good. The compounds toluene, ethylbenzene, trichloroethylene, and hexane, were also chosen for investigation of the agreement; the physical parameters which are used in the calculation are listed in **Table 4-2** and the results are listed in **Table 4-3**.

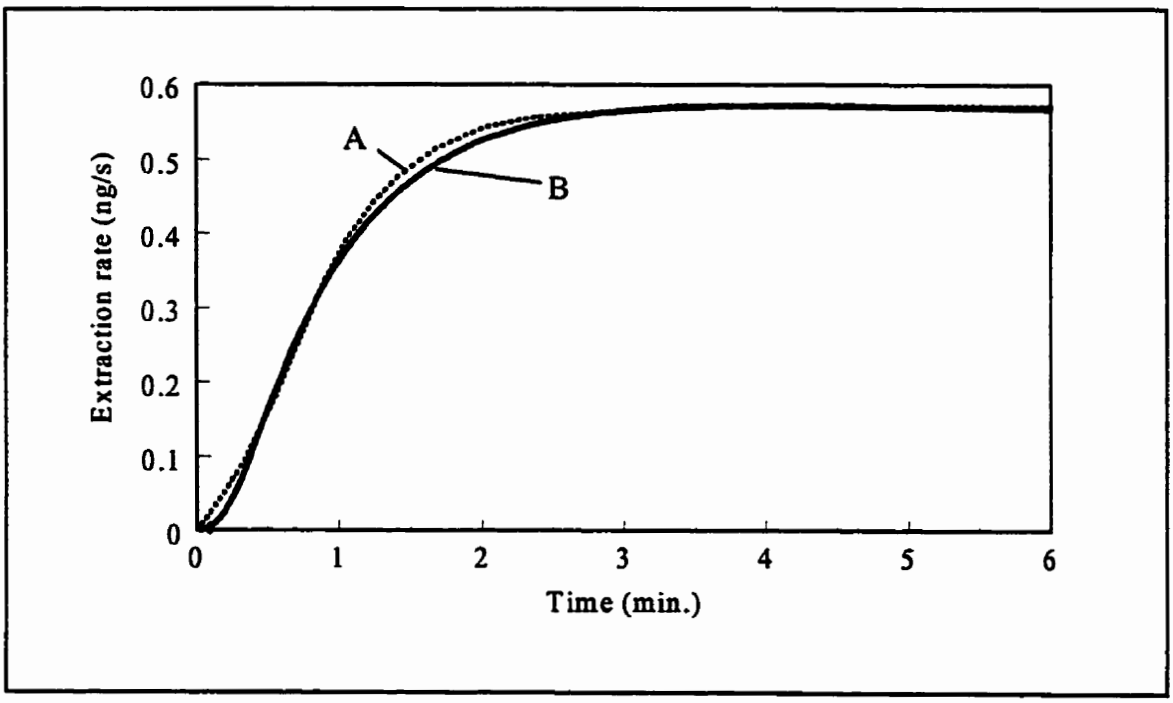

Figure 4-7. Extraction time profiles of benzene. Curve A: model prediction; Curve B: experimental result.

Table 4-3. Comparison of theoretical and experimental results. RSD % are based on five replicates.

	$t_{90\%}$, determined by use of Eq. (1) [s]	Response times, determined experimentally [s]		% Difference between theoretical and experiment $t_{0\text{-}90\%}$	G_e determined by use of Eq. (3) [ng s^{-1}]	G_e (%RSD) determined experimentally [ng s^{-1}]	% Difference between theoretical and experimental G_e
		$t_{0\text{-}90\%}$ (%RSD)	$t_{100\text{-}10\%}$ (%RSD)				
Benzene	136	113 (3.9)	106 (6.2)	–16.9	0.55	0.55 (3.3)	0
Toluene	347	269 (5.8)	308 (7.8)	–22.5	0.73	0.72 (4.2)	–1.4
Ethylbenzene	701	641 (5.9)	856 (6.5)	–8.5	0.91	0.95 (3.8)	4.4
TCE	163	131 (3.7)	157 (2.4)	–19.6	0.45	0.41 (3.4)	–8.9
Hexane	113	120 (2.1)	296 (6.7)	–6.2	0.32	0.28 (3.7)	–12.5

The good agreement between model and experiment implies that the model of membrane extraction accurately describes the dominant natural processes in MESI. **Figures 4-8** and **4-9** illustrate the theoretical relationship between response time and mass transfer resistance at the outside membrane surface, i.e. the dependence of $t_{90\%}$ on k_1', and the relationship between response time and mass transfer resistance at the inside membrane surface, i.e. the dependence of $t_{90\%}$ against k_l. Calculations with Eqs (1) and (3) show that response time and steady-state extraction rate will be influenced by boundary effects at the membrane outside surface if:

$$\frac{1}{Nu_0 D_s} > \frac{0.015}{K_{ms} D_m} \qquad (7)$$

i.e. if $k_1' > 0.03$, for the aspect ratio of the membrane used in this study, $\phi = 2.08$. Likewise response time and steady state extraction rate will be influenced by boundary effects at the membrane inner surface if:

$$\frac{1}{3.65D_g} + \frac{\pi f L}{Q} > \frac{0.03}{K_g D_m} \qquad (8)$$

i.e. if $k_l > 0.06$, for the aspect ratio $\phi = 2.08$.

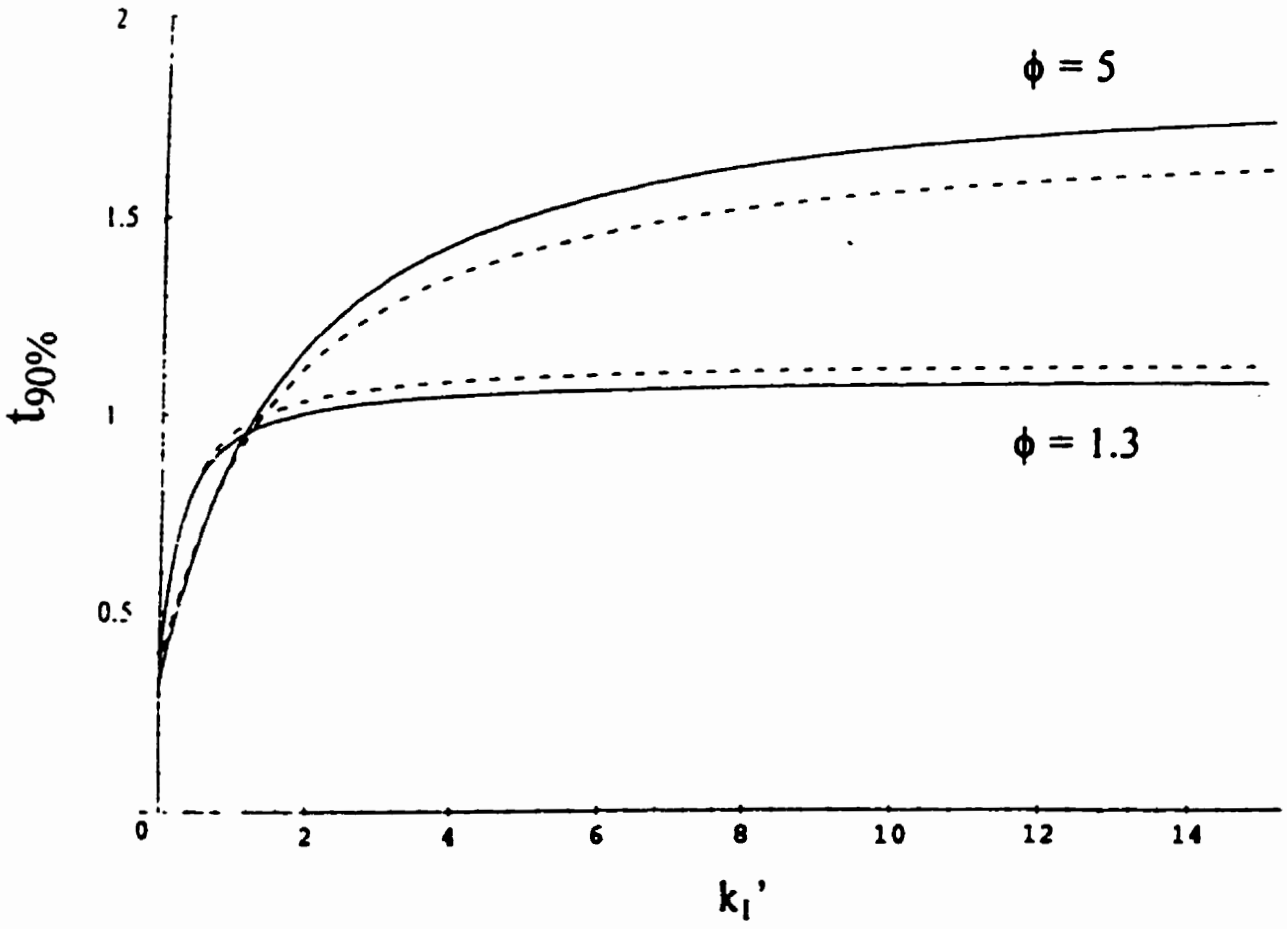

Figure 4-8. Relationship between response time (min) and the parameter for mass transfer at the outside membrane surface, k_l'. The solid line is that calculated by use of the exact model (Appendix III, Eq. 12), the dashed line is that calculated by use of the approximation formula (Eq. 1).

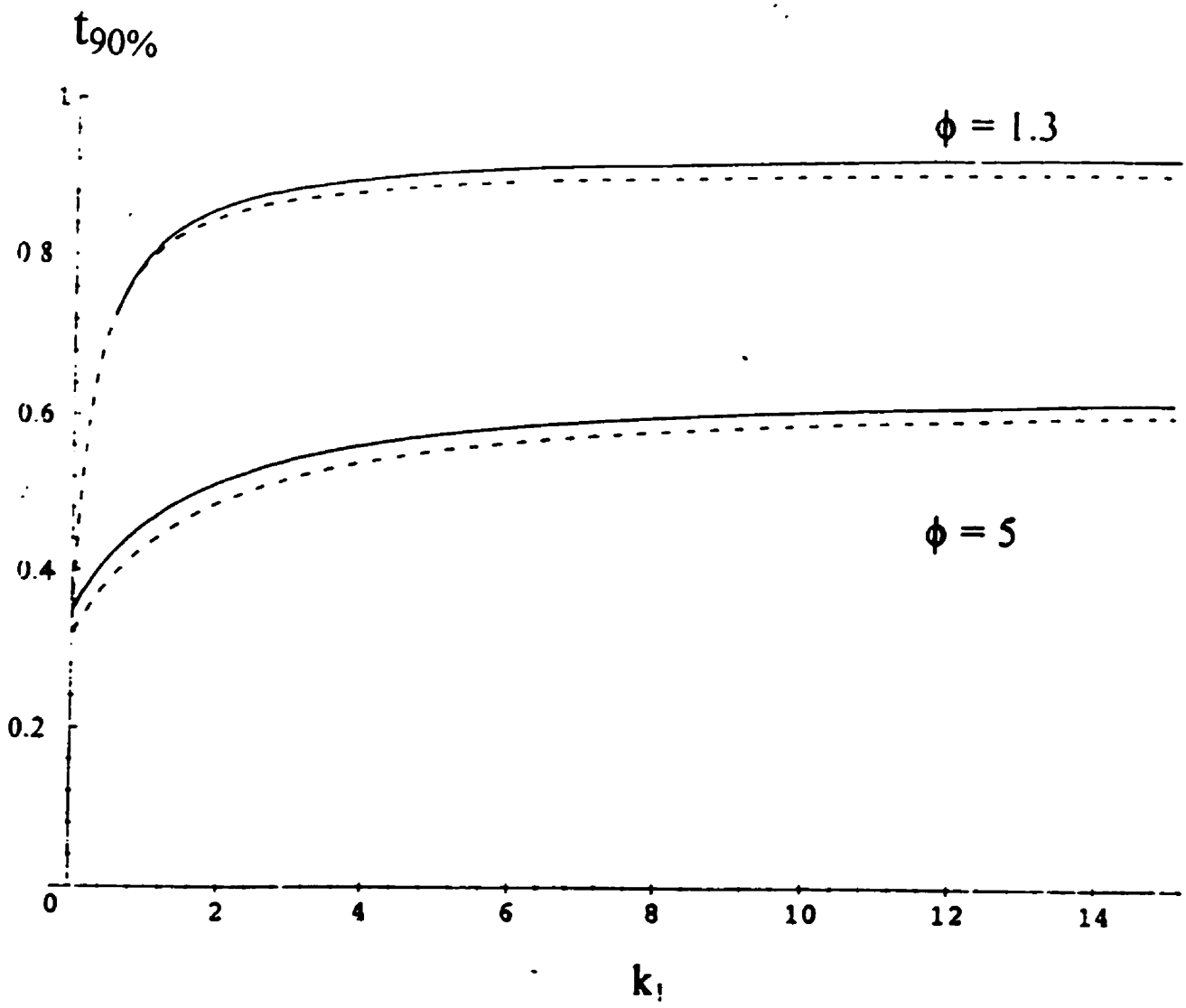

Figure 4-9. Relationship between response time (min) and the parameter for mass transfer at the inside membrane surface, k_1. The solid line is that calculated by use of the exact model (Appendix III, Eq. 12), the dashed line is that calculated by use of the approximation formula (Eq. 1).

Table 4-4 summarizes the range of parameter values possible for VOCs in air and water. Theory predicts boundary effects can be significant for extraction from air or water, especially when compounds have high partition coefficient between membrane and sample, on the basis of the criteria of Eqs 7 and 8 and the parameter values in **Table 4-4**. The outside boundary effect, i.e. k_1', will probably be significant for extraction from air if $K_{ms} > 2000$, and for extraction from water in most cases. One consequence of this characteristic is that if the outside boundary effect is significant the sample flow speed must be constant for system reproducibility. The membrane can be surrounded by a chamber with a stirrer to enable control of sample flow speed. Use of such a mechanism to increase sample flow speed will also shorten response time and minimize trapping time.

Making general conclusions on the properties of the MESI system is not simple because diffusion coefficients of VOCs in polymers can vary by orders of magnitude for one compound in different polymers, or for different compounds in one polymer. For example, at room temperature D for benzene is 0.48×10^{-12} cm^2 s^{-1} in polyvinyl acetate and 1.3×10^{-5} cm^2 s^{-1} in natural rubber; in polyacrylate, D is 6.2×10^{-10} cm^2 s^{-1} for benzene and 1.0×10^{-7} cm^2 s^{-1} for methanol.[32] Diffusion in polymers can also be sensitive to compounds absorbed in the polymer, so extraction rate could vary irreproducibly for samples, such as effluents or biological fluids, containing high concentrations of organic compounds. The diffusion coefficient is assumed constant for the analyte concentration ranges in this study.

The boundary condition at the inside surface is measured by the value of k_l. This parameter can be controlled by variation of the experimental settings, and it varies little with experimental conditions such as temperature. A short membrane and high mobile phase flow rate will reduce k_l. Occasionally experimental settings can be chosen such that boundary effects have a

negligible influence on extraction rate and response time, i.e. k_l' and k_l become negligible. An experimental setup with negligible boundary effects was used to measure D_m. The equation, similar to Eq. (2), was based on extraction from air with a stripping gas flow rate.[42]

Because there were simple relationships between response time and extraction rate and temperature, as an example, the relationships were calculated for benzene (**Figures 4-10 and 4-11**). These calculations used the parameter values determined for this experimental system, and all of their individual relationships with T as described in **Table 4-4.** The variation in response time with T was dominated by the variation in the polymer diffusion coefficient, D_m. The extraction rate variation was dominated by the variation in the value of $K_{ms}D_m$. The overall influence on extraction rate depends on $K_{ms}D_m$. The relationship between temperature and extraction rate has been experimentally observed in **Figure 4-4**.

When designing a MESI system for a new application a membrane with a low value of $\ln\phi/K_{mg}D_m$ is desirable, because this can enable practical calibration by use of Eq. 5, the simplest and most reliable calibration. Membrane types could be compared according to their value of $\ln\phi/ K_{mg}D_m$. Likewise when choosing membrane length and stripping gas flow rate, a value of L/Q that enables calibration by use of Eq. 5 would be ideal. Increasing L/Q increases the response time, but by at most a factor of 2 for aspect ratio $\phi = 2.08$ (Eq. (1)). Increasing the stripping gas flow rate can also increase extraction rate, so a shorter trapping time, and thus a shorter effective response time, would result in the same response. A high stripping gas flow rate results in analyte breakthrough in the sorbent trap, however. Choice of membrane also depends on characteristics such as selectivity, and mechanical or chemical durability. Besides the factors described above, if MESI is applied directly to an effluent stream or biological system rich in organic compounds, significant interference could cause high background noise

or affect, non-reproducibly, the parameters that govern response time and extraction rate. Humic or other materials in a sample could foul a membrane. In that situation, a headspace approach is more suitable.[63]

Table 4-4. The range of parameter values at 300 K and how each varies with T over ambient temperatures in different phases of the MESI system. All symbols are defined in the Glossary

	ν [$cm^2\ s^{-1}$]	D, for VOCs [$cm^2\ s^{-1}$]	K_{ms}, for VOCs [dimensionless]	Other
Air sample:	0.15, $\sim T^{1.8}$ [Ref. 55]	0.05–0.16, $\sim T^{1.8}$ [Ref. 55]	0.1–115000, $\sim e^{-\Delta H/RT}$ [Refs 64, 65] Example values of $\Delta H/R$: 5160 for benzene 4700 for toluene [Ref. 56]	$Nu_o D_s = 0.015 + 0.099(ub)^{1/2}$ to $0.045 + 0.39(ub)^{1/2}$ [g-cm-s]. An analyte at constant mole fraction will vary concentration [ML^{-3}] with $1/T$.
Water sample:	$\nu(T) \cong 0.1083 - 0.000332T$ [Ref. 55]	0.5–1.5 × 10^{-5}, $\sim T/\nu(T)$ [Ref. 55]	0.1–7000, [Refs 64, 66] $\sim e^{-\Delta H/RT}$ or ~1/solubility(T). Example values of $\Delta H/R$, estimated from water solubility tables 525 for benzene [Ref. 70]	$Nu_o D_s = 0.00057(ub)^{1/2}$ to 0.0012 $(ub)^{1/2}$ [g-cm-s] $\sim \nu(T)^{2/3}/T^{6/6}$.
Polymer membrane		10^{-13}–10^{-5}, $\sim e^{-Ed/RT}$ [Refs 67, 35] Example values of E_d/R: 7700 benzene in natural rubber, 2900 toluene in polystyrene , 300 benzene in the membrane used in this study, estimated from measurements reported before [Ref. 35]		D is sensitive to compounds absorbed in the polymer. (PDMS will absorb 720 μg cm^3 water [Ref 68] with D of water = 7×10^{-5} $cm^2\ s^{-1}$ [Ref. 35].) e.g., in poly(vinyl acetate): compared with 1 ppm, 1000 ppm of allyl chloride changes its D 60%; water in polymer greatly accelerates the sorption rate of acetone. [Ref. 35]
Gas mobile phase:	0.1–1.0, $\sim T^{1.8}$ [Ref. 55]	0.022–0.38, $\sim T^{1.8}$ [Refs 55, 67]	Partition coefficients between polymer and any gas are practically the same as between polymer and air [Ref. 49].	At a constant mass flow rate the volumetric flow rate Q will vary with T. (If tank and needle valve are at ambient temp T, and the valve is not adjusted, mass flow rate will not vary significantly with T [Ref. 69].)

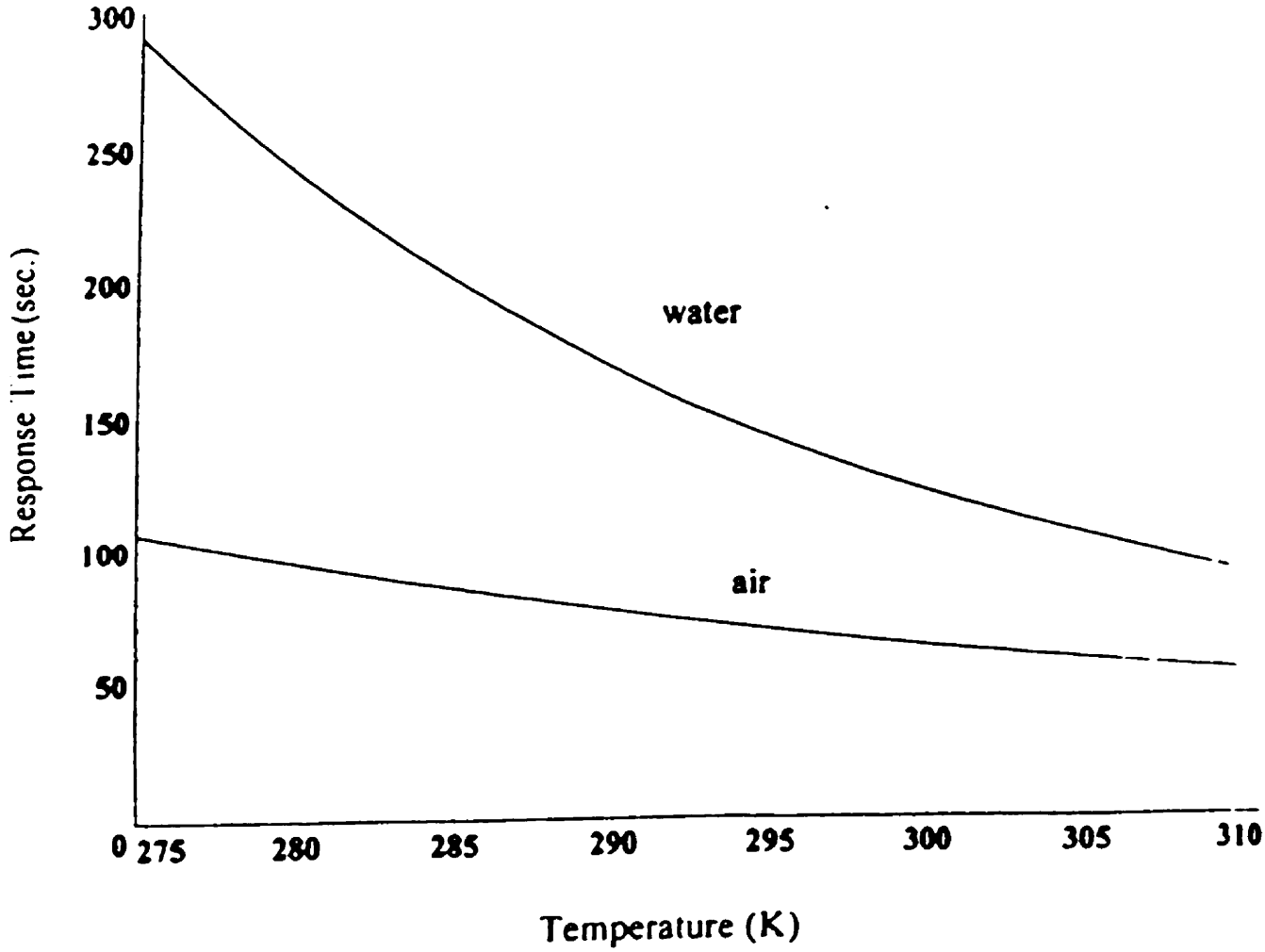

Figure 4-10. Relationship between response time with temperature as calculated by use of the relationship given in **Table 4-4**. For air extraction, $D=T^{1.5}$; for aqueous sample, $D=T/v$, $v \approx 0.1083-0.0000332T$.

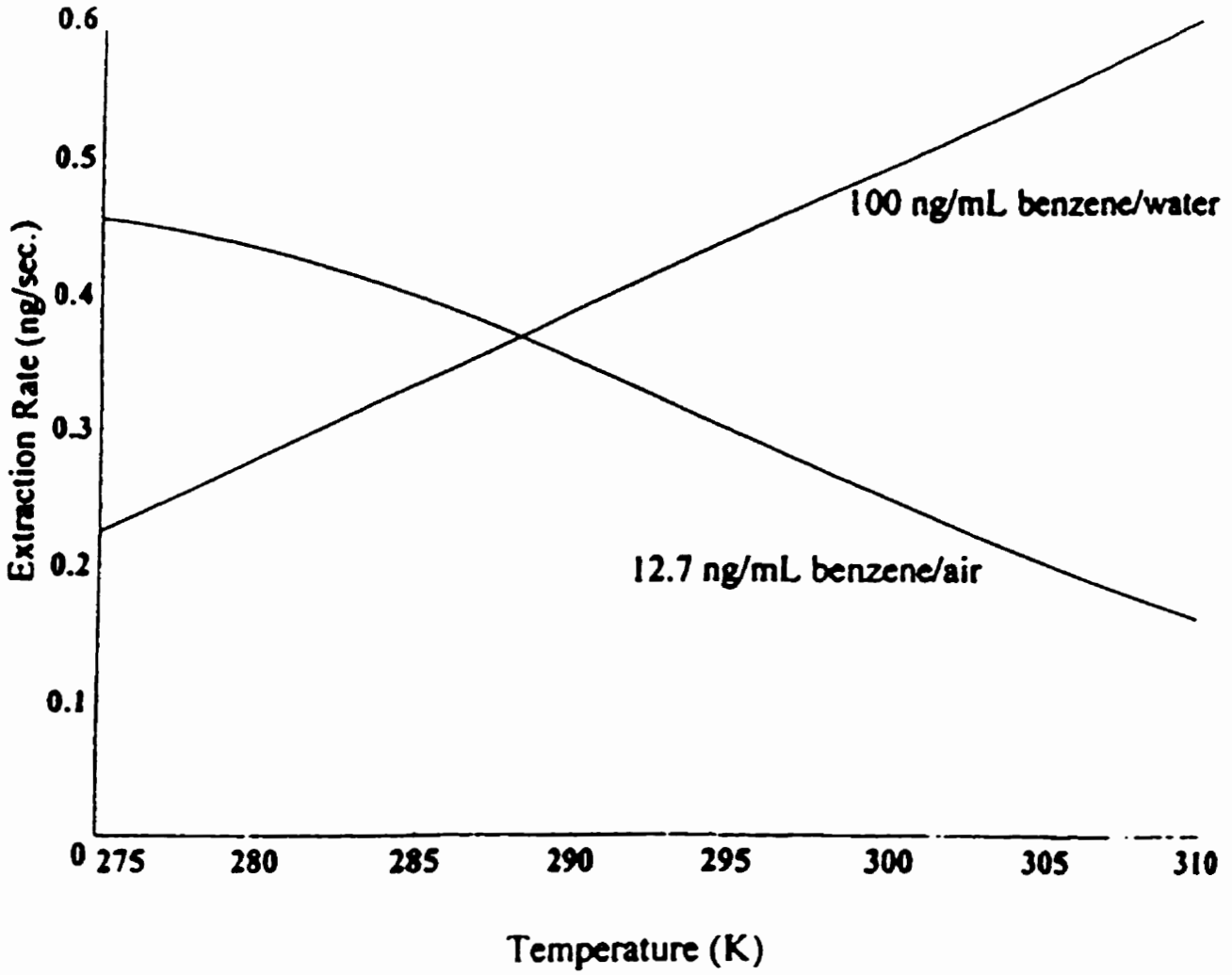

Figure 4-11. Relationship between extraction rate with temperature, as calculated by use of the relationship given in **Table 4-4**. For air sample, $D=T^{1.8}$, $K=c^{-\Delta H/RT}$; for aqueous sample, $D=T/v$, $v=0.1083-0.000332T$.

4.6 Conclusion

A mathematical model has been derived to describe direct membrane extraction of aqueous samples. The boundary layers between the aqueous phase and the membrane, and between the inner membrane surface and the stripping gas were considered. In aqueous sample extraction, reduction of the boundary layer between the sample matrix and the membrane can significantly improve the extraction efficiency. Sample stirring and sample heating were investigated and found to improve extraction efficiency. It was found experimentally that a small headspace could result in more efficient extraction. The extraction rate and response time predicted by use of the model were in good agreement with experimental results. The relationship between membrane thickness and the response time was studied theoretically. This showed that a thinner membrane resulted in a faster response.

CHAPTER 5

CALIBRATION OF MESI FOR AIR ANALYSIS

CHAPTER 5

CALIBRATION OF MESI FOR AIR ANALYSIS

5.1 Basics of Quantitation without Calibration

Calibration is an important issue in MESI analysis. Experimental investigation[75] has shown that external calibration results in high precision and wide linear range. For field application, however, because of the need for rapid, simple, and accurate analysis, traditional calibration methods such as internal and external calibration are not appropriate, and occasionally are not applicable. A new calibration method, which can fulfil the requirements of field analysis, is introduced in this chapter. In MESI analysis, the extraction process dominates the analysis step, and governs the sensitivity and selectivity of the method. In air monitoring, extraction can be regarded as three major processes—analyte partitioning on the membrane outer surface, analyte diffusion through the membrane, and analyte removal by the stripping gas from the membrane inner surface. The amount extracted Z at time t can be expressed as (Appendix II, Eq. 16)

$$Z(t) = AC_s DK_s \{\frac{t}{\theta + a\ln b/a} - \frac{2}{aD}\sum_{n=1}^{\infty}(1 - e^{-D\alpha_n^2 t})\frac{J_0(b\alpha_n)[\theta\alpha_n J_1(a\alpha_n) + J_0(a\alpha_n)}{F(\alpha_n)\alpha_n^2}\}$$

Where $\theta = ADfK_g/Q$

At steady-state extraction, the amount extracted, Z, can be expressed as[42]:

$$Z = \frac{AC_s DKt}{\frac{ADfK}{Q} + a\ln(b/a)} \qquad (1)$$

Where a and b are the inner and outer radius of the membrane, respectively. A is the membrane inner surface area, C_s is the concentration in air, D is the diffusion coefficient in the membrane, f is the ratio of the average concentration of the stripping gas and the concentration of

the stripping gas at the exit of the end of the membrane, K is the membrane/air partition coefficient, Q is the stripping gas flow rate, and t is the trapping time. The other notation is explained in Appendix II.

To express the relationship between the concentration in air, C_s, and other parameters, Eq. 1 can be rearranged to:

$$C_s = \frac{Z}{t}\left(\frac{f}{Q} + \frac{a \ln b/a}{ADK}\right) \qquad (2)$$

In Eq. 2, a, b, A and Q are constant. The trapping time (t) can be experimentally fixed. D and K are constant if the extraction temperature is constant (assuming low sample concentration). K and D values are available in the literature or can be measured on site. Parameter f is a constant when extraction conditions such as stripping gas flow rate and extraction temperature, are constant. Therefore, Eq. 2 can be simplified to:

$$C_s = BZ \qquad (3)$$

Where the constant $B = \frac{1}{t}\left(\frac{f}{Q} + \frac{a \ln(b/a)}{ADK}\right)$, and can easily be calculated. Eq.3 shows that at steady state extraction, the concentration in air is proportional to the amount extracted. In other words, if the amount extracted is known, the concentration in air can be calculated. The amount extracted, Z, can be obtained from the analyte peak area and the FID (flame ionization detector) response factor. Thus no external calibration is required.

5.2 Temperature Effect and Model Evaluation

The above discussion is true if extraction conditions are stable. In some circumstances, however, the conditions are not stable, mainly because of temperature variation. Temperature variation results in changes in the stripping gas flow rate, the size of the membrane probe, and K and D values. The effect on probe size is usually very small and can be ignored. The effect on the

flow rate of the stripping gas can be calculated by use of Gay-Lussac's Law (pressure is constant)[41]:

$$\frac{V_1}{V_2} = \frac{T_1}{T_2} \qquad (4)$$

Where V_1 and V_2 are the volumes at temperature T_1 and T_2 (Kelvin), respectively. The gas volume V is equal to the flow rate, Q, multiplied by the time, t. So, Eq. 4 can be expressed as:

$$\frac{Q_1 t}{Q_2 t} = \frac{Q_1}{Q_2} = \frac{T_1}{T_2} \qquad (5)$$

Where Q_1 and Q_2 are the stripping gas flow rates at temperature T_1 and T_2, respectively. If the temperature change is in the range ±5°C at 25°C, the change in flow rate is only ±1.7%, and is regarded as insignificant.

The effects of temperature on K and D are, however, significant. **Table 5-1** shows how the values of K (membrane/air) and D (in the membrane) for benzene are affected by temperature. Methods for determining K and D have been described elsewhere.[42] It is apparent that when the temperature changes by ±5°C at 30°C, K and D values change significantly, and implies that the effects of temperature on these two parameters should be of concern.

Table 5-1. K and D values at different temperatures.

Temperature (°C)	25	30	35
K	485	358	290
Percentage change in K	35	–	–19
D (10^{-6} cm^2 s^{-1})	2.12	2.39	3.18
Percentage change in D	–11	–	33

To evaluate the effect of changes of these parameters on the calibration, the mathematical model was tested by varying K and D. The change ranges selected were ±2, ±5, and ±10%. **Table**

5-2 lists the results of the calculation. It is apparent from this table that varying the stripping gas flow rate has little impact on the extraction rate, but K, D, and membrane length have a large effect. The impact of membrane length can be avoided by carefully measuring the probe. In general, temperature variations do not cause significant changes in membrane dimensions.

In **Table 5-2**, when a single parameter effect was considered, the effect on extraction was significant when a ±10% change was assumed. However, the percentage change of these parameters was for the theoretical calculation only. For real-case modeling, two important factors should be considered—reasonable values for the change ratio and combination effects. In the above testing, a ±10% change in the stripping gas flow rate was unrealistically large—this would require a 30°C change in the extraction temperature, which would be rare for air extraction. For K and D values, however, a 10% change can be caused by temperature change of ~1°C, which is quite reasonable. When the total effect is assessed for a real situation, a positive or negative contribution of the parameters to the amount extracted should be obtained. In **Table 5-2**, for example, a temperature change has opposite effects on K and D, so when the change in K is positive, that in D is negative (last row of the table). When the total effect was assessed, ±20% variation of K and D values was used; this corresponds to a temperature change of ±3°C. It can be seen that the total effect was not significant. In other words, temperature variation during an extraction will not result in a large calibration error. Experimentally, for a temperature change of ±3°C, variations in the amounts of selected analytes extracted were ±5 ~10%, slightly more than the method precision of RSD 3–6%. A small temperature change does not, therefore, affect the calibration.

Table 5-2. Effect of parameter changes (%) on the extraction rate (%). Parameter variation was based on the values $Q = 2.2$ mL min^{-1}, $L = 4$ cm, $K = 485$, $D = 2.12 \times 10^{-6}$ (cm^2 s^{-1}).

Flow rate Q (mL min^{-1}) (%)	Membrane length L (cm) (%)	Partition coefficient *K* (%)	Diffusion coefficient *D* (%)	Percentage change in extraction rate
±2				±0.91
±5				±1.81
±10				±3.62
	±2			±1.35
	±5			±3.17
	±10			±5.88
		±2		±0.91
		±5		±3.17
		±10		±6.33
			±2	±0.92
			±5	±3.18
			±10	±6.33
±2	±1	∓20	±20	±2.31

In field analysis the temperature can vary from day to day and from place to place. Temperature differences can be several degrees to several tens of degrees in different applications. For example, the temperature in a chimney vent can be greater than 100°C; that in a meat storage room can be below 0°C. In these situations the effect of temperature on the amount extracted is no longer insignificant. **Figure 5-1** shows the chromatogram obtained during continuous monitoring of BTEX during a temperature change from 97°C to 25°C. In the experiment, a 4 cm membrane was used. The flow rate of stripping gas was 2.2 mL L^{-1}. The concentration of BTEX were: benzene: 12.7 μgL^{-1}, toluene 15.2 μgL^{-1}, ethylbenzene 15.7 $\mu gL^{-1}$and o-xylene 12.5 μgL^{-1}.

Obviously, in this case K and D values calculated at room temperature should not be used, because this would cause a large calibration error. K and D values obtained at different temperatures should be used to ensure the calibration is correct.

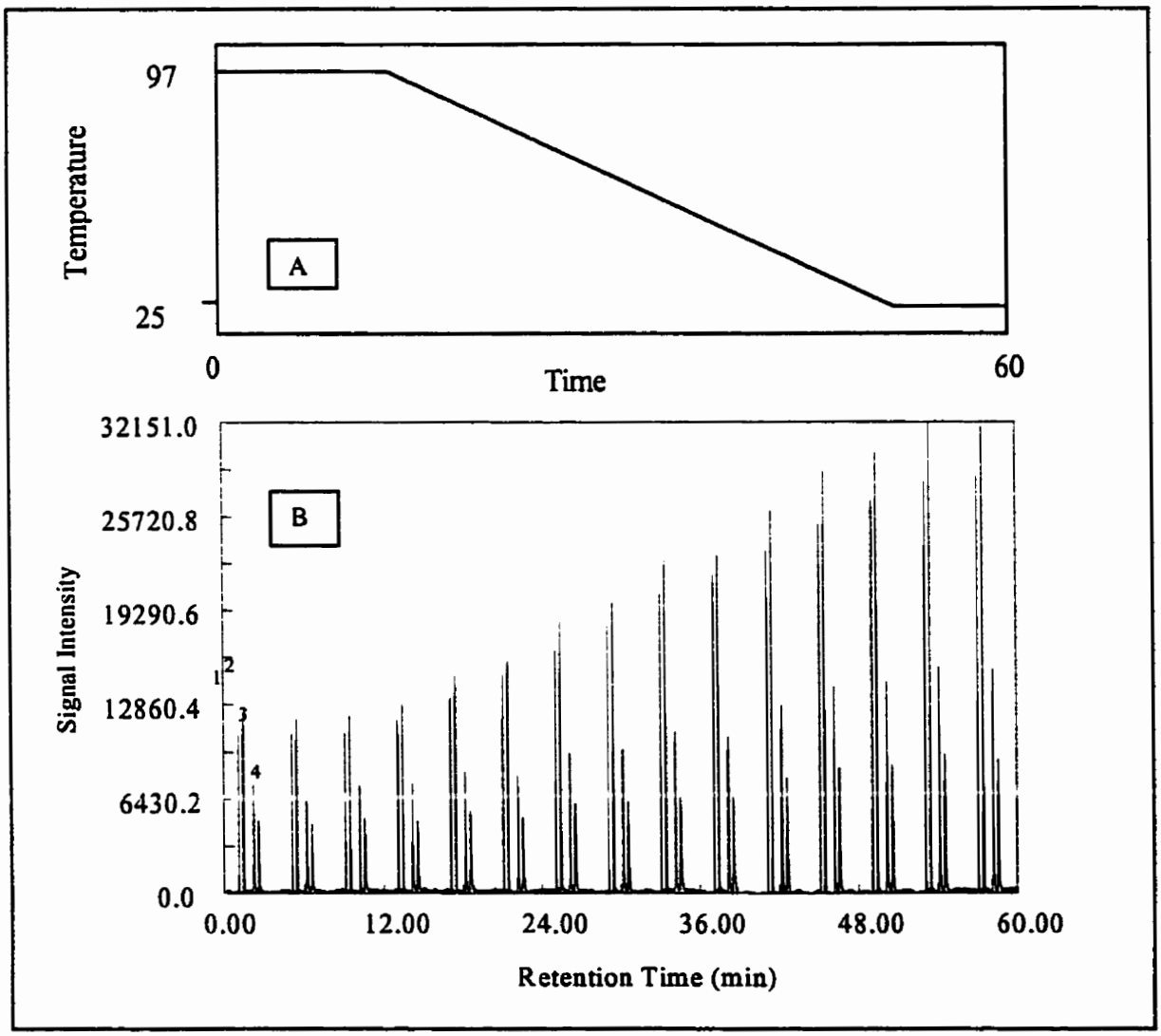

Figure 5-1. (A) Plot of temperature change. (B) Chromatogram obtained for BTEX during a change in the extraction temperature. 1, benzene; 2, toluene; 3, ethylbenzene; 4, *o*-xylene.

5.3. Measurement of Partition Coefficient and Diffusion Coefficient

The partition coefficient K (membrane/air) and diffusion coefficient D values (in the membrane) for analytes at different temperatures can be obtained from the literature or can be measured by methods described elsewhere[42]. There are several ways of measuring the diffusion coefficient of an analyte in the membrane.[31,35,36]

The MESI method can be employed for on-line determination of the K and D values of analytes without external calibration. To measure the K and D values, the PDMS sorbent used in the previous work was replaced by a piece of membrane which was the same material as that used for the membrane probe. The sorbent tube was kept at the same temperature as the membrane probe. No cooling or heating was used for room-temperature extraction. In this example the measured D value corresponds to that at room temperature. In an absorption process, before equilibrium, the amount absorbed by the sorbent increases as the absorption time is extended. The diffusion process can, therefore, be monitored by monitoring the increase in the absorption amount. The amount absorbed by the sorbent can be thermally desorbed into the GC column and then detected. To monitor the amount absorbed with time, a series of absorption times were used. To ensure, initially, a constant concentration in the stripping gas, the membrane probe was left to equilibrate with the sample matrix while the stripping gas did not pass through the sorbent. After a constant concentration had been obtained in the stripping gas, the gas was switched to flow through the sorbent. The heating pulse was then sent to the sorbent at different times, e.g. 10, 20, 30, 40, 50, 60, 80, 100, 120, 150, 180, 200 s... until a constant signal was obtained. A time profile was obtained and is shown in **Figure 5-2**. This time profile can be used to calculate the diffusion coefficient by use of the equation[43] $D = d^2/2t_{½}$, where d is the membrane wall thickness, and $t_{½}$ is the half-time to reach steady-state diffusion. By use of this method, the D values for three

compounds shown in **Figure 5-2** were found to be 2.70 (±0.05), 1.70 (±0.06), and 0.91(0.04) (10^{-6} cm^2 s^{-1}), respectively. These values are relatively close to values determined previously[42]— 2.12 (±0.03), 1.59 (±0.05), and 1.09 (±0.05) (10^{-6} cm^2 s^{-1}), respectively.

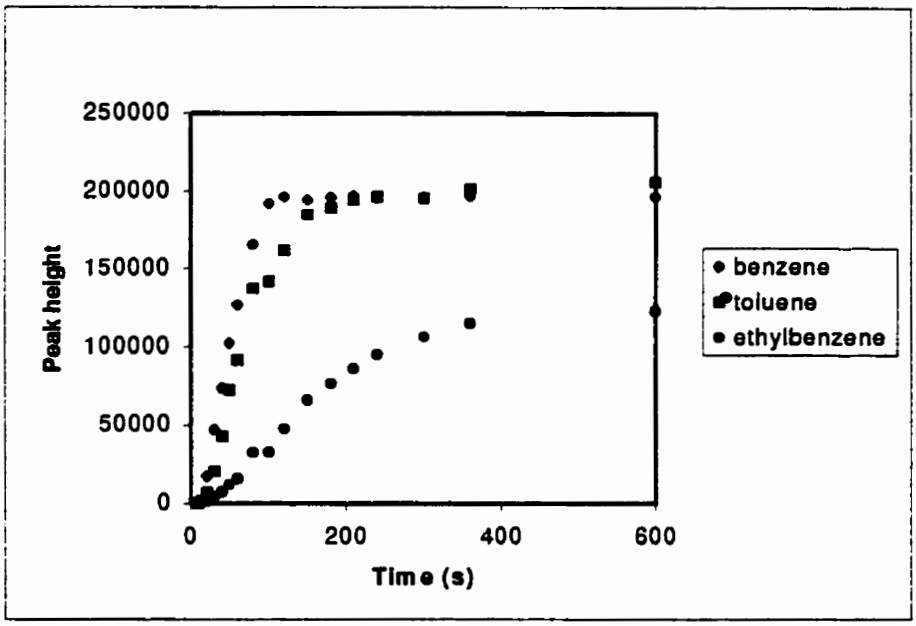

Figure 5-2. Diffusion time profiles for benzene, toluene, and ethylbenzene in the membrane at room temperature (25°C). Membrane length: 4 cm, flow rate of stripping gas: 2.2 mL L^{-1}. Concentration, benzene: 12.7 μgL^{-1}, toluene: 15.2 μgL^{-1}, ethylbenzene: 15.7 μgL^{-1}.

The partition coefficient K is the concentration ratio in two phases at equilibrium; this can be expressed as:

$$K = \frac{C_m}{C_c} \qquad (5)$$

where C_m and C_c are the concentrations in the membrane and the stripping gas, respectively. Eq.5 can be changed to:

$$K = \frac{n_m / V_m}{C_c} \qquad (6)$$

where n_m and V_m are, respectively, the amount absorbed by the membrane sorbent at equilibrium and the sorbent volume. The membrane volume V_m can be obtained by determining the membrane density and weight (by use of a microbalance). The amount absorbed can be determined by desorbing the analyte from the sorbent on to the GC column, and can be expressed as

$$n_m = H_m r_f \qquad (7)$$

where H_m is the peak area (or height) counts and r_f is FID response factor. The analyte concentration C_c can be obtained by trapping analytes from the stripping gas and then determining the amount trapped. The concentration C_c can be expressed as:

$$C_c = \frac{n_c}{v_c} = \frac{n_c}{Qt} \qquad (8)$$

where n_c is the amount of analyte in the stripping gas of volume v_c. Q is the stripping gas flow rate, and t is the trapping time. To determine n_c, the trapping mode of MESI was used. Experimentally, the sorbent interface was cooled to –40°C by use of a 3-stage semiconductive cooler,[19] and the trapping time was 1 min. Like n_m, the amount of analyte in the stripping gas can be expressed as:

$$n_c = H_c r_f \qquad (9)$$

where H_c is the peak area (or height) counts. Combining Eqs 7–9, Eq. 6 can be rewritten as:

$$K = \frac{H_m Qt}{H_c V_m} \qquad (10)$$

Eq. 10 indicates that the value of K can be calculated by use of MESI by measuring the peak area (or height) counts. It can be seen that no additional external calibration is needed for calculation of K. **Figure 5-3A** shows the chromatogram obtained from the analytes after cryofocusing trapping and **Figure 5-3B** is the chromatogram of the same analytes after room-

temperature trapping. The results from the calculation are listed in **Table 5-3**. It can be seen that the approach is in very good agreement with the SPME method.

The determinations of *K* and *D* are only based on the chromatograms of the analytes, and no additional external calibration was used. For unknown analytes, if the *K* and *D* values are obtained the unknown analyte could be identified by comparing these two parameters with literature or other data, because it is rare to find two compounds with the same *K* and *D* values. In other words, the *K* and *D* values might be useful for qualitative analysis, although further investigation is needed. Occasionally, identification is not necessary, because the total amount of a series of homologous compounds is important, such as in the monitoring of total alkanes or alkenes. Each compound's *K* and *D* values can be measured, and an equal detector response factor for all organic compounds is assumed.[79] Calibration can then be performed on the basis of the above discussion.

Table 5-3. *K* values (the values are based on three replicate measurements).Membrane length: 4 cm, flow rate of stripping gas: 2.2 mL L^{-1}. Concentration, benzene: 12.7 μgL^{-1}, toluene: 15.3 μg L^{-1}, ethylbenzene: 8.9 μgL^{-1}.

	Conc. in the stripping gas (peak area counts, average)	Conc. in the membrane (peak area counts , average)	*K* value by this method of measurement	*K* value reported previously[42]
Benzene	10506250	5409609720	514 (± 3)	485
Toluene	358750	623159057	1737(± 5)	1872
Ethylbenzene	123125	391200295	3177 (± 6)	3379

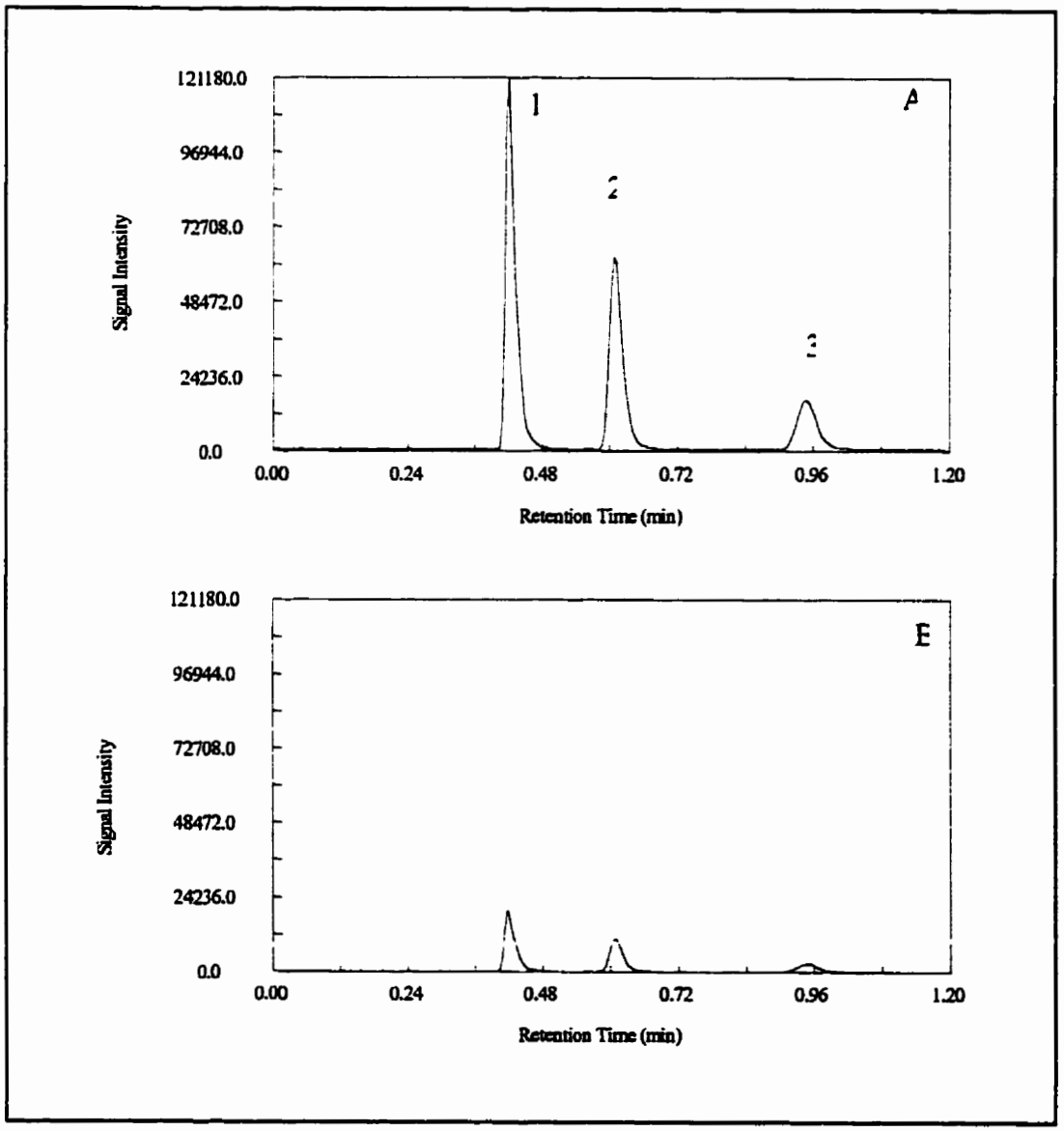

Figure 5-3. Chromatograms obtained for benzene, toluene, and ethylbenzene for measurement of partition coefficients: (A) cryofocusing trapping; (B) room temperature trapping. Membrane length: 4 cm, flow rate of stripping gas: 2.2 mL L^{-1}. Concentration, benzene: 12.7 μg L^{-1}, toluene: 15.2 μg L^{-1}, ethylbenzene: 15.7 μg L^{-1}.

Another way of measuring D is to detect the permeation process of the analyte in the membrane probe. In this method, the MESI setup is modified. The sorbent interface and the GC column are replaced by 20 cm × 0.32 mm i.d. deactivated silica tubing connected directly to the extraction probe and the FID detector. The measurement is based on Eq. 11.[36,47,48.]

$$D = 0.14\, d^2/t_{½} \qquad (11)$$

where d is the membrane wall thickness, $t_{½}$ is the half-time of permeation reaching steady-state. In Eq. 11 the membrane thickness d is known and $t_{½}$ can be obtained by experiment. Thus D can be calculated. It should be pointed out that Eq. 11 is only valid when the concentration of analyte is constant on one side of the membrane and zero on the other side. In this study, the concentration at the outside of the membrane was constant because the membrane was exposed to a continuously flowing gas stream containing a constant concentration of analyte. To make the concentration zero on the inner surface of the membrane a high flow rate must be used. The theory used for the calculation implies that the flow rate must be greater than 25 mL min^{-1} for a 4 cm length of membrane. The $t_{½}$ can be checked experimentally with different flow rates from 1 to 30 mL min^{-1}. It was found that for benzene $t_{½}$ was minimum and remained constant when the flow rate was 25 mL min^{-1}. This flow rate was, therefore, used to measure D for benzene. **Figure 5-4** shows the permeation time profile of benzene. $t_{½}$ was 18 s; by using Eq. 11 the D value for benzene at 25°C was found to be 2.12×10^{-6} cm^2 s^{-1}. Note that for other analytes, the required minimum stripping gas flow rate should be different, because of the different K values.

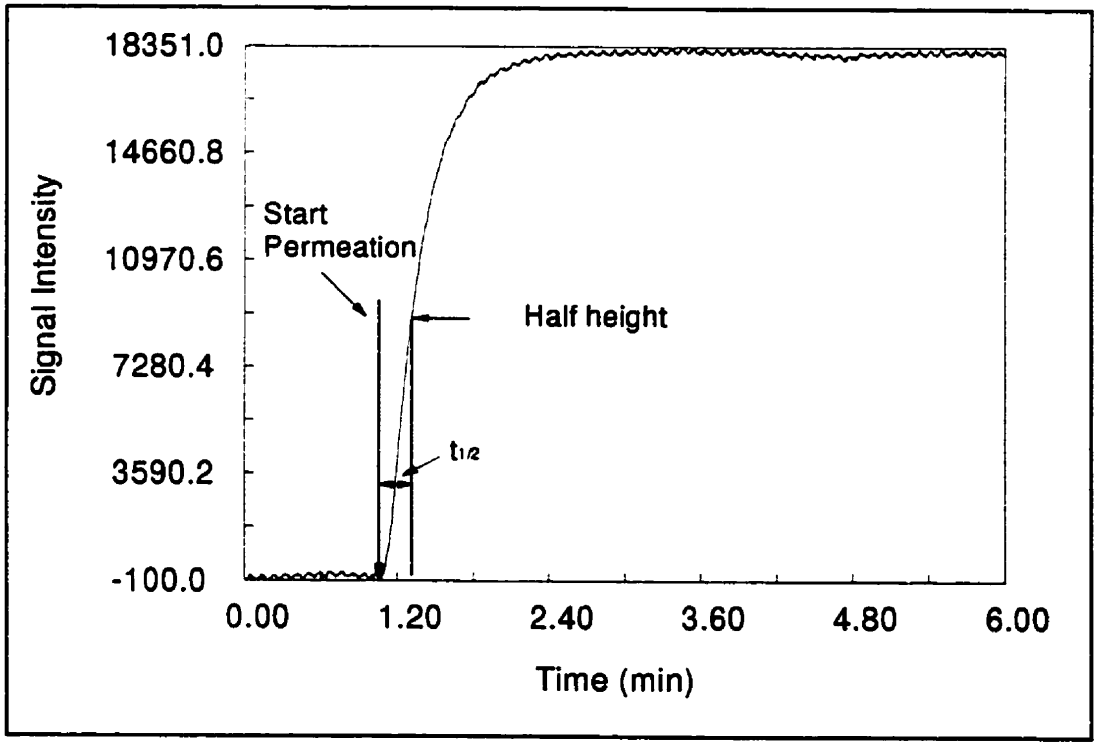

Figure 5-4. Permeation time profile of benzene. Stripping gas flow rate = 25 mL min^{-1}, temperature = 25°C. Membrane length: 4 cm, benzene concentration: 12.7 μgL^{-1}.

Alternatively, SPME can be used to measure *D*. Details of the SPME method are available in the literature.[43–46,49] In the measurement, an SPME–membrane device was used instead of an SPME–fiber assembly. The membrane device was a modification of the fiber assembly. The original SPME fiber assembly was replaced by a length of stainless steel tubing (6 cm long, 18 gauge), and a stainless steel needle (8 cm length 30 gauge) was used to support the membrane, **Figure 5-5** shows the assembly of SPME–membrane sampling device. In the SPME method, the SPME–membrane was exposed to the air sample to extract the analyte. The extraction time was selected as 10, 20, 30, 40, 50, 60, 80, 100, 120, 180, 300, and 600 s. The amount extracted after each time was detected by placing the membrane in the GC injector for thermal desorption then

GC analysis. A constant extraction temperature was maintained during the measurement. **Figure 5-6** shows the extraction time profile obtained by the SPME method

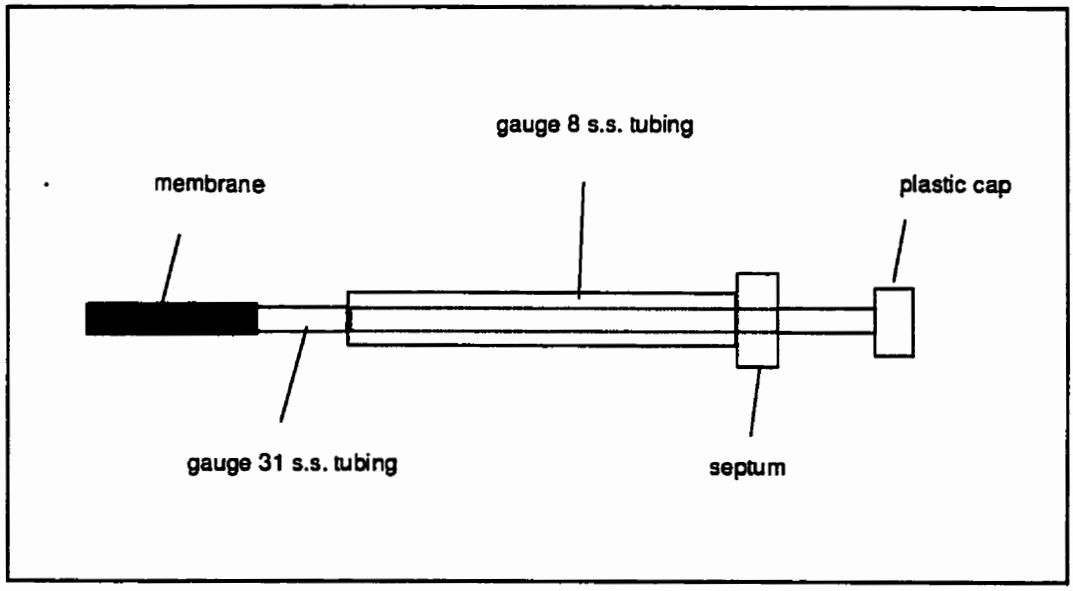

Figure 5-5. The assembly of the SPME–membrane sampling device.

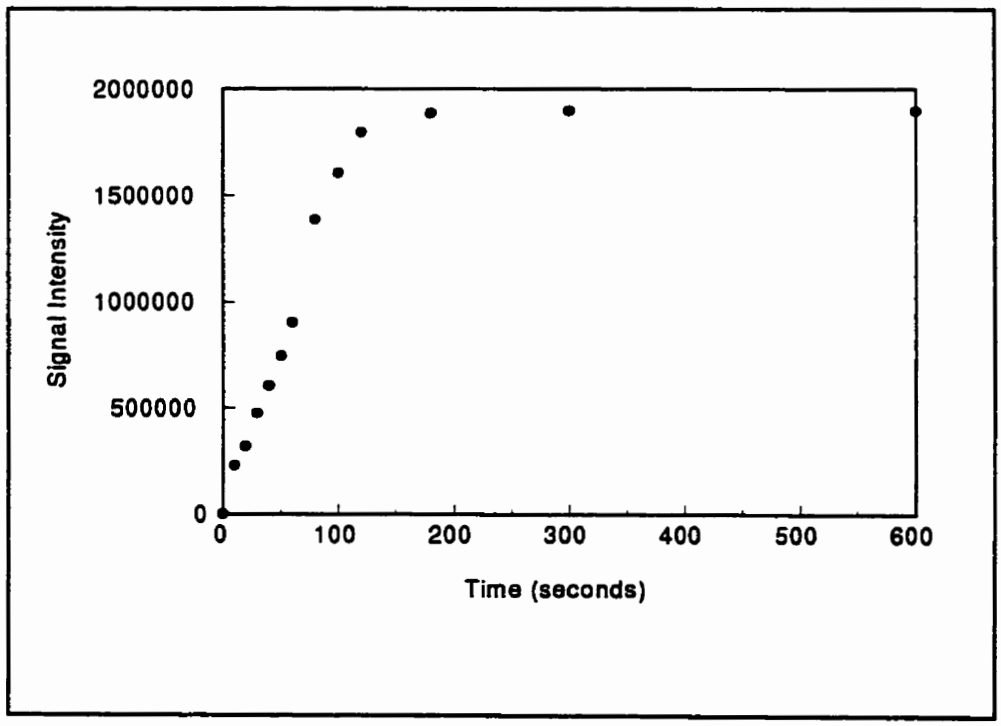

Figure 5-6. Extraction time profile of benzene for benzene/air sample. Extraction temperature 25°C. Benzene concentration: 12.7 μg L^{-1}. Membrane length: 1cm.

This profile depicts the extraction process, hence the diffusion process in the membrane. The D value then can be calculated by use of the appropriate model, in which D is expressed as $D = d^2/2t_{½}$. In **Figure 5-6**, $t_{½}$ is 65 s and the D is 2.09×10^{-6} cm^2 s^{-1}. This value is close those obtained by the techniques depicted in **Figures 5-3** and **5-4**.

Alternatively, the partition coefficients can be measured by the SPME method. In this method, the membrane is exposed to a known gas sample. After the absorption equilibrium has been reached, the membrane is exposed in the GC injector for thermal desorption. The amount absorbed was determined by comparison after calibration by standard syringe injection.

In the SPME method the retention index can be used to calculate the partition coefficients of alkanes and alkenes.[79] The same method can also be used with the SPME–membrane technique to measure the K values of these compounds.

5.4 Agreement

Table 5-4 lists the calibration results obtained for the analysis of a standard gas mixture of benzene, toluene, ethylbenzene, *o*-xylene, hexane, and 1, 1, 1-trichloroethylene. The membrane length was 4 cm and the flow rate of the stripping gas was 2.2 mL L^{-1}. It is apparent that the method is highly accurate.

Table 5-4. Air concentration without external calibration (25°C).

	B	Area counts (average of 5 replicates)	FID response factor (area ng^{-1})	Air concentration (experiment) ($\mu g\ L^{-1}$)	Standard air concentration ($\mu g\ L^{-1}$)
Benzene	0.71	214700000	25618	1.19 ($\pm$ 0.05)	1.25
Toluene	0.58	208500000	301645	1.18 ($\pm$ 0.04)	1.12
Ethylbenzene	0.44	136500000	336972	0.92 ($\pm$ 0.06)	0.94
o-Xylene	0.38	126500000	387630	0.86 ($\pm$ 0.07)	0.88
1,1,1-Trichloroethlyene	0.69	46550000	45385	1.49 ($\pm$ 0.05)	1.58
Hexane	0.65	24850000	22347	1.71 ($\pm$ 0.05)	1.62

5.5 Calibration Based on Membrane Probe Heating

This section describes a method for determining K and D values and estimating air concentrations in a single experiment.

It is known that SPME is a sophisticated method for measurement of K. In SPME, at equilibrium, the concentration in the liquid polymer coating is uniform. In MESI we know that for steady-state extraction there is a constant concentration gradient in the membrane (Chapter 3). If the difference between the amounts absorbed by the SPME–membrane and MESI–membrane techniques can be determined, K can be calculated. In MESI–GC the amount absorbed can be obtained by thermal desorption of the membrane probe. To perform membrane heating the membrane probe is wrapped with a heating coil, which can be the same coil used in the sorbent interface. During membrane heating, however, the absorbed analyte cannot be completely

desorbed into the stripping gas, some analytes return to the air stream, so only a fraction can be detected. Experimental examination showed that the amount desorbed into the stripping gas was constant if the extraction and desorption conditions were constant. Thus determination of the difference between the amounts absorbed by the SPME–membrane and MESI–membrane techniques is equivalent to determination of the difference between the amount absorbed by the SPME–membrane technique and the fraction of the amount adsorbed which is desorbed by the MESI–membrane technique.

To obtain the fraction of the amount adsorbed by the MESI–membrane technique which is subsequently desorbed, pulse heating is applied to the membrane probe after steady-state permeation. **Figure 5-7** shows a chromatogram obtained for benzene by membrane pulse heating. The two highest peaks, 1 and 2, correspond to two heating pulses, hence thermal desorption from the membrane. The two peaks are the same height, which means that a constant amount was desorbed. The fraction desorbed into the stripping gas is represented by the difference between the intensity of peak 1 (or peak 2) and the average intensity of the peak obtained at steady-state, which aligns with curve a. Curve a is a smooth plot of each peak height from non-steady-state to steady-state.

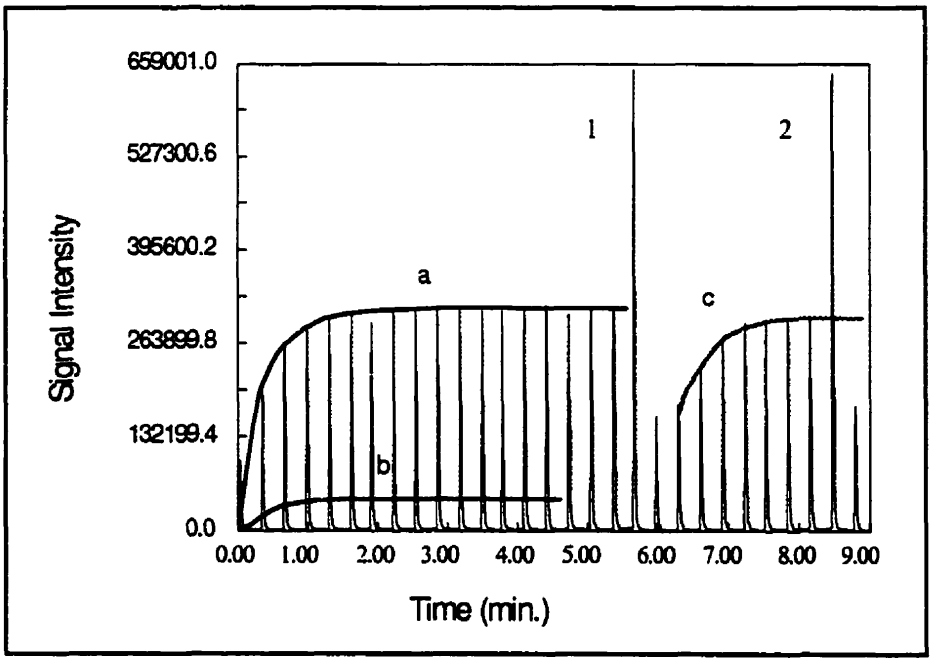

Figure 5-7. Chromatogram of Benzene in probe pulse heating. Concentration 12.7 μg L^{-1}; membrane probe length: 4 cm; flow rate of stripping gas: 2.2 mL min^{-1}; extraction temperature: 25°C; pulse voltage on the membrane probe and sorbent interface: 38.6 V; pulse width: 1 s; trapping temperature at sorbent interface: - 40 °C; trapping time: 40 s.

To obtain the amount absorbed by SPME, an SPME–membrane device was exposed in the same extraction chamber to extract analyte; this analyte was then desorbed into the injector of the same GC for analysis. Because the same extraction and GC conditions were used, the results are comparable. **Table 5-5** lists the *K* values measured by experiments at different temperatures. This table verifies that when the amount of electrical heating pulse was fixed, the percentage desorbed from the membrane to the stripping gas was constant. The amount desorbed by MESI was approximately 38% of the amount absorbed by SPME. After use of an adjustment factor of 38%, for the difference between the peak 1 (or 2) and the peaks at steady state,the *K* values determined by MESI are close to those obtained by SPME.

Table 5-5. *K* value measurement and adjustment (benzene).

Temperature (°C)	23	25	30	35	40
K Value by SPME method [1]	550	485	358	290	242
K Value by membrane heating pulse in monitoring (before adjustment) [2]	208	183	139	112	94
Difference before adjustment (%)	37.8	37.7	38.8	38.6	38.8
K Value after adjustment (adjust ratio = 38%)	547	481	365	294	247

(1) reference 42

(2) experimental conditions: refer Fig. 5-4

In MESI, because the analytes which penetrated the membrane cannot immediately arrive at the detector, the permeation process in the membrane cannot be detected instantly. Sorbent trapping is the major reason for the delayed detection of the penetrated analytes. For example, 40 s trapping results in 40 s delay. In **Figure 5-7**, curve b is a permeation time profile of benzene. The curve was obtained by use of the method, discussed in Section 5.3, for measuring *D* by use of Eq 11. Curve b indicates more closely the permeation process of benzene in the membrane. Because a high flow rate of stripping gas and no sorbent trap were included, the analytes were quickly transported to the detector by the stripping gas after membrane permeation. Compare curves a and b; $t_{½}$ is larger for curve a. The membrane permeation processes are, however, similar in both measurements, therefore *D* is the same. The difference between the $t_{½}$ values for curves a and b can be found experimentally. On the basis of this difference *D* can be measured by using curve a.

In Eq. 11 the constant 0.14 is valid for a high stripping gas flow rate without trapping. At a low flow rate with trapping, to get the same D value (because D is not changed) the 0.14 value must be adjusted because $t_{½}$ has changed. The adjustment factor can be obtained by comparing $t_{½}$ for curves a and b. Experimentally, the adjustment factor was obtained by measuring $t_{½}$ at different temperatures, **Table 5-6** lists the results. The adjustment factor 0.42 was obtained from the comparisons. From this table it is apparent that when extraction and GC conditions are constant D for benzene can be estimated from curve a.

Table 5-6. D value measurement and adjustment (benzene). Concentration 12.7 μg L^{-1}; membrane probe length 4 cm; flow rate of stripping gas 2.2 mL min^{-1}, extraction temperature 25°C.

Temperature (°C)	2	25	30	35
$t_{½}$ (s)	0	18	16	12
D (10^{-6} cm^2 s^{-1}) = $0.14d^2/t_{½}$	.91	2.12	2.39	3.18
$t_{½}'$ (s)	9	55	50	35
D' (10^{-6} cm^2 s^{-1}) = $0.42\ d^2/t_{½}$	.94	2.08	2.29	3.27

Note: $t_{½}$ and D were obtained with no trapping and at a high flow rate (25 mL min^{-1}); $t_{½}'$ and D' were obtained with sorbent trapping and at a low flow rate (2.2 mL min^{-1}) (refer fig. 5-4)

An alternative method for estimation of D is based on membrane pulse heating under conditions of steady-state permeation. In **Figure 5-7** curve a and curve c are similar, (curve c is

the smooth line of the peak heights after second pulse heating) they overlap each other if the two curves are moved together. This is easily understood. A certain amount of benzene in the membrane was desorbed during the pulse heating (peak 1). As the extraction conditions were restored after desorption, the same concentration gradient was formed in the membrane. The permeation followed the same evolution as in the initial extraction from the non-steady-state to the steady-state. In the experiment, the pulse heating required to heat the membrane to 263°C was approximately 1 s; approximately 30 s was required for cooling to room temperature. **Figure 2-8** shows the profile of membrane temperature against time. For 40-s trapping the first peak after peak 1 was not counted, because during this time the membrane temperature was decreasing, and this causes the D value to change. The permeation curve was counted from the second peak after the heating pulse. In these circumstances the D value can be calculated in the same way as in the method based on curve a. It is clear that this method for measurement of D is easy to handle, because it is not necessary to measure the exposure time of the membrane probe to the air.

The K and D values for benzene can be obtained from the chromatogram shown in **Figure 5-7**. Under conditions of steady-state permeation, the peak area or height count can be used to calculate the amount extracted by use of the FID response factor. Then the concentration in air can be calculated by use of Eq. 3. In practice, the equation and the adjustment factors can be stored in a computer in advance. A calculation program can be developed for frequent reporting of the results of air analysis. **Table 5-7** shows the results obtained for air concentration measurements by the external calibration method and by the membrane probe heating method. It is apparent there is a good agreement between the two methods and the estimate of the air concentration is close to the real value.

Table 5-7. Comparisons of benzene concentrations in air by the external calibration and membrane probe heating methods. Extraction temperature 25°C; membrane length 4 cm; flow rate of stripping gas 2.2 mL min^{-1}.

Actual air concentration ($\mu g\ L^{-1}$)	External calibration ($\mu g\ L^{-1}$)	Membrane probe heating ($\mu g\ L^{-1}$)
0.12	0.13 (± 0.03)	0.10 (± 0.04)
0.53	0.55 (± 0.02)	0.62 (± 0.02)
0.91	0.85 (± 0.03)	0.75 (± 0.06)
1.24	1.31 (± 0.03)	1.11 (± 0.06)
5.31	5.17 (± 0.05)	4.84 (± 0.07)
8.25	7.97 (± 0.05)	9.05 (± 0.05)
11.7	11.4 (± 0.6)	12.9 (± 0.9)

5.6 Conclusion

Quantitation without external calibration was investigated for air extraction. The method was based on the derived mathematical model, and a relatively good accuracy and precision were obtained. The effect of temperature on the calibration was discussed and it was found that K and D were the most important properties affected by temperature changes. Several methods for measurement of K and D value were introduced and compared. The membrane probe heating method had the advantages of simplicity, relatively high accuracy and precision, and suitability for on-site measurement of K and D.

CHAPTER 6

QUANTITATION

CHAPTER 6

QUANTITATION

6.1 The Basics of Quantitation in MESI

Extraction in MESI comprises two processes—non-steady-state and steady-state. **Figure 6-1** illustrates these processes for benzene/air sample extraction. This extraction time profile corresponds to the conditions of constant air sample concentration and temperature during the extraction. The extraction rate at steady-state can be expressed as (Chapter 3, Eq. 5):

$$G_{ss} = AC_s DK_s \frac{1}{\theta + a \ln b/a} \qquad (1)$$

Where A is the membrane inner surface area, C_s is the sample concentration, D is the diffusion coefficient in the membrane, K_s is the distribution constant for membrane/sample, $\theta = ADK_s / Q$, and Q is the stripping gas flow rate. It is apparent that when the extraction conditions, including temperature, mixing, and stripping gas flow rate are fixed, Eq. 1 can be simplified to:

$$G_{ss} = kC_s \qquad (2)$$

where $k = ADK_s \frac{1}{\theta + a \ln b/a}$. Under steady-state conditions, therefore, the extraction rate is proportional to sample concentration. This is fundamental to quantitation under steady-state extraction conditions.

At non-steady-state, the extraction rate $G(t)$ can be expressed as:

$$G(t) = kC_s - \sum g(t) \qquad (t = 1...\infty) \qquad (3)$$

where $\sum g(t)$ is a function of time. Eq. 3 implies that for non-steady state extraction, the extraction rate is not proportional to sample concentration. In similar time periods, however, the

range of change of extraction rates is the same; the amount extracted in this time period is, therefore, proportional to sample concentration. This is the basis of quantitation by external calibration under non-steady-state extraction conditions.

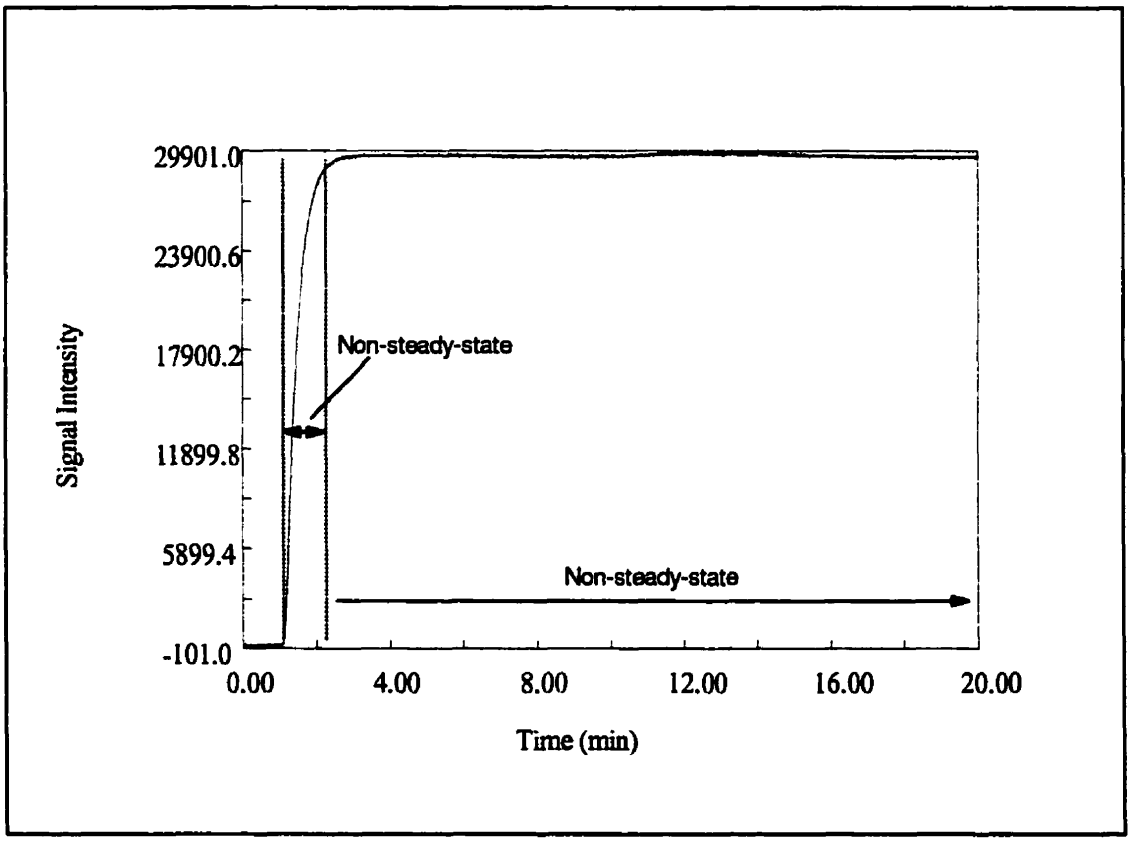

Figure 6-1. Permeation time profile for benzene/air. Benzene concentration: 12.7 μg L^{-1} Membrane length: 4cm; flow rate of stripping gas: 2.2 mL min^{-1}; extraction temperature: 25 °C.

It was seen that in an extraction process, if the sample concentration changed, the extraction rate also changed. The reason for changing sample concentrations is mainly the dynamic nature of the extraction process of MESI. In this process, analyte is removed continuously from the sample by the membrane probe. If the sample volume is not sufficiently large, the concentration can be rapidly depleted, and this depletion results in a change in the rate

of extraction, and hence a change in the amount extracted. **Figure 6-2** shows the extraction time profile for benzene/water sample in a 40-mL vial with 1500 rpm stirring. The profile was obtained by directly connecting the membrane probe to the FID detector via a piece of silica tubing. It is apparent that the extraction processes changes from non-steady-state (rate increase), to steady-state (constant rate) and again to non-steady-state (rate decrease). In MESI, the conditions for quantitation include constant mixing, temperature, pressure, stripping gas flow rate, extraction time, and GC conditions. If one of the conditions changes, then the amount extracted changes. Consistent experimental conditions are, therefore, required.

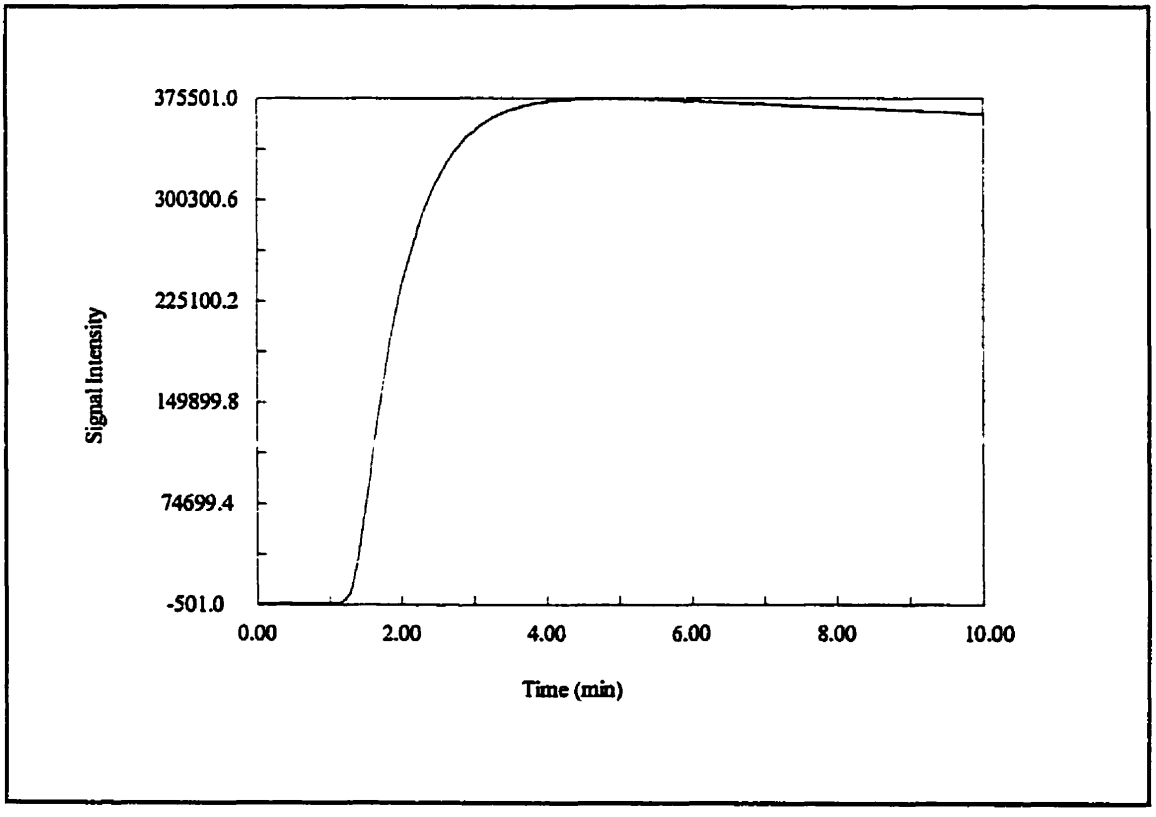

Figure 6-2. Permeation time profile for benzene/water. Concentration 200 ppb; sample size 40 mL; membrane length: 4cm; extraction temperature 25 °C; the sample was stirred at 1500 rpm.

6.2 Quantitation Based on Non-steady-state Extraction

In this extraction process, the extraction rates vary with time. Initially, the extraction rate is 0 at the moment the membrane is exposed to the sample. Then, the extraction rate increases with extraction time. Because the rate of extraction varies with time during the extraction process, if the extraction time-range is not consistent, the amount extracted will be different. For example, for ethylbenzene/air extraction, when the extraction time-range was changed from 0-60 s to 10-70 s, although the extraction time was the same, 60 s, the difference between the amounts extracted was 23.3%. **Table 6-1** shows how the amount of BTEX extracted from air varies when different initial extraction times are used. It is clear that control of the initial extraction time is critical, because the initial extraction time decides the position of the time slot. When the initial time was strictly controlled, good precision was obtained. **Figure 6-3** shows the calibration curve for MESI extraction of BTEX from an aqueous sample, in which the extraction was started 20 s after exposure of the membrane to the sample. A wide concentration range was obtained from 1 to 5000 ppb with square regression of 0.9958-0.9990; the RSD for each testing point was less than 7% (3 replicates).

Table 6-1. Effect of initial extraction time on the amount of BTEX extracted from air. The data shown are ratios (%) of the amounts extracted (average of three replicates) under non-steady-state and steady-state conditions. Trapping time was 1 min.

Initial time delay (s)	Benzene	Toluene	Ethylbenzene	*o*-Xylene
10	–33.4	–51.9	–66.7	–72.1
20	–21.3	–43.1	–58.2	–67.7
30	–14.6	–33.2	–49.2	–55.0

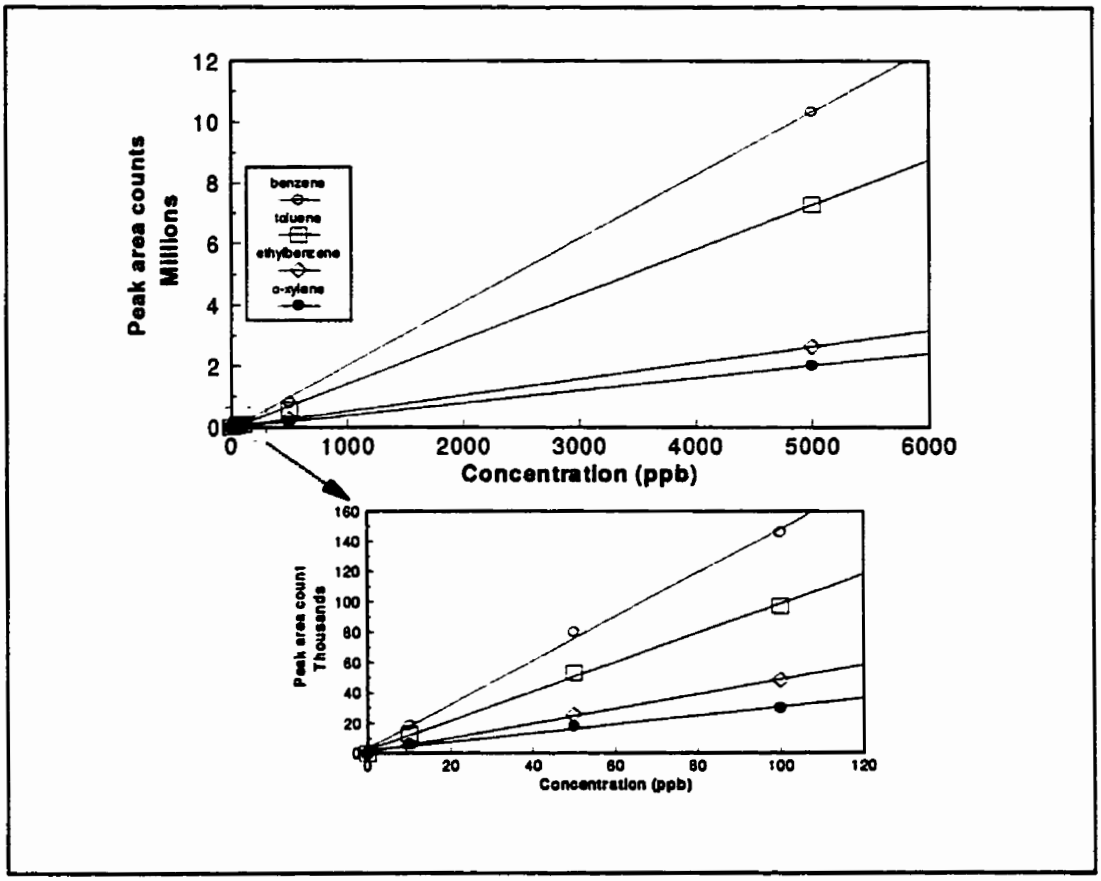

Figure 6-3. Calibration curve for non-steady-state extraction of BTEX from water.

Usually ensuring a consistent initial extraction time is difficult. Variation as a result of inconsistent initial extraction times can, however, be reduced by extending the trapping time. This is illustrated by the results in **Table 6-2**. It is apparent that short extraction times lead to greater variance and that longer extraction times result in insignificant differences between the amounts extracted. To achieve good reproducibility, therefore, a relatively long extraction time is preferred. Occasionally, such as in real time monitoring, or when the analyte has a small diffusion coefficient in the membrane (which results in a long non-steady-state time), quantitation is better under non-steady-state conditions, which enable rapid monitoring or

analysis. Quantitation based on non-steady-state extraction is rapid, but sensitivity is low, because extraction rates are low.

Table 6-2. Effect of trapping time on the amount extracted. The data show differences (%) between the amounts extracted (average of three replicates) after initial time delays and after no delay.

	Benzene difference	Toluene difference	Ethylbenzene	*o*-Xylene
Trapping 1 min				
Time delay (s)				
10	15.9	14.8	23.3	31.3
20	42.9	35.9	61.7	68.7
30	53.1	59.46	98.3	134.7
Trapping 4 min.				
Time delay (s)				
10	0.5	1	2.3	2.9
20	0.8	1.6	5.8	7.3
30	4.9	4.1	7.8	9.2

6.3 Quantitation Based on Steady-state Extraction

Quantitative analysis based on steady-state extraction is more convenient than that based on non-steady-state extraction, because accurate control of the initial trapping time is not required. Obviously, the sensitivity of this method is good because the extraction rate reaches its highest level; reproducibility also is good, because the extraction rates are constant. **Table 6-3**

shows the precision of the extraction of benzene from air under steady-state conditions, and **Figure 6-4** shows the calibration curves obtained for extraction of BTEX from an aqueous sample. A wide linear concentration range was obtained. The square regression for each curve ranged from 0.9989 to 0.9995, and the RSD of each testing point was <3% (3 replicates). Apparently, under steady-state conditions also longer extraction times are needed to ensure reproducible extraction. This condition is easy to satisfy for large sample volumes, such as indoor air, rivers, and lakes. For small sample volumes, however, (e.g. the conditions used to produce **Figure 6-2**) the duration of steady-state extraction is too short—less than 2 min. In analysis it is not easy to exploit such a short duration. Of course, 2-min duration of the steady-state is not a large problem for short-term extraction, 0.5 min for example. If, however, the sample volume is smaller, the duration of steady-state extraction decreases—or might not even exist. In these circumstances this approach is useless, in particular because uncertainty of the initial extraction time is significant. Another possible drawback of this approach is low work efficiency. This is attributed to some analytes having low diffusion coefficients in the membrane; this leads to a long non-steady-state process before the steady-state.

Table 6-3. Reproducibility of extraction of benzene from air under steady-state conditions. RSD% was obtained from three replicate analyses.

Flow rate (mL min^{-1})	RSD %			
	Benzene	Toluene	Ethylbenzene	*o*-Xylene
1.56	2.3	1.1	2.1	2.6
3.2	0.7	0.6	0.6	0.7
4	0.6	0.7	0.6	0.3

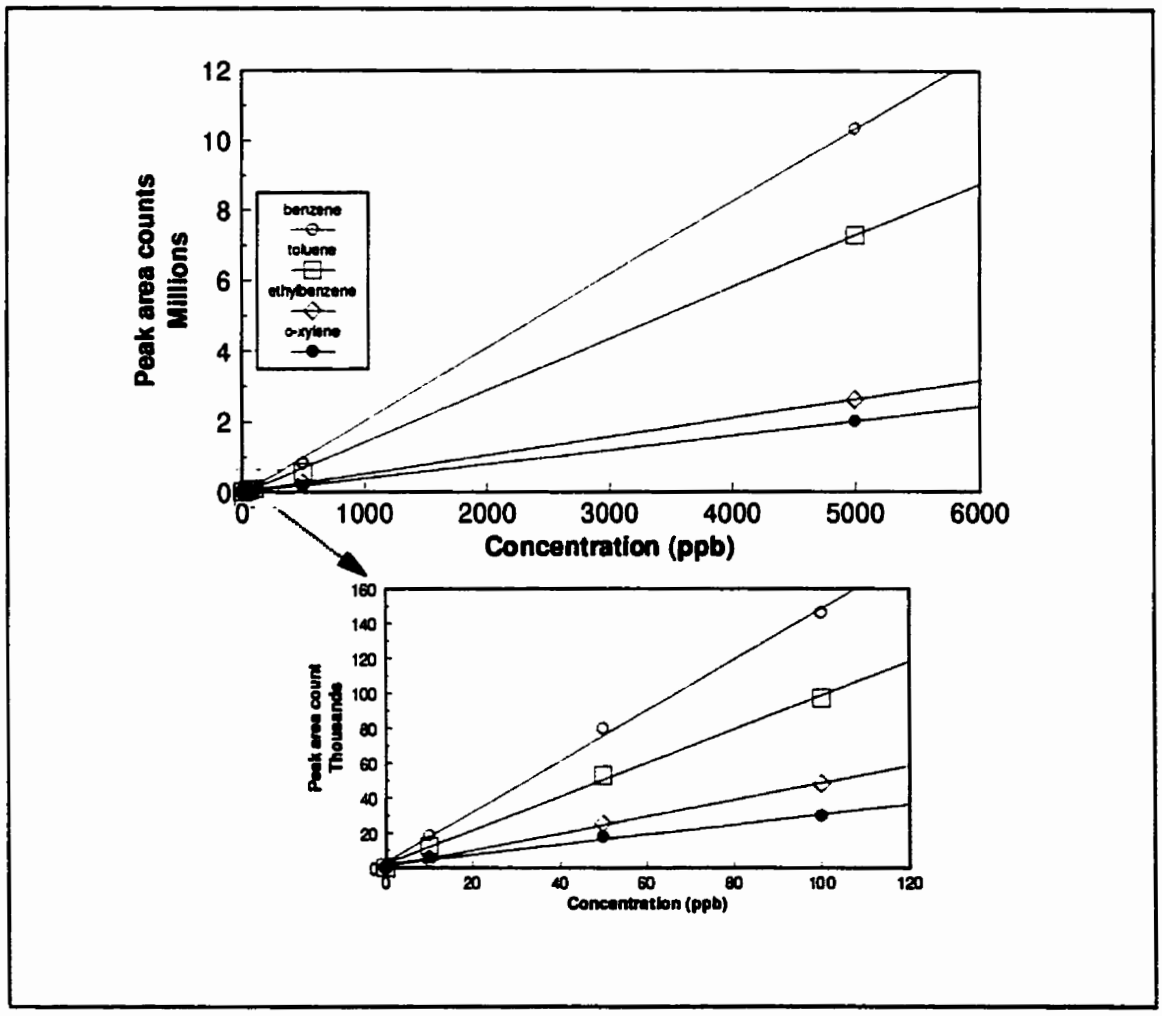

Figure 6-4. Calibration curve for steady-state extraction of benzene from water. Membrane length: 4cm; extraction temperature: 25 °C; sample stirring at 1200rpm; flow rate of stripping gas: 2.2 mL min^{-1}; trapping time: 1 minute.

To extend the duration of steady-state extraction, large sample volumes should be used. If a large sample volume is not available or is inconvenient, static conditions or a low stirring speed can be used for the extraction. **Figure 6-5** shows the extraction time profile of benzene/water for

static extraction; the duration of steady-state extraction was longer, but the sensitivity was very low, because of low mass transport of analyte from the sample to the membrane.

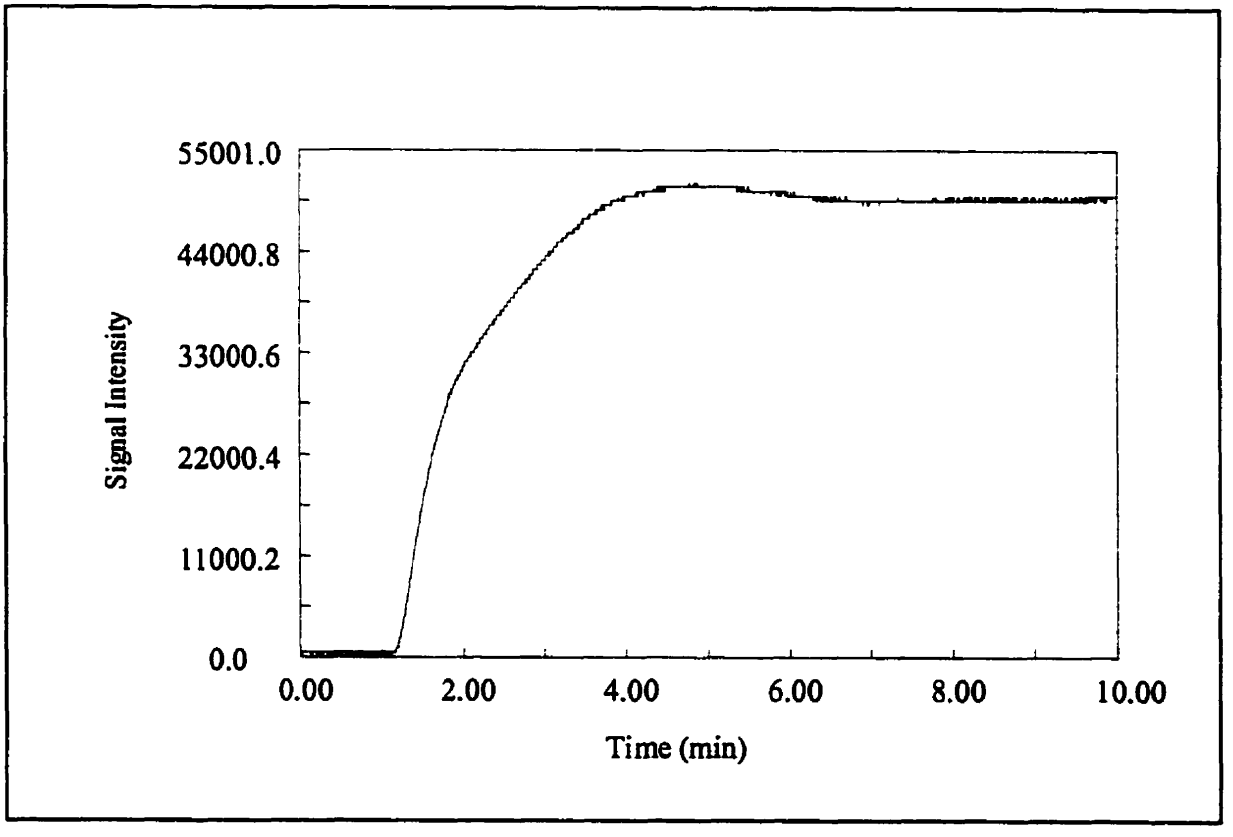

Figure 6-5. Extraction time profile for extraction of benzene from water under static conditions. Benzene concentration: 200 ppb; membrane length: 4cm; flow rate of stripping gas: 2.2 mL min^{-1}; extraction temperature: 25 °C.

A short non-steady-state time is desirable for the purpose of work efficiency in this approach. We have previously shown[42] that several methods can be used to obtain a short non-steady-state time; these include increasing the stripping gas flow rate, good mixing, use of thinner-wall membranes, and higher extraction temperature. When the stripping gas flow rate reaches a certain level, a further increase cannot significantly shorten the non-steady-state time.

The extraction rate can, however, be increased substantially. **Figure 6-6** illustrates the effect of stripping gas flow rate on non-steady-state time and extraction rate of benzene. Note that the high flow rate should correspond to a short trapping time because of breakthrough. Increasing the extraction temperature is good for aqueous analysis, but not suitable for air extraction because the extraction efficiency is reduced by increasing the temperature. Membranes with thinner walls have the advantages of short non-steady-state time and a small amount absorbed in the membrane probe.

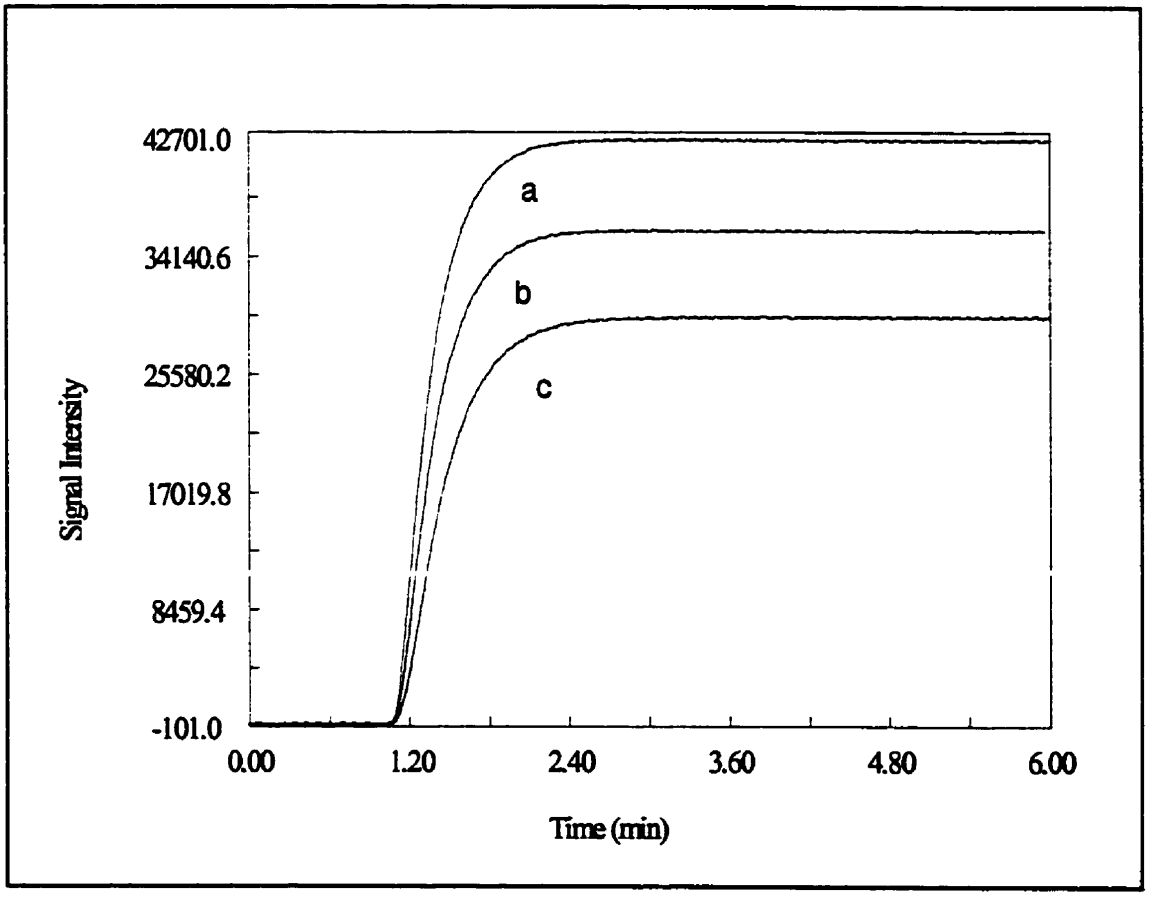

Figure 6-6. Effect of stripping gas flow rate on non-steady-state time and extraction rate (a) 6.4 mL min^{-1}, (b). 4.4 mL min^{-1}, (c). 2.2 mL min^{-1}. Benzene concentration (in air)12.7 μg L^{-1}; extraction temperature: 25 °C

6.4 Quantitation Based on Non-steady-state and Steady-state Extraction

Occasionally, when small-volume samples of low concentration are available, the steady-state extraction process is too short to be captured and short extraction times under non-steady-state cannot reach the detection limit. In these circumstances a longer extraction time is preferred. Obviously, this longer extraction time encompasses non-steady-state and steady-state processes. **Figure 6-7** shows the linear relationship between extraction time and amount extracted in the time range 30 s to 20 min. In the experiment, the membrane length was 4 cm. Concentration for BTEX was 200 ppb. The sample was stirred by magnetic stirring at 1200 rpm. The extraction temperature was 25 °C. Obviously, a longer extraction time leads to extraction of a large amount, hence high sensitivity. Because of the longer extraction time, variation of the initial trapping time is not significant. For example, when the trapping time was 10 min and the variation of the initial trapping time was approximately 10 s, variations in the amount extracted were below 1%. The limitation of longer trapping times is breakthrough. This shortcoming can be overcome by use of a lower trapping temperature or more sorbent.

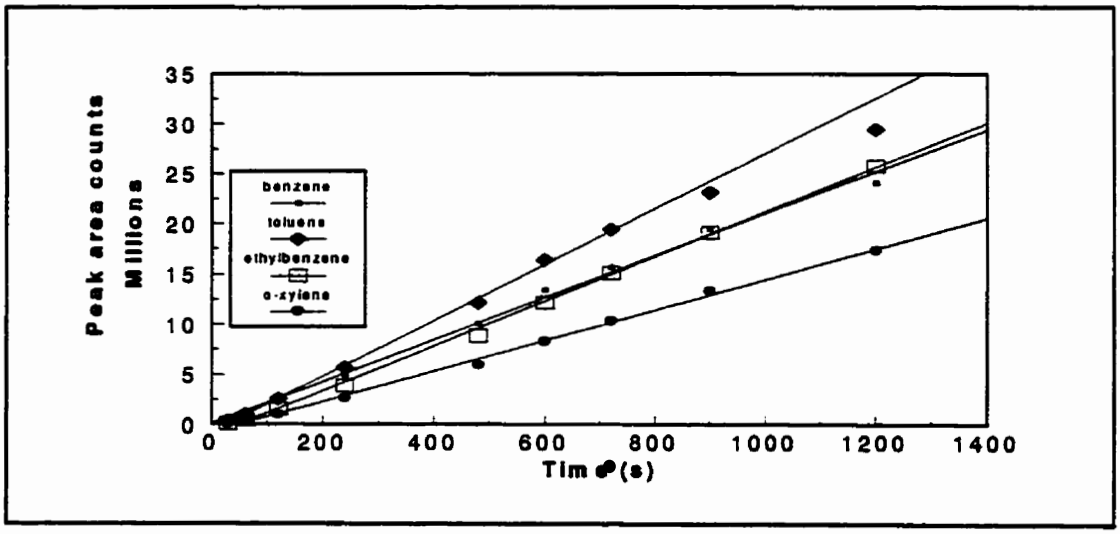

Figure 6-7. Linear relationship between extraction time and the amount extracted.

6.5 Quantitation Based on Stop Flow

An alternative means of reducing variation of the initial trapping time, eliminating waiting time in steady-state extraction, and improving the limit of detection is to measure the first injection after the absorption equilibrium of the membrane. In this method, the membrane is initially exposed to the sample without stripping gas flow inside. The purpose of this step is to establish equilibrium between the membrane and the sample. After equilibrium is reached, the stripping gas is then passed through the membrane to strip the analyte from the inner membrane surface. Because equilibrium has been reached, the concentration at the inner membrane surface is high and high mass transport is obtained during initial stripping. **Figure 6-8** depicts the concentration change in the process.

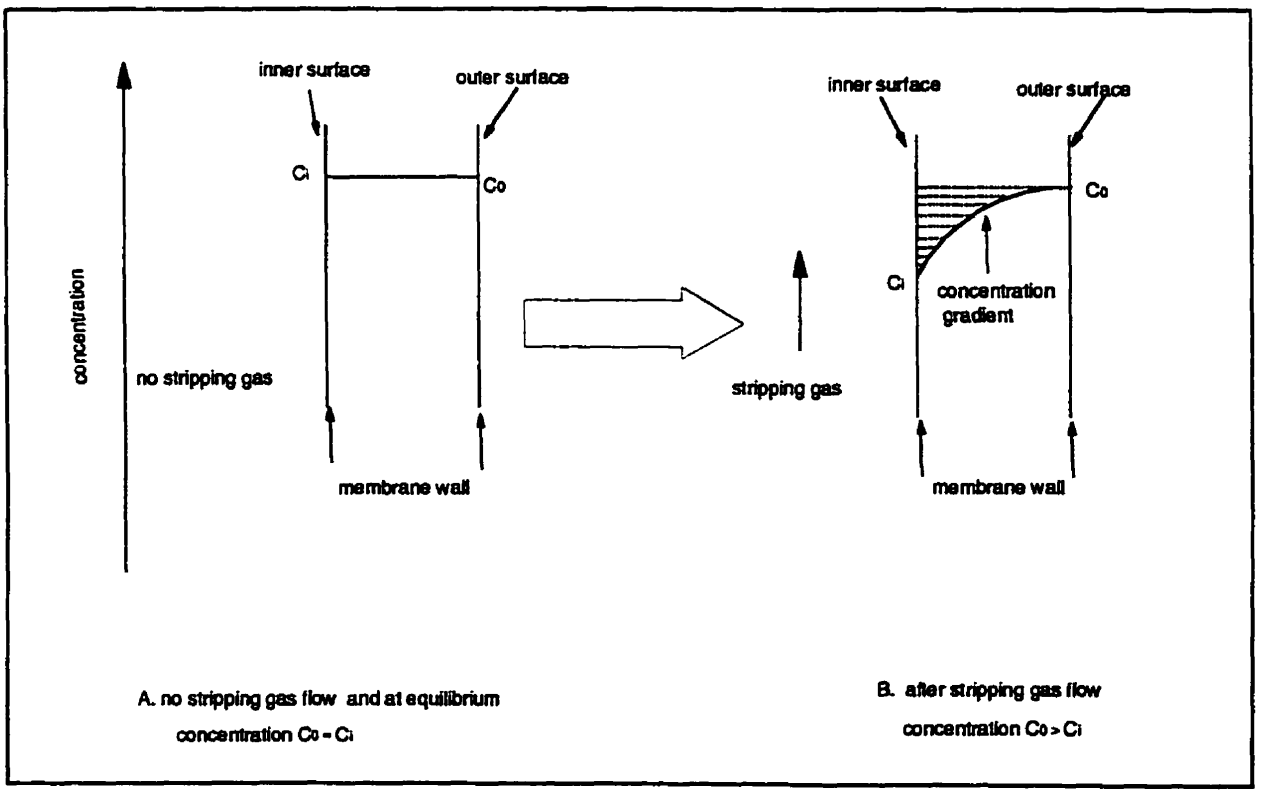

Figure 6-8. Concentration gradient before and after flow of stripping gas through the membrane.

It is apparent that when equilibrium is reached, distribution in the membrane is homogeneous. When the stripping gas suddenly flows inside the membrane, the analyte on the inner membrane surface is stripped off and the concentration in the membrane is changed. After a while, a constant concentration gradient is formed. The shadowed area in **Figure 6-8** indicates the extra amount of analyte stripped as a result of the pre-equilibrium. This accumulates in the sorbent trap and leads to a surge peak in the first injection. **Figure 6-9** shows the extraction time profile for benzene and the chromatogram from continuous monitoring with nine-cycle injection.

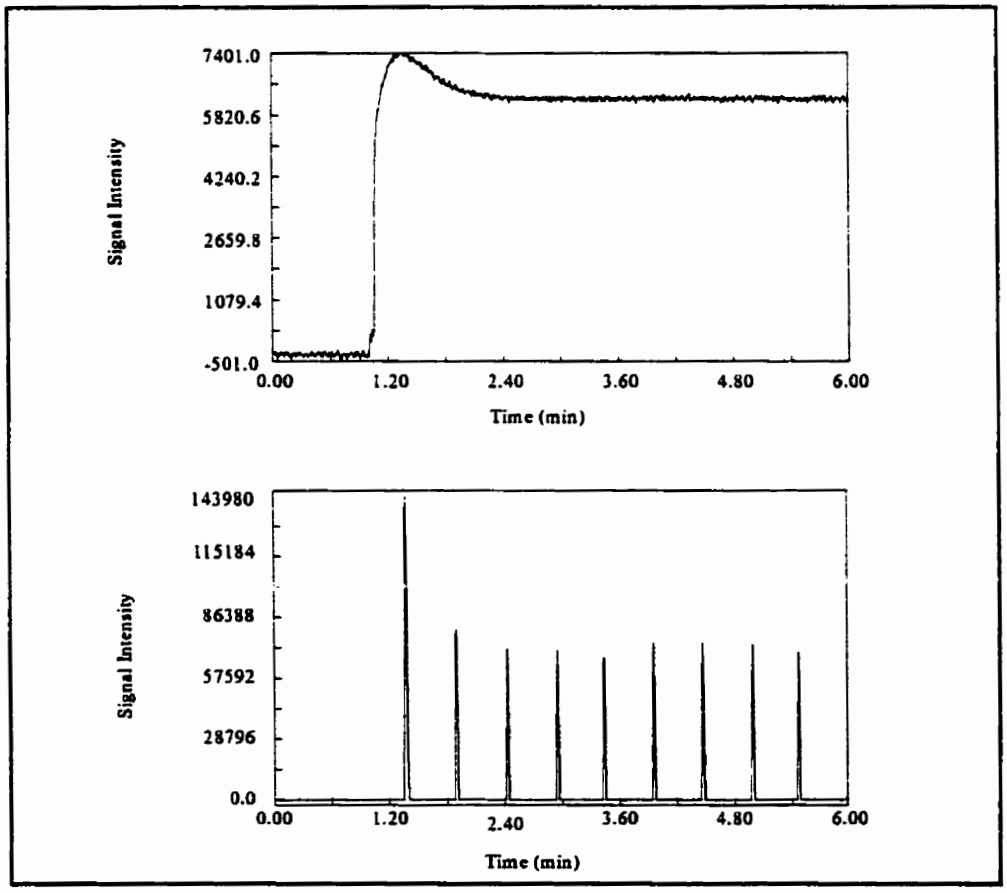

Figure 6-9. Extraction time profile and chromatogram for analysis of benzene by the membrane saturation method. Benzene concentration: 12.7 μg L^{-1}; membrane length: 4cm; flow rate of stripping gas: 4.6 mL min^{-1}; extraction temperature: 25 °C

From **Figure 6-9** it is apparent that when the stripping gas flow rate was 2.2 mL min^{-1} the surge wave (peak) lasted approximately 68 s. This can be regarded as the non-steady-state time and is very close to the value measured previously,[42] when the membrane concentration was increased from 0 to a constant level. In this approach, there is no mass transfer from sample to the sorbent interface during stop flow, so the initial time at which the membrane is exposed to the sample is not the issue. The increase in the amount of the first peak extracted depends on the distribution constant of the analyte between the stripping gas and the membrane. Obviously, an analyte with small partition coefficient is easily stripped off and the amount extracted is a greater. **Table 6-4** shows, for the components of BTEX, the percentage increase in the area of the first peak obtained under these conditions compared with that obtained under steady-state conditions. It was expected that the increase for benzene would be the greatest for this group of compounds. On the other hand, the analyte diffusion coefficient determines the time needed to establish a constant concentration gradient across the membrane after the start of the flow of stripping gas—for analytes with large diffusion coefficients formation of the concentration gradient is rapid. The time taken to form a constant concentration gradient can be investigated by checking the permeation time profile of the analyte.

Table 6-4. Increase in the amount extracted compared with membrane absorption equilibrium in steady-state extraction. The stripping gas flow rate was 4.6 mL min^{-1}.

	Benzene	Toluene	Ethylbenzene	*o*-Xylene
Increase (%)	74.3	65.4	47.4	54.8
	(±0.7)	(±0.7)	(±0.8)	(±0.9)

Figure 6-10 shows the time profiles for the components of BTEX. It is apparent that the time taken to establish the concentration gradient is shortest for benzene; *o*-xylene takes much longer. It is also apparent from this figure that when gas flow rate is 2.2 mL min^{-1}, no surge wave was observed for ethylbenzene and *o*-xylene. This because these two analytes have larger partition coefficients—the analytes at the inner membrane surface could not be effectively stripped off at the slow stripping gas flow rate. When the flow rate of stripping gas was increased, the surge wave was observed. **Figure 6-11** shows the effect of stripping gas flow rate on extraction time profile. It is apparent that high flow rates resulted not only in short formation time but also high peak intensity. This approach must, therefore, use higher gas flows. **Figure 6-12** shows the chromatogram obtained for BTEX at a gas flow rate of 4.2 mL min^{-1} with 1 min trapping. The first group of peaks correspond to the first injection after exposure of the membrane to the BTEX/air sample for 5 min (in this instance equilibrium was reached). Sensitivity was, apparently, higher than for steady-state extraction. Again, good calibration curves were obtained; these are shown in **Figure 6-13.** The concentration range was from 1 to 5000 ppb. The calibration curves presented square regression of 0.9999-0.9990; the RSD for each testing point was <4% (three replicates).

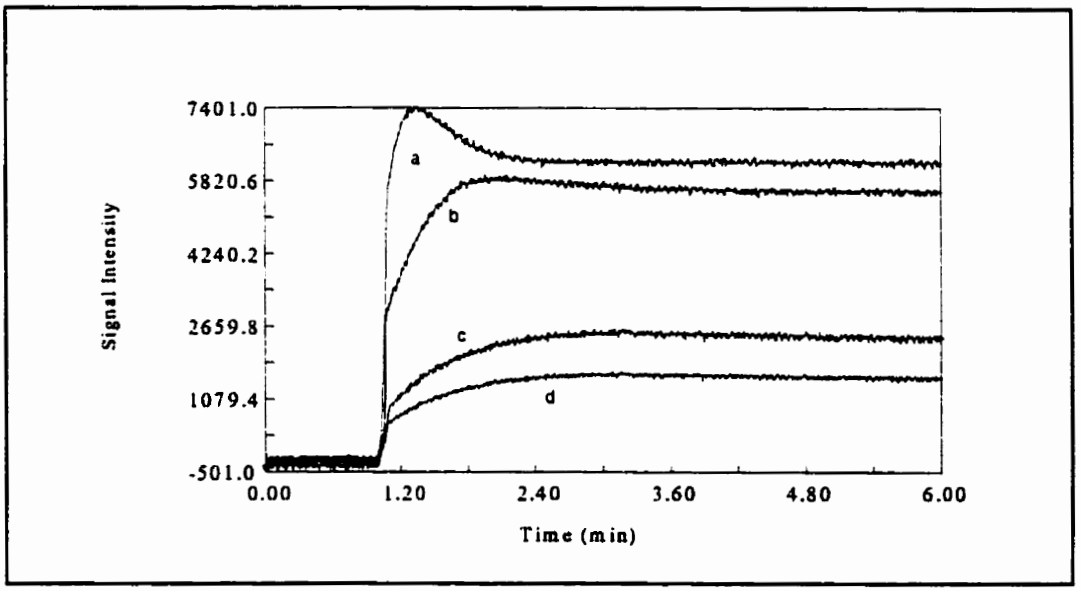

Figure 6-10. Permeation time profiles of BTEX when stripping gas was switched to flow through the membrane after previous membrane saturation. (a) benzene, conc.: 12.7 μg L^{-1}; (b) toluene, conc.: 15.3 μg L^{-1}; (c) ethylbenzene, conc.: 10.9 μg L^{-1}; (d) *o*-xylene, conc.: 9.8 μg L^{-1}.

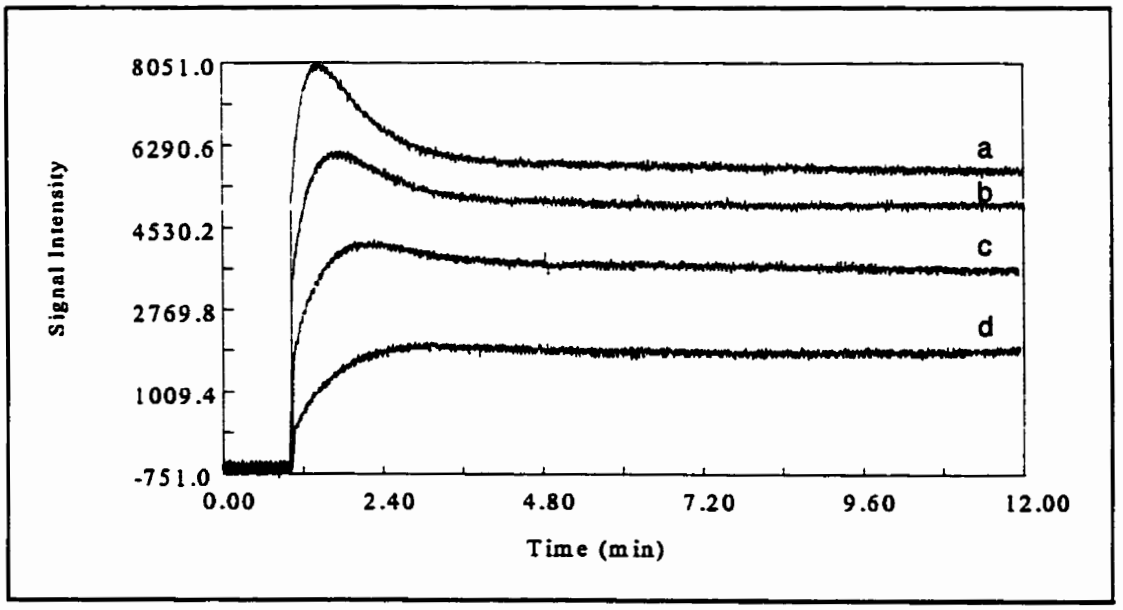

Figure 6-11. Effect of stripping gas flow rate on the permeation time profile of ethylbenzene. Flow rate: (a) 10.5 mL min^{-1}; (b) 6.5 mL min^{-1}; (c) 3.9 mL min^{-1}; (d) 2.0 mL min^{-1}. Concentration:10.9 μg L^{-1}; extraction temperature: 25 °C.

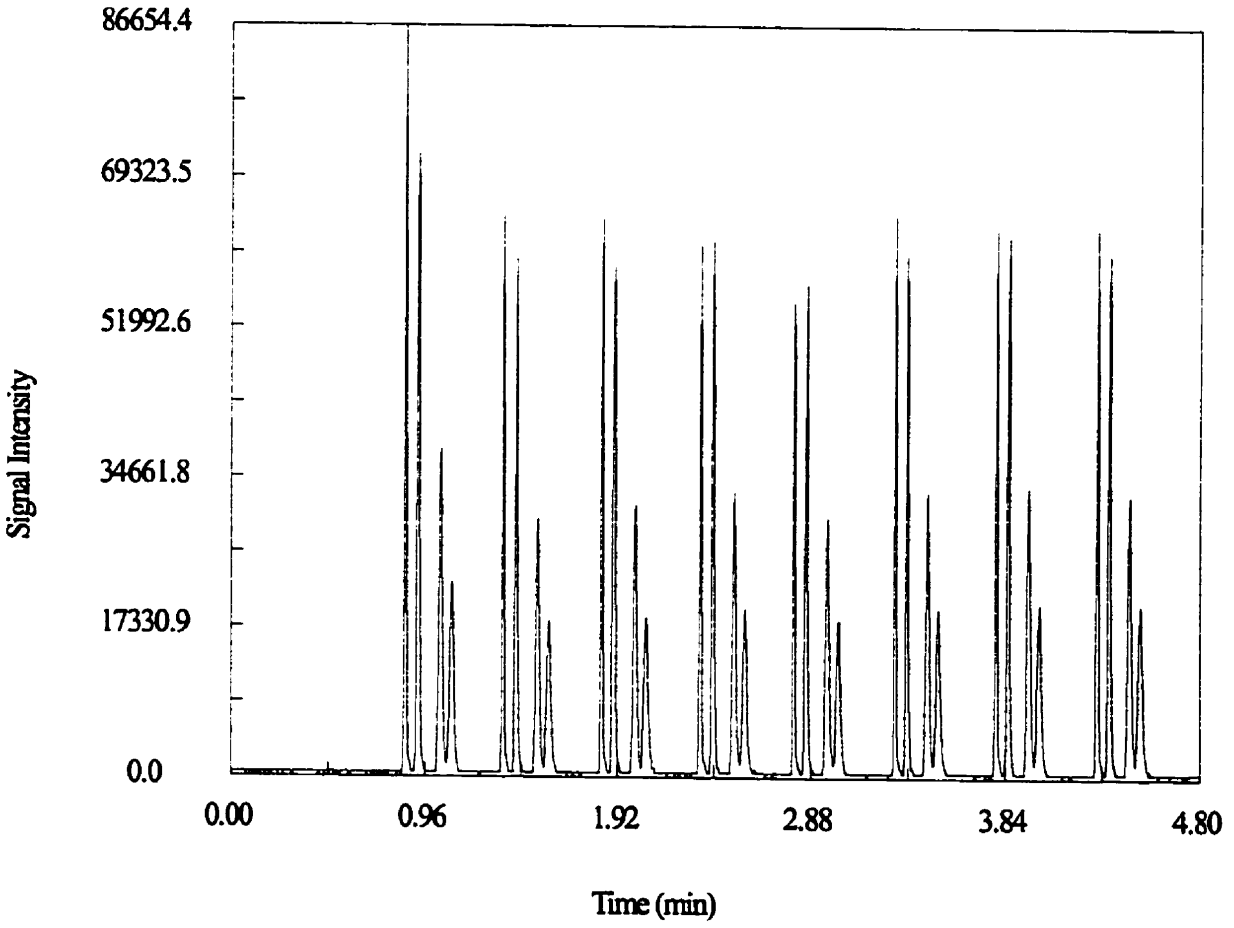

Figure 6-12. Monitoring of BTEX in air when the stripping gas was switched to flow through the membrane after previous membrane saturation.The stripping gas flow rate was 4.2 mL min^{-1}.

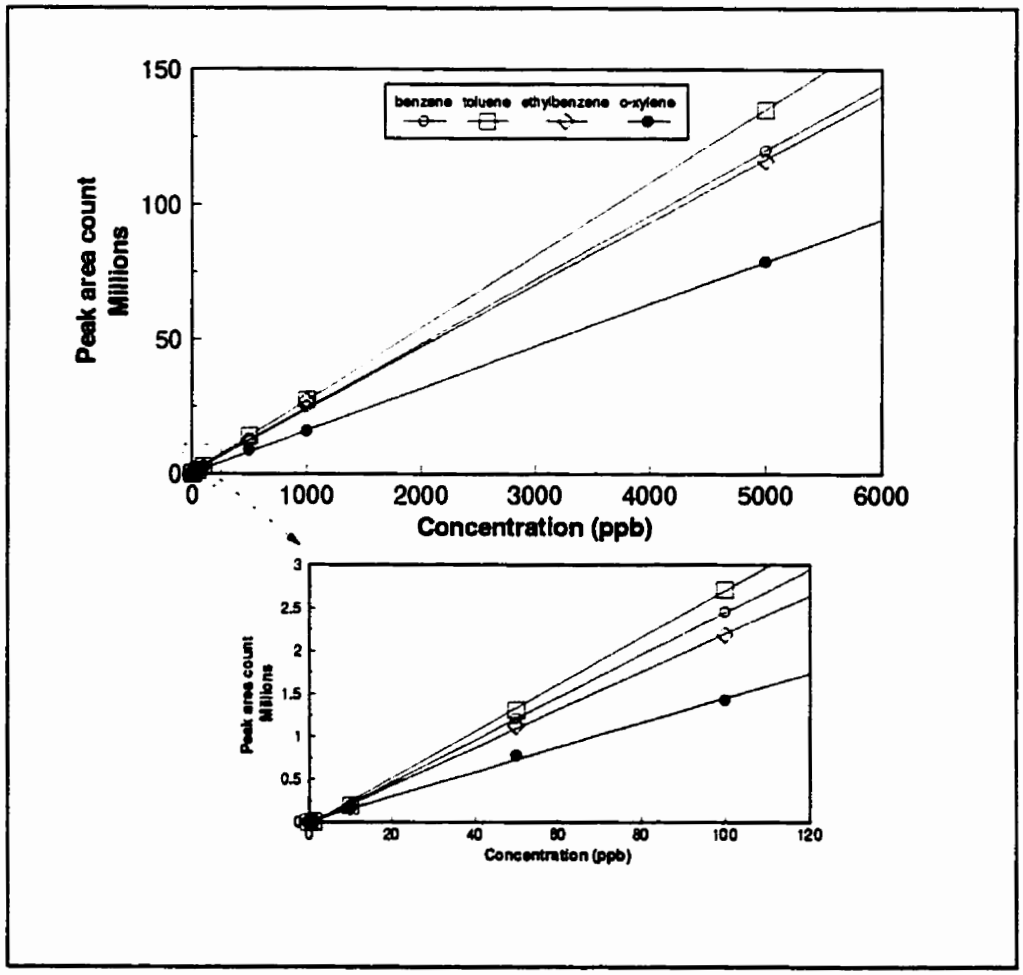

Figure 6-13. Calibration curves for BTEX/water analysis by stop-flow extraction.

6.6 Quantitation Based on Exhaustive Extraction

Quantitative MESI measurements can be performed by exhaustive membrane extraction, which eliminates the need for standards and minimizes temperature and matrix effects. In this method, the membrane probe is exposed to the sample to extract analyte continuously until the concentration is below the detection limit. The peak heights or area counts of analyte are then added together to furnish the total amount in the sample. If the detector (e.g. FID) response factor is known, no calibration is needed (Chapter 5). This method is used in sealed sample

systems only. The shortcoming of this method is the long analysis time, usually measured in hours. The analysis time can be reduced by good mixing and use of thinner wall membranes. A small sample volume is preferable because it results in rapid concentration depletion. **Figure 6-14** shows chromatograms obtained from BTEX after 80 min analysis. This investigation was performed on a 1g sample of spiked sand with BTEX concentration of 100 ppb and the extraction was performed in a 2 mL vial. The flow rate of stripping gas was 2.2 mL $min^{-1}$and trapping gas was 1 minute. The recovery was 89 ($\pm$ 0.7)% with sample matrix heating.

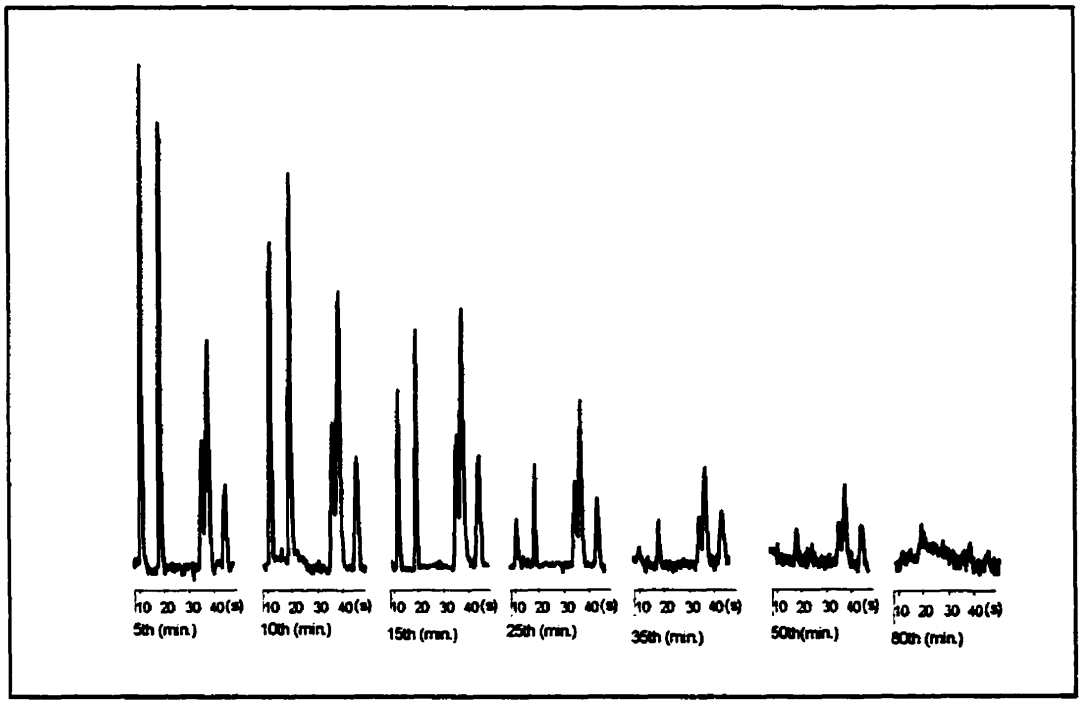

Figure 6-14. Chromatograms obtained from BTEX after exhaustive extraction.

6.7 Limit of Detection

In MESI the limit of detection depends on the extraction conditions, for example sample matrix, mixing, temperature, etc. When the extraction conditions are constant, trapping time is the main factor. A longer trapping time results in a lower detection limit. The detection limits

obtained for the components of BTEX in air by use of the approaches discussed in this chapter were compared for a 1-min trapping time. The results are shown in **Table 6-5**. As expected, the limit of detection was lowest for the stop-flow method.

Table 6-5. Limit of detection (ppb). The trapping time was 1 min.

	Benzene	Toluene	Ethylbenzene	*o*-Xylene
Non-steady-state extraction, initial time delay 10 s	1	2	6	7
Steady-state extraction	0.2	0.1	0.1	0.2
Stop flow	0.1	0.05	0.05	0.2

6.8 Conclusion

It has been shown that quantitation in MESI can be performed in several ways, including non-steady-state extraction, steady-state extraction, combined non-steady- state and steady-state extraction, stop-flow extraction, and exhaustive extraction. If non-steady-state extraction is used and a short extraction time is necessary, control of the time at which the extraction starts is essential for precision. Steady-state extraction resulted in good precision and high sensitivity, with the advantage that the timing of the start of the extraction was unimportant. Analysis with a longer extraction time based on non-steady-state and steady-state processes is time-efficient and of high sensitivity. The stop-flow method is the most sensitive, precision is good and operation is simple. Overall, flexible-time extractions and wide linear calibration ranges have been achieved with these methods. Exhaustive extraction has the advantage that no calibration is required. Such methods lead to a wide linear range and high precision and sensitivity. All of these aspects demonstrate the potential of MESI for VOC analysis and monitoring.

CHAPTER 7

MESI IN ON-SITE MONITORING

CHAPTER 7

MESI IN ON-SITE MONITORING

7.1 Membrane Headspace Extraction

Membrane extraction in air, aqueous phase, and headspace analysis has been investigated; the corresponding mathematical models can be used to describe the extraction process.[42,63,71] In membrane extraction, the partition coefficient between the membrane and air is greater than that between the membrane and water and, because VOCs can be effectively extracted from the headspace of aqueous samples, MESI is suitable for on-site monitoring.[72–74] Headspace extraction precludes contact of the membrane with the aqueous matrix and keeps the membrane probe clean, ensuring good performance. This enables the application of MESI in different environments. On the other hand, headspace extraction of VOCs requires that they are efficiently distributed into the headspace; good mixing is, therefore, generally necessary. This chapter describes the use of a small extraction module designed for water headspace extraction.

7.2 Cap-MESI for Headspace Water Extraction

7.2.1 Construction of Cap-MESI and Experimental Setup

The headspace membrane extraction module can be made rugged and suitable for long-term field monitoring application. The extraction cap is shown in **Figure 7-1.** The cap was modified from a powder funnel (Nalgene); the diameter of the bottom was 65 mm. The neck of the funnel was tightly sealed with a Teflon cap and the membrane probe was supported by two pieces of silica tubing which was positioned inside the cap. To agitate the headspace, a microfan (0.5 W, 5 V; 1 cm × 1 cm × 0.5 cm; Sunon, Taiwan) was suspended in the cap. The microfan

was supported by two stainless-steel needles which were hung on the Teflon cap. A hole was drilled in the Teflon lid and was sealed by means of a stainless-steel rod. The hole can be opened by removal of the rod to enable adjustment of the headspace pressure.

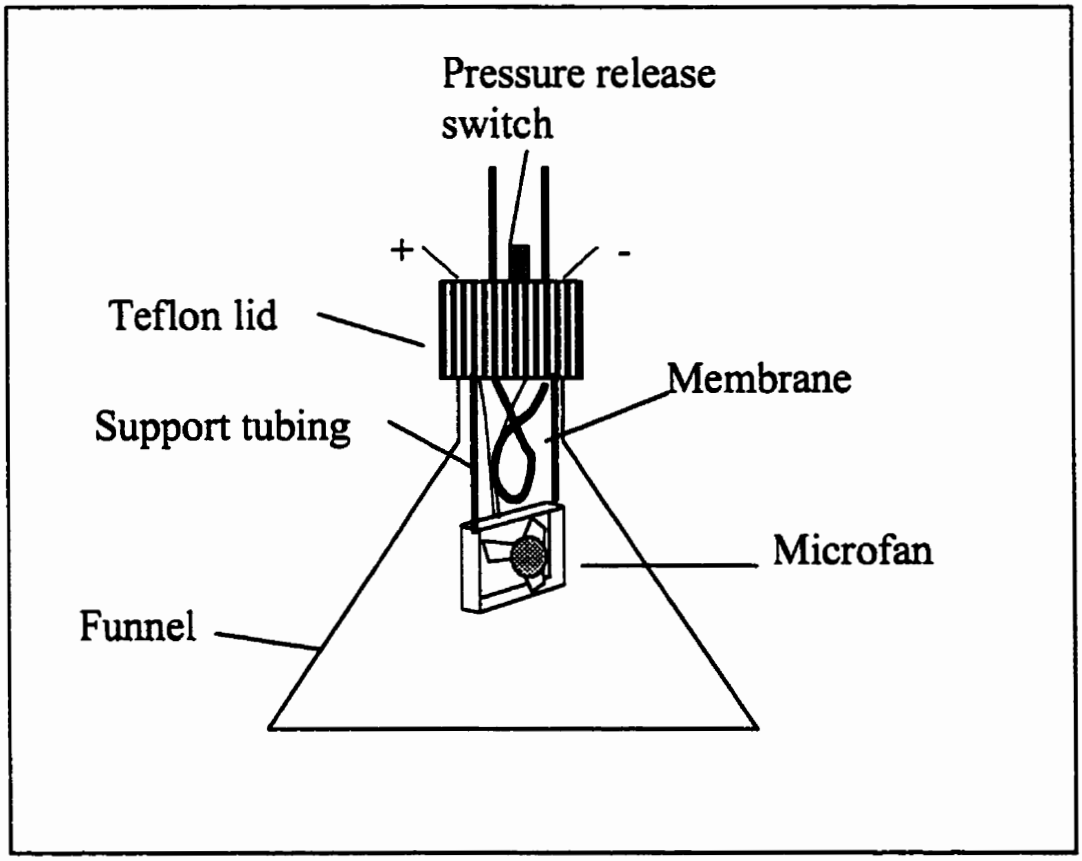

Figure 7-1. Schematic diagram of the construction of extraction cap.

The aqueous sample used in this investigation was a mixture of benzene, toluene, ethylbenzene, *o*-xylene and trichloroethylene (TCE). In all aqueous samples the exact concentrations of

benzene, toluene, ethylbenzene, *o*-xylene, and trichloroethylene were 88, 172, 156, 156, and 88 ppb (*w/w*), respectively.

To perform surface water monitoring, the extraction cap was placed on the water surface. The aqueous sample was in a water bath glass container. The headspace was at ambient pressure. For under water monitoring, the extraction cap was positioned in an aqueous sample at a depth of 25 cm. When the cap was in deep water, the headspace pressure was higher than ambient because of the depth of water. To introduce a 1-cm depth of water inside the cap, the headspace pressure was adjusted by opening and closing the pressure release switch shown in **Figure 7-1**. During extraction the position of the extraction cap was fixed by means of a clamp to hold the neck of the cap and the cap in tight contact with the bottom of the bath container. This contact ensures proper sealing and prevents exchange of the sample inside with that outside the cap. Monitoring of VOCs was performed after 4 min trapping and 1 s thermal desorption. **Figure 7-2** shows the chromatograms obtained for a group VOCs after headspace monitoring of an aqueous sample. The sample concentration was: benzene 180 ppb, toluene 400 ppb, ethylbenzene 200 ppb, o-xylene 200 ppb, trichloroethylene 250 ppb. The extraction was at room temperature.

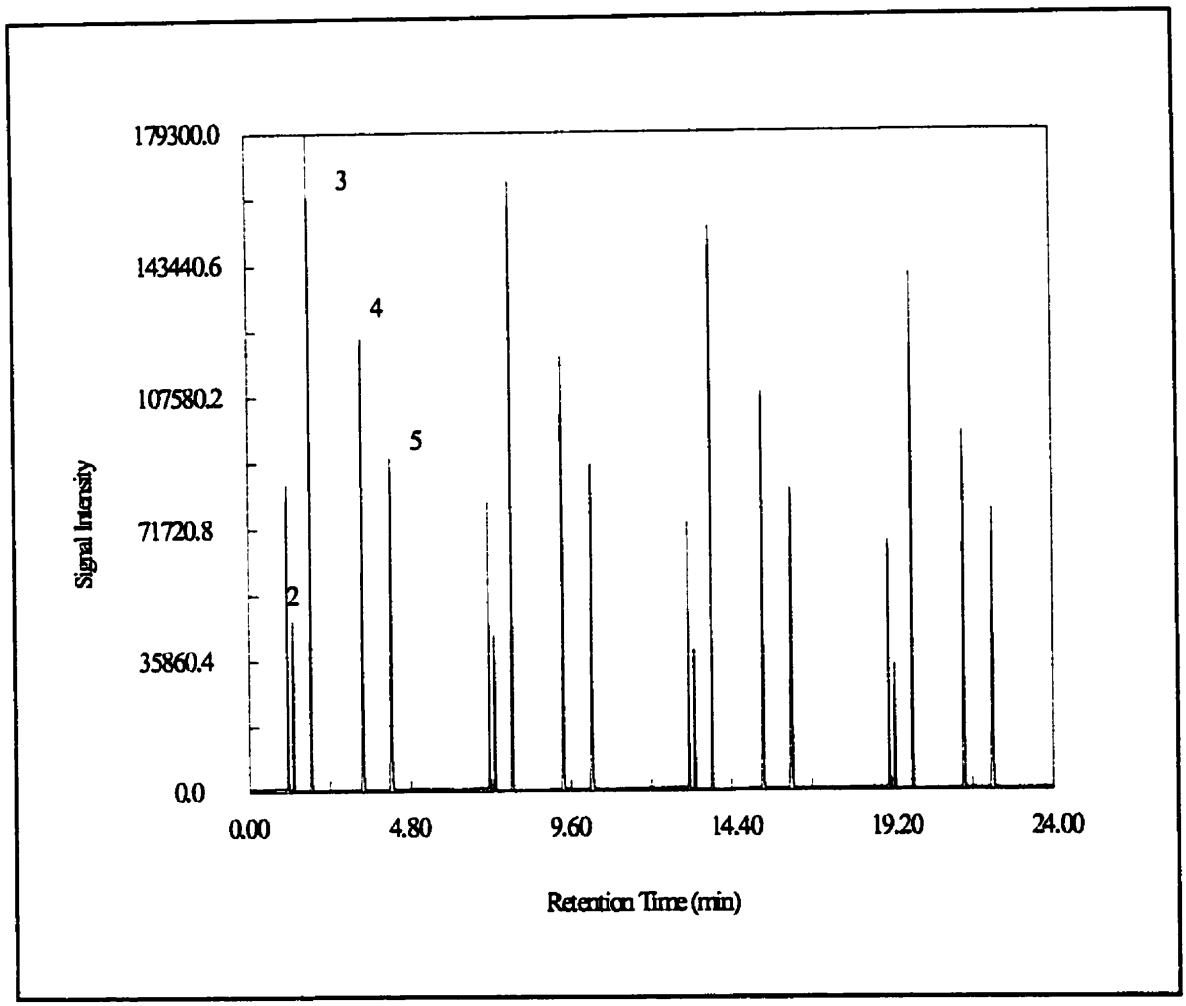

Figure 7-2. Chromatograms obtained from a VOC mixture by continuous Cap-MESI headspace monitoring: 1, benzene; 2, trichloroethylene; 3, toluene; 4, ethylbenzene; 5, *o*-xylene.

7.2.1 Surface Water Extraction

Surface water headspace analysis can supply information about the release of volatile organic compounds to air from ponds, lakes, and rivers, and help environmentalists to monitor

air and water quality. When Cap-MESI is used the extraction can be treated as a normal headspace extraction, because there is no pressure difference between the capped headspace and the outside. Analyte must diffuse from the bulk solution to the aqueous surface, then partition to the headspace, diffuse from the headspace to the membrane outer surface, partition into the membrane, diffuse to the inner wall of the membrane, and then partition into the stripping gas to the MESI system where it is analyzed. Among these processes, because of the small diffusion coefficient of the analyte in the aqueous phase, analyte transport from the bulk solution to the solution–membrane surface is the rate-determining step. Mixing is the most important means of improving mass transfer, and magnetic stirring is a popular method for aqueous sample mixing. Stirring can rapidly bring VOCs to the water surface, enabling rapid distribution of the analytes into the headspace; the equilibrium between the headspace and water can, therefore, be reached in a short time. When the equilibrium is reached, the greatest extraction efficiency will be obtained. The amounts of benzene extracted in continuous monitoring with different mixing are compared in **Figure 7-3**.

From **Figure 7-3** it is apparent that for 48 min monitoring static conditions resulted in extraction of the smallest amount, and that steady-state extraction was reached slowly. Both water stirring and headspace microfan agitation result in extraction of greater amounts and steady-state extraction being achieved in a shorter time. Combination of magnetic stirring and microfan headspace agitation shows that the former led to the steady-state being reached in a shorter time and the extraction of a greater amount in the initial extraction. Peak size decreased irrespective of the mode of agitation used; this was attributed to concentration depletion in the bulk solution owing to removal of the analytes during extraction. From **Figure 7-3** it is apparent that the two different modes of agitation resulted in extraction of similar amounts in 48 min. We

know magnetic stirring is an effective method for water agitation; the experiment showed, however, that similar mixing was achieved with the microfan. There are three possible explanations of this phenomenon. Firstly, microfan agitation moved not only the air of the headspace but also the water surface; the formation of many ripples could greatly increase the water surface area and result in faster mass transfer from the aqueous phase to the headspace. Secondly, when the microfan was circulating the air, the water was also agitated. As the depth of the solution was only 1 cm, the analytes could easily be brought to the water surface from the bulk solution. Thirdly, the rapidly moving air in the headspace could more efficiently strip analytes from the water surface, bring more analytes to the membrane, and simultaneously reduce the boundary layer around the membrane. From **Figure 7-3**, it is also apparent that simultaneous use of water stirring and headspace agitation resulted in extraction of the largest quantities; the time taken to reach steady-state was too short to be observed in the experiment. Because the rapid removal of analytes resulted in concentration depletion, peak intensities declined rapidly.

To understand the effect of headspace mixing on the amount extracted, two experiments were designed. In one experiment, the microfan was adjusted to face the membrane probe and the water, i.e. the microfan was positioned so that it blew both air and the water. In another experiment, the microfan was adjusted to face the membrane probe only—to reduce the agitation of the water. The results are shown in **Table 7-1**. It is apparent that with the microfan blowing on the water surface the amount extracted is greater. This result supports the above explanation that the microfan can significantly mix the water.

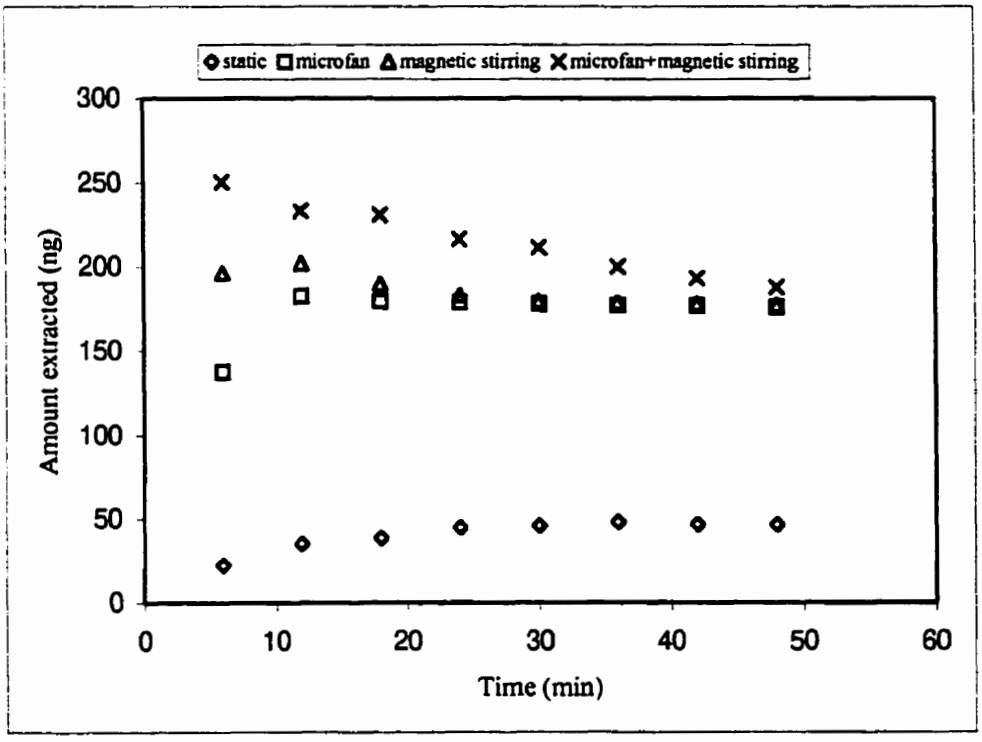

Figure 7-3. Extraction time profiles for headspace extraction of benzene with different agitation of the water surface. Benzene concentration: 180 ppb, extraction temperature: 25 °C.

Table 7-1. Comparison of the amounts of *o*-xylene extracted (average peak height from four replicates) in continuous Cap-MESI headspace monitoring. Concentration 200 ppb, temperature 25ºC.

Time (min)	4	8	12	16	20	24	28	32
Agitation A	49500	78000	83500	82500	83800	82800	79500	74500
Agitation B	54500	92500	91800	92500	89500	82500	80500	76500

Agitation A: microfan facing the membrane probe only

Agitation B: microfan facing the membrane probe and the aqueous sample

7.2.2 Under-Water Headspace Extraction

For under-water headspace monitoring the extraction cap was positioned in relatively deep water. Because the top of the cap was efficiently sealed, a headspace was formed inside the cap. It has been found experimentally that extraction under water was different from that at the water surface. With under water extraction it took longer to reach steady-state extraction and the total amount extracted (sum of all peaks) was lower. This is because of the different headspace pressure. When the extraction cap was positioned under the water, because of the depth of the water the headspace pressure was greater than that at the water surface. When the headspace is at higher pressure, the speed of mass transfer from the aqueous phase to the headspace is reduced, as is the partial vapor pressure of analyte in the headspace.[12] When the partial vapor pressure of the analyte in the headspace is reduced, the amount extracted is obviously reduced, because it is proportional to sample concentration.[8] In this study the extraction was performed under 25 cm water, so the headspace pressure would not be very high. The amount extracted at steady-state was not significantly different from that at the water surface, but different times were taken to reach steady-state. Better mixing is, apparently, needed to improve the mass transfer rate. For field monitoring, mixing can be achieved by use of a motor rotor with two sets of paddles for simultaneous stirring of water and headspace. A fan with more power would also mix better and should result in greater extraction efficiency.

Although this investigation was performed in 25 cm water only, it can be predicted that in deeper water the amount extracted would be significantly lower and the sensitivity would be correspondingly worse. To deal with the problem of increased pressure, the headspace pressure must be reduced. In practice a taller cap can be used and the headspace pressure can be released by opening the pressure release switch (**Figure 7-1**) to introduce the water to the upper level.

The reason for using a taller cap is to ensure that the cap covers more water, so that when the pressure is reduced, a proper headspace for membrane probe and agitation is still maintained. Alternatively, the deep water can be brought to the water surface for extraction at ambient pressure. To bring the deeper water to the water surface a long tube or pipe can be connected to the extraction cap; the tube or pipe is dipped into the water to the target depth, but the extraction cap remains at the water surface. The pressure release switch (**Figure 7-1**) can then be opened to guide the water gradually to the surface water level. The headspace pressure is then the same as at the water surface. Good sensitivity can be obtained.

7.2.3 Quantitation

Quantitation is an important issue in field monitoring. For external calibration, quantitation based on steady-state extraction can lead to good reproducibility. For steady-state extraction a long steady-state extraction time is expected, and the time depends on the sample volume. We have previously[13] shown that a large sample volume resulted in a longer steady-state extraction time. The sample volume in field monitoring is usually very large, i.e. rivers, lakes, and underground water, so the change from steady-state to non-steady-state as a result of depletion of analyte by the extraction can be ignored.

In Cap-MESI headspace analysis the headspace pressure is important for quantitation, and constant headspace pressure is needed. Any variation in depth will affect the amount extracted. To simplify the calibration, the headspace pressure can be controlled at ambient, which will also result in the highest extraction efficiency. The temperature in deep water should also be considered. Normally, the temperature in deep water is below that at the water surface. This would affect the distribution of analytes in the headspace. In an external calibration, the

correct temperature should be used. Alternatively, when mixing is perfect a method without external calibration can be used. This method for air analysis has been discussed elsewhere.[14]

To simplify discussion of quantitation, only surface water monitoring was investigated in this study. Extraction was performed with microfan mixing because water stirring is not convenient in most field applications. To ensure a large sample volume in the investigation, a 1-L aqueous sample was used. VOC peaks of constant height were used for calibration to ensure the chromatogram was obtained under conditions of steady-state extraction. The calibration curves for these compounds are shown in **Figure 7-4**. Good linearity was obtained for concentrations from 1 ppb to 5 ppm; values of R^2 were from 0.9831 to 0.9998. RSD was always below 7%. Good detection limits were obtained for the VOCs; these are listed in **Table 7-2**.

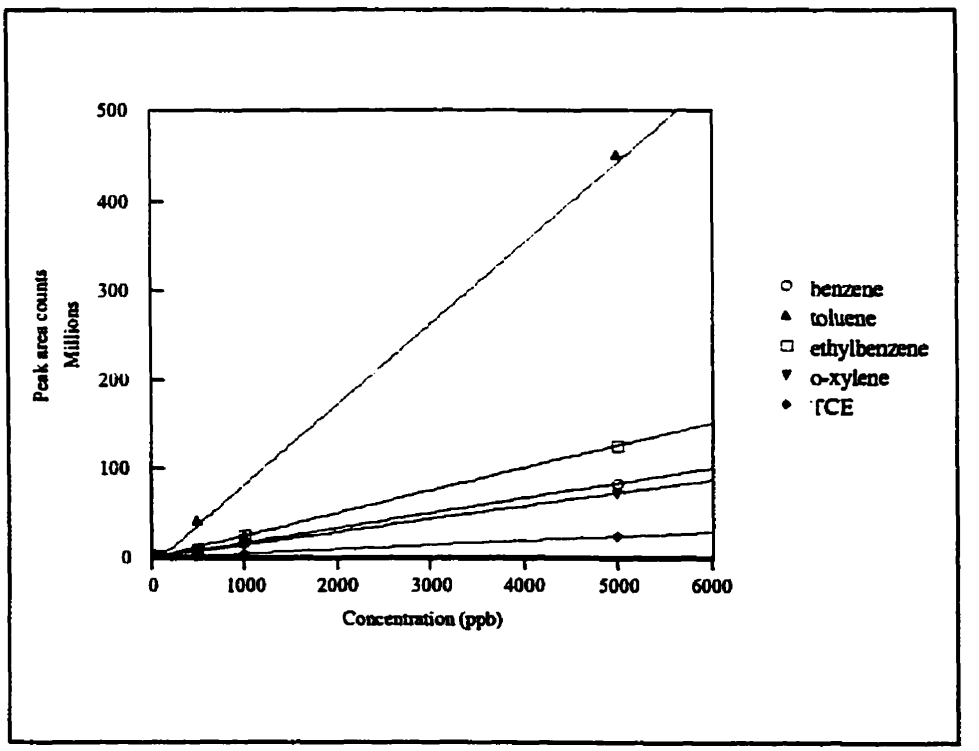

Figure 7-4. Calibration curves obtained for benzene, toluene, ethylbenzene, *o*-xylene, and TCE by Cap-MESI surface water headspace analysis.

Table 7-2. Precision and limit of detection. The trapping time was 4 min.

	Benzene	Toluene	Ethylbenzene	*o*-xylene	TCE
Precision (RSD%)*	4.2	3.8	3.9	4.5	6.2
Limit of detection (ppb)	0.1	0.1	0.1	0.1	1

*The precision was obtained from five replicate analyses at a concentration of 200 ppb.

7.3 On-site and On-line Headspace Fermentation Monitoring by MESI–GC–MS

When MESI is applied directly to an effluent stream or biological system rich in organic compounds, significant interference could cause high background noise or affect, non-reproducibly, the parameters that govern response time and extraction rate. Humic or other materials in a sample could foul a membrane. In that situation, a headspace approach is more suitable.

MESI has been applied for on-site and on-line headspace fermentation monitoring by coupling to GC–MS. For monitoring the membrane probe was simply exposed to the headspace of a fermentation broth; the sample was not mixed. The extraction (sampling) time was 3 min and the temperature of sorbent trapping was below –40°C. Changes in the composition of the volatile organic products monitored during the fermentation process could be easily observed by MESI–GC–MS. **Figure 7-5** shows the chromatograms obtained 1, 10, and 24 h after the start of fermentation. It is apparent that the products and their concentration varied with time. From this application we can conclude that MESI–GC–MS is suitable for real-time monitoring.

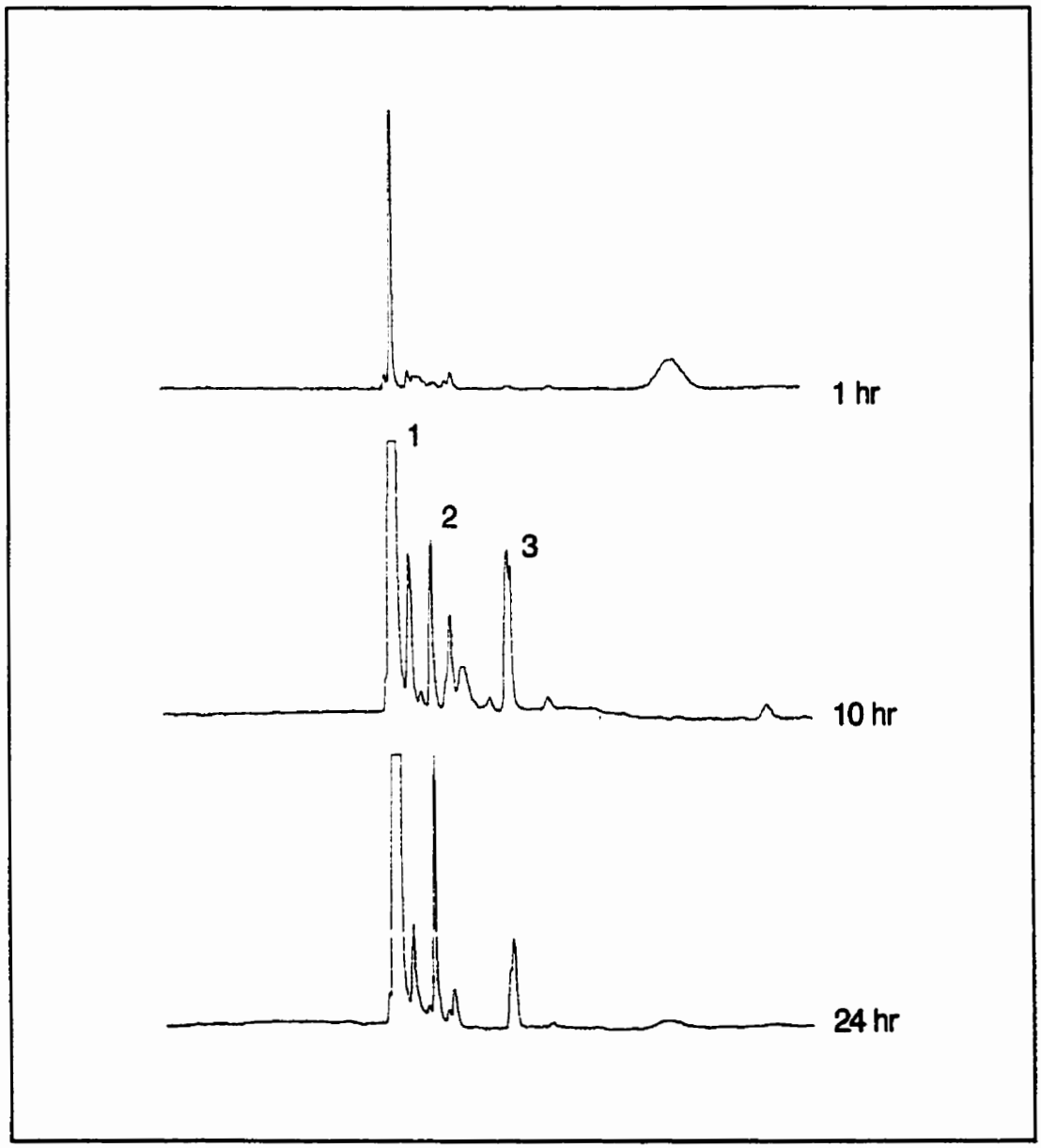

Figure 7-5. Fermentation monitoring: 1, ethanol; 2, acetic acid; 3, acetoin.

7.4 Conclusion

MESI has potential for on-site monitoring and Cap-MESI should be a useful tool for field analysis and monitoring. The extraction cap can be placed at the water surface or at depth to perform on-site or on-line monitoring. Because headspace extraction is used, the membrane in not in contact with the sample matrix, which avoids a reduction of membrane performance. This ensures the extraction probe can be placed in the environment for long-term monitoring without any need for membrane replacement. In deep water monitoring, headspace pressure and low temperatures are major factors causing low extraction efficiency. To reduce the effect of pressure, the water matrix and the headspace should be efficiently mixed. To obtain good extraction efficiency in deep water monitoring, water should be brought to the water surface to enable ambient headspace pressure monitoring. Quantitation based on external calibration should take into consideration the actual extraction temperature and pressure, particularly for deep water monitoring. Good linearity, precision, and detection limits were obtained for quantitation based on surface water headspace extraction. This study demonstrates that Cap-MESI is a potential practical approach for field monitoring because of its simplicity, cost, time efficiency, ease of automation, good sensitivity, selectivity, and reliability. Fermentation monitoring by MESI–GC–MS demonstrated the application of MESI in on-site monitoring and identification.

References

1. Ong, C. P.; Lee, H. K.; Li, S. F. Y. *Environ. Monit. Assess.* **1991**, 19, 63.

2. Noble, D. *Anal. Chem.* **1993**, 65, 693A.

3. Callis, J. B.; Iiman, D. L.; Kowalski, B. R. *Anal. Chem.* **1987**, 59, 624A.

4. Boyd-Bond, A. A; Chai, M.; Luo, Y. Z.; Zhang, Z.; Yang, M. J.; Pawliszyn, J.; Gorecki, T. *Environ. Sci. Technol.* **1994**, 28, 569A.

5. Warren, D. *Anal. Chem.* **1984**, 56, 1592A.

6. Jönsson, J. Å; Mathiasson, L. *Trends Anal. Chem.* **1992**, 11,106.

7. Lindegård, B.; Bjork, H.; Jönsson, J. Å; Mathiasson, L.; Olsson, A. *Anal. Chem.* **1994**, 66, 4490.

8. Thordarson, E.; Pálmarsdóttir, S.; Mathiasson, L.; Jönsson, J. Å. *Anal. Chem.* **1996**, 68, 2559.

9. Lotiaho, T.; Lauritsen, F. R.; Choudhury, T. K; Cooks, R. G.; Tsao, G. T. *Anal. Chem.* **1991**, 63, 875A.

10. Bier, M. E. and Cooks, R. G. *Anal. Chem.* **1987**, 59, 597.

11. Lauritsen, F. R.; Gylling, S. *Anal. Chem.* **1995**, 67, 1418.

12. LapPack, M. A; Tou, J. C.and Enke C. G. *Anal. Chem.* **1990**, 62, 1265.

13. Virkki, V. T.; Ketola, R. A; Ojala, M.; Kotiaho, T.; Komppa, V.; Grove, A.; Facchetti, S. *Anal. Chem.* **1995**, 67, 1421.

14. Blanchar, R. D.; Hardy, J. K. *Anal. Chem.* **1984**, 56, 1621.

15. Blanchar, R. D.; Hardy, J. K. *Anal. Chem.* **1986**, 58, 1529.

16. Melcher, R. G.; Bakke, D. W. Hughes, G. H. *Anal. Chem.* **1992**, 64, 2258.

17. Pratt, K. F.; Pawliszyn, J. *Anal. Chem.* **1992**, 64, 2101.

18. Pratt, K. F.; Pawliszyn, J. *Anal. Chem.* **1992**, 64, 2107.

19. Luo, Y. Z.; Yang, M. J.; Pawliszyn, J. *J. High Resol Chromatogr.* **1995**, 18, 27.

20. Yang, M. J.; Harms, S.; Luo, Y. Z.; Pawliszyn, J. *Anal. Chem.* **1994**, 66, 1339.

21. Hoc, G.; Kok, B. *Arch. Biochem. Biophys.* **1963**, 101, 160.

22. Bokatka, S.; Degn, H. *Rapid Commun. Mass Spectrom.* **1991**, 5, 433.

23. Rotzscge, H., *Stationary Phase in Gas Chromatography.* Elsevier Science Publishers, Amsterdam, The Netherlands, **1991**. Page 201-213.

24. Clarson, S. J.; Semlyen, J. A. *Polymer* **1986**, 27, 91.

25. Zhang, Z.; Pawliszyn, J. *Anal. Chem.* **1995**, 67, 34.

26. Brettell, T. A; Grob, R. A. *American Lab.* **1985**, Oct. 19.

27. Gorecki, T.; Pawliszyn, J. *Anal. Chem.* **1995**, 67, 3265

28. Stern, S. A. *Membrane Separation Technology;* Elsevier, Amsterdam, **1995**. Page103-105.

29. Skelland, A. H. P., *Diffusional Mass Transfer*, John Wiley & Sons, New York, **1974**. Page 27.

30. LaPack, M. A.; Tou, J. C.; Enke, C. *Anal Chem.* **1990**, 62,1265.

31. Mulder, M. *Basic Principles of Membrane Technology;* Kluwer Academic Publishers, Dordecht, The Netherlands.**1991**. Page 77.

32. Carslaw, H. S.; Jeaeger, J. C. *Conduction of Heat in Solids, 2nd ed;* Clarendon Press, Oxford, **1986**.section 13.4

33. Andrew, P., Smith, A. F.; Wood, R. *Analyst*, **1971**, 96, 528.

34. Bertom, G., Liberti, F. A.; Perrino, C. *J. Chromatogr.* **1981**, 203, 263.

35. Crank, J.; Park, G. S. *Diffusion in Polymers*; Academic Press, London, **1968**. Page 46.

36. Ziegel, K. D.; Frensdorff, H. K.; Blair, D. E. *J. Polymer. Sci. Part A-2, 7*, **1969**, 809.

37. Wijmans, J. G.; Baker, R. W. *J. Membrn Sci.* **1995**, 107, 1.

38. Baker, R. W.; Yoshioka, N.; Mohr, J. M.; Khan, A. J. *J. Membrn Sci* **1987**, 31, 259.

39. Watson, J. M.; Baron, M. G. *J. Membrn Sci.* **1996**, 110, 47.

40. Brun, J.; Lachet, C.; Bulvester, G.; Auclair, B. *J. Membrn Sci.* **1985**, 25, 55.

41. Atkins, P. W. *Physical Chemistry;* Oxford University Press, London, **1978**. Page 32-35.

42. Luo, Y. Z.; Adams, M.; Pawliszyn, J. *Anal. Chem.* **1998**, 70, 248.

43. Pawliszyn, J. *Solid Phase Microextraction: Theory and practice*; Eley-VCH Press, New York, **1997**. Chapter 2.

44. Zhang, Z.; Pawliszyn, J. *Anal. Chem.* **1993**, 65, 1843.

45. Zhang, Z.; Yang, M. J.; Pawliszyn, J. *Anal. Chem.* **1994**, 66, 844A.

46. Louch, D.; Motlagh, S. *Anal. Chem.* **1992**, 64, 1187.

47. LaPack, M. A.; Tou, J. C.; McGuffin, V. L.; Enke, C. G. *J. Polym. Sci.* **1994**, 86, 263.

48. LaPack, M. A.; Tou, J. C.; *Anal. Chem.* **1991**, 63, 1631.

49. Berezkin, V.G.; Korolev, A.A.; Maluykova, I.V. *Proceedings of the 18th Int. Symp. on Cap. Chrom.* **1996**. Page. 396-404.

50. Mitr, S.; Zhang, L.; Zhu, N.; Guo, X. *J. Microcolm Sep.* **1996**, 8, 21.

51. Ortner, E. K.; Rohwer, E. R. *J. High Resol Chromatogr* **1996**, 19, 339.

52. Burger, B.; Burger, W. J. G.; Bureger, I. *J. High Resol Chromatogr* **1996**, 19, 346.

53. Mitr, S.; Zhu, N.; Zhang, X.; Kebbekus, B.; *J. Chromatogr.* **1996**, 737, 165.

54. Bauer, S.; Solyom, D.; *Anal. Chem.* **1994**, 66, 4422.

55. Edwards, K. et al ed. *Transfer Processes, 2nd Edition*; Hemisphere Publishing: New York, **1978**. Page 438.

56. Martos, P.; Pawliszyn, J. *Anal. Chem.* **1997**, 69, 206.

57. *Maple V Release 4*, Waterloo Maple Inc.: Waterloo, Canada, **1996**.

58. Cussler, E. L. *Diffusion- Mass Transfer in Fluid;* Syndicate of the University of Cambridge, Cambridge.**1987**. page 105-112.

59. CRC *Handbook of Chemistry and Phisics*, 64th ed.; CRC press, Inc.: Boca Raton, FL, **1983**; mpp F-5 and F-38

60. Kinston, H. M; Jassie, L.B. *Introduction to Microwave sample preparation*; American Chemical Society, Washington, DC, **1988**. Page 17.

61. Barnabas, I. J.; Dean, J. R; Fowlis, I. A; Owen, S.P. *Analyst*, **1995**,120, 1897.

62. Ganzler, K., Salago, A; Calko, K. *J. Chromatogr.* **1986**, 371, 299.

63. Yang, M. J.; Adams, M.; Pawliszyn, J. *Anal. Chem.* **1996**, 68, 2782.

64. Pan, L.; Adams, M.; Pawliszyn, J. *Anal. Chem.* **1995**, 67, 439.

65. Zhang, Z.; Pawliszyn, J. *J. High Resol. Chromatogr.* **1996**, 2, 155.

66. Langenfeld, J.; Hawthorne, S.; Miller, D. *Anal. Chem.* **1996**, 68, 144.

67. Jost, W. *Diffusion in Solids, Liquids. Gases*; Academic Press Inc.: New York, **1960**, page 412.

68. Klunder, G. L.; Russo, R. E. *Apl. Spec.* **1995**, 49, 379.

69. McGraw-Hill, *McGraw-Hill Encyclopedia of Science and Technology*; **1997**, article on "Nozzles". Page 124-126.

70. Freier, R. K. *Aqueous Solutions*, Walter de Gruyter, Berlin, 1976. 11. 365.

71. Luo, Y. Z.; Adams, M.; Pawliszyn, J. *Analyst.* **1997**, 122,1461.

72. Charalambous, G. *Analysis of food and beverages, Headspace Technique*; Academic Press: New York, **1978**. Page 71.

73. Kolb, B. *Applied Headspace Gas Chromatography* Heyden: London, **1980**. Page 169.

74. Ioffe, B. V.; Vitenberg, A. G. *Headspace Analysis and Related Methods in Gas Chromatography;* Wiley: New York, **1984**. Page 218.

75. Luo, Y. Z.; Pawliszyn, J. *Quantitative Analysis of Membrane Extraction with a Sorbent Interface*, in preparation.

76. Luo, Y. Z.; Pawliszyn, J. *Calibration of Membrane Extraction with a Sorbent Interface for air analysis*, in preparation.

77. Hayduk, W.; Laudie, H. *AIChEJ* **1974**, 20, 611.

78. Lugg, G.A.; *Anal. Chem.* **1968**, 40, 1072.

79. Martos, P.; Saraullo, A.; Pawliszyn, J. *Anal. Chem.* **1997**, 69, 402.

APPENDIX I. LIST OF ABBREVIATIONS

BTEX	a mixture of benzene, toluene, ethylbenzene, and xylene
FID	flame ionization detector
GC	gas chromatography gas chromatograph
HPLC	high performance liquid chromatography
ID	inner diameter
LOD	limit of detection
MIMS	membrane introduction mass spectrometry
MS	mass spectrometer
MESI	membrane extraction with a sorbent interface
OD	outer diameter
PC	personal computer
PDMS	Poly (dimethylsiloxane)
PTFE	poly tetraflouroethylene
RSD	relative standard deviation
SLM	supported liquid membrane
SPME	solid phase microextraction
STP	standard temperature and pressure
TCE	1,1,1-trichloroethylene
VOCs	volatile organic compounds

APPENDIX II. MODEL FOR AIR EXTRACTION

The boundary conditions

At the outside surface boundary, r = b, the boundary condition can be written

$$\frac{1}{K_s} C\big|_{r=b} = C_s \tag{1}$$

where K_s is the distribution constant between membrane and sample. To simplify the notation and to make it consistent with the reference,[32] the above equation is rewritten

$$k_1' \frac{\partial C}{\partial r} + k_2' C = k_3' \tag{2}$$

where $k'_1 = 0$, $k'_2 = 1/K_s$, $k'_3 = C_s$

At the inside surface boundary, r = a, the boundary condition can be written

$$\frac{C\big|_{r=a}}{K_g} = \overline{C_g} \tag{3}$$

where $\overline{C_g}$ is the average, lengthwise concentration in the stripping gas, and K_g is the distribution constant between membrane and stripping gas.

The method to calculate $\overline{C_g}$ is derived. The concentration in the stripping gas will change along the length of the membrane as the gas accumulates analytes. The concentration in stripping gas is expected to increase non-linearly. To analyze the non-linear concentration profile along the axis of the membrane, let x represent the distance along the membrane. The concentration in the stripping gas will change with x according to

$$C_g(x) = \int_0^x \frac{2\pi a}{Q} D \frac{\partial}{\partial r} C\big|_{r=a} dx \tag{4}$$

at the inside surface boundary, r =a, the boundary condition can be written

$$k_1 \frac{\partial C}{\partial r} - k_2 C = k_3 \tag{5}$$

where k_1=0, k_2=-1/Kg, $k_3 = \int_0^x \frac{2\pi a}{Q} D \frac{\partial}{\partial r} C|_{r=a} dx$

This problem is solved only for the steady-state condition. At the steady-state, the concentration in the membrane is considered a function of two variables, C (r, x). To solve this problem, the Laplace transformation is applied in the variable x. The unknown function C (r, x) becomes its Laplace transform L {C}. The boundary condition coefficients become $k_1 = -\frac{2\pi aD}{Qp}, k_2 = -\frac{1}{K_g}, k_3 = 0$, and k'_1=0, k'_2 =1/K_s, k'_3 =C_s /p. The solution, from the reference:[32]

$$L\{C\}(r,p) = \frac{bk'_3 k_1 + abk_2 k'_3 \ln(r/a)}{ak_2 k'_1 + bk_1 k'_2 \, abk_2 k'_2 \ln(b/a)} \tag{6}$$

the above expression has two poles at p=0 and p=p_0, where $p_0 = -\frac{2\pi D k_g}{Q \ln b/a}$, The inverse Laplace transform gives the result

$$C(r,x) = K_s C_s (1 - \frac{\ln b/r}{\ln b/a} e^{p_0 x}) \tag{7}$$

At steady-state the average concentration in the stripping gas with respect to length is

$$\overline{C}_g = \frac{1}{L} \int_0^L C_g(x) dx \tag{8}$$

and the average stripping gas concentration as a function of its exit concentration is

$$f = \frac{\overline{C_g}}{C_g(L)} \tag{9}$$

At steady-state this value can be calculated from the equations (4), (7) and (8).

Equations of Diffusion and Extraction Rates

The extraction rate of the MESI process can be predicted by solving the diffusion equation for the membrane geometry and boundary conditions. The equation describing diffusion according to Fick's second law in cylindrical polar coordinates is

$$\frac{D}{r}\frac{\partial}{\partial r}\left(r\frac{\partial}{\partial r}C(r,t)\right)=\frac{\partial}{\partial t}C(r,t) \qquad (10)$$

To predict the extraction versus time profile, i.e., the non-steady-state process, we consider only the diffusion average, lengthwise. The concentration profile in the stripping gas along the length of the membrane is assumed to have the same shape from the start of extraction until steady-state. In other words, the value of "f" is assumed to be constant from the start of extraction until steady-state.

For this simplified average diffusion model, the flux is considered equal everywhere along the length of the membrane. The concentration in the stripping gas exiting the membrane equals the analyte flux across the inner surface, multiplied by inner surface area, divided by flow rate. Thus the boundary condition at r = a is

$$\frac{C|_{r=a}}{K_g}=\overline{C_g}=\frac{2\pi afl}{Q}D\frac{\partial}{\partial r}C|_{r=a} \qquad (11)$$

If we consider only the average conditions, the boundary conditions at r = b are formula (3) with $k'_1 = 0$, $k'_2 = 1/K_s$, $k'_3 = C_s$, and at r = a formula (6) with $k_1 = 2\pi af\,LD/R$, $k_2 = 1/K_g$, $k_3 = 0$. The solution to this problem, to predict extraction rate versus time, is given in the reference.[32] The solution is

$$C(r,t)=K_sC_s\frac{\theta+a\ln r/a}{\theta+a\ln b/a}-K_sC_s\sum_{n=1}^{\infty}e^{-D\alpha_n^2t}\frac{J_0(b\alpha_n)\{\theta\alpha_nJ_1(a\alpha_n)+J_0(a\alpha_n)\}}{F(\alpha_n)}H(r,\alpha_n) \qquad (12)$$

where $\theta = ADfK_g/Q$, A is the membrane inner surface area, $A = 2\pi aL$, and the α_n are the positive roots of

$$-[\theta\alpha J_1(a\alpha)+J_0(a\alpha)]Y_0(b\alpha)+[\theta\alpha Y_1(a\alpha)+Y_0(a\alpha)]J_0(b\alpha)=0 \qquad (13)$$

In the above expression,

$$F(\alpha_n)=[\theta\alpha_n J_1(a\alpha_n)+J_0(a\alpha_n)]^2-(\theta^2\alpha_n^2+1)[J_0(b\alpha_n)]^2 \qquad (14)$$

and

$$H(r,\alpha_n)=J_0(r\alpha_n)[\theta\alpha_n Y_1(a\alpha_n)+Y_0(a\alpha_n)]-Y_0(a\alpha_n)[\theta\alpha_n J_1(a\alpha_n)+J_0(a\alpha_n)]$$

(15)

From this solution we can calculate extracted amount at time t by

$$Z(t)=AC_sDK_s\{\frac{t}{\theta+a\ln b/a}-\frac{2}{aD}\sum_{n=1}^{\infty}(1-e^{-D\alpha_n^2 t})\frac{J_0(b\alpha_n)[\theta\alpha_n J_1(a\alpha_n)+J_0(a\alpha_n)}{F(\alpha_n)\alpha_n^2}\} \qquad (16)$$

and the extraction rate by

$$G(t)=\frac{\partial}{\partial t}Z(t)=AC_sDK_s\{\frac{1}{\theta+a\ln b/a}-\frac{2}{a}\sum_{n=1}^{\infty}e^{-D\alpha_n^2 t}\frac{J_0(b\alpha_n)[\theta\alpha_n J_1(a\alpha_n)+J_0(a\alpha_n)}{F(\alpha_n)}\} \qquad (17)$$

The above formula can be used to calculate the time to reach steady-state extraction. A computer program must be used to find the roots of Eq. 13 and then calculate extraction rate or extraction amount. At steady-state, the formula for C (r, t) simplifies to

$$C(r)=K_sC_s\frac{\theta+a\ln r/a}{\theta+a\ln b/a} \qquad (18)$$

The extraction rate at steady-state is

$$G_{ss}=AC_sDK_s\frac{1}{\theta+a\ln b/a} \qquad (19)$$

APPENDIX III. MODEL FOR WATER EXTRACTION

Mass Transfer Process

1. Convection and diffusion through sample to the membrane outside surface. This complex phenomenon is understood by the fluid dynamics theory. At the membrane outer surface, i.e. at r = b where r represents radius from the membrane axis, the mass transfer can be described by [32]

$$(C_s - \frac{C|_{r=b}}{K_{ms}})h_0 = D_m \frac{\partial C}{\partial r}|_{r=b} \qquad (1)$$

where C_s is analyte concentration in the bulk sample, assumed constant [μg/L]; h_o is coefficient of mass transfer from sample to the membrane outer surface [kg/sec m^2]; K_{ms} is distribution constant of analyte between sample and membrane, concentration in membrane divided by concentration in sample at the interface [dimensionless, μg/L: μg/L]; $C|_{r=b}$ is the analyte concentration in the membrane at its outer surface [μg/L]; and D_m is the analyte's diffusion coefficient in the membrane [cm^2/sec].

The mass transfer coefficient is given by $h_o = Nu_o \cdot D_s/2b$ where Nu_o is the Nusselt number, and D_s is the analyte's diffusion coefficient in the fluid. The Nusselt number for a cylinder in a fluid cross flow is [55]

$$Nu_0 = 0.3 + \frac{0.62\,Re_d^{0.5}\,Sc^{1/3}}{[1+(0.4/Sc)]^{1/4}} \qquad \text{for } Re_dSc>0.2 \text{ and } Re_d<10{,}000 \qquad (2)$$

where Re_d is the Reynolds number and Sc the Schmidt number of the fluid, defined $Re_d = u^2b/v$, $Sc = v/D_s$ where u is fluid velocity [cm/sec] and v its kinematic viscosity [cm^2/s].

Let $k'_1 = K_{ms}D_m/bh_o = 2K_{ms}D_m/Nu_oD_s$. The parameter k'_1 is a measure of the resistance to mass transfer at the membrane outer surface. When $k_1' = 0$, concentration in the membrane at r = b is equal to sample bulk concentration multiplied by the distribution constant, i.e. concentration in the membrane is at its maximum possible. As k_1' increases the concentration at r = b decreases from this maximum possible, i.e. a concentration drop occurs due to mass transfer resistance of the boundary layer.

2. Partitioning between sample and membrane at its outer surface. This process follows Henry's law for an air sample, and Nernst's law for a water sample. Henry's law states that the ratio of analyte partial pressure to $C|_{r=b}$ at the interface is constant over low concentrations, and varies with exp(ΔH/RT), where ΔH is the heat of sorption from sample to membrane and R is the gas constant. Since K_{ms} is a ratio of mass-per-volume concentrations and pressure is assumed to be 1 atm constant, K_{ms} will vary with exp(ΔH/RT)/T. For non-polar solutes partitioning between air and polymer, ΔH is approximately equal to heat of vaporization, available from published tables.[56] Nernst's law states that K_{ms} is constant over low concentrations and varies with exp(ΔH/RT).

3. Diffusion through membrane. Initial analyte concentration is constant throughout the sample, and zero in membrane and stripping gas. End effects of the membrane are assumed negligible so diffusion is symmetric about and along the membrane axis, which is described by Fick's law in one dimension, radius r,

$$\frac{D_m}{r}\frac{\partial}{\partial r}\left(r\frac{\partial}{\partial r}C(r,t)\right) = \frac{\partial}{\partial t}C(r,t) \qquad (3)$$

where t is the time from the start of extraction. The analyte diffusion coefficient in a polymer varies with exp(-E_d/RT), where E_d is the apparent activation energy for diffusion and R is the gas constant.

4. Partitioning between membrane and stripping gas at the membrane inner surface. This mass transfer step follows Henry's or Nernst' law, as in step 2.

5. Diffusion and convection of analyte into stripping gas which flows out the membrane. This mass transfer step is understood by fluid dynamics theory, as in step 1, but concentration is not constant in the stripping gas. The boundary condition at r = a is modeled

$$D_m \frac{\partial C}{\partial r}\Big|_{r=b} = h_i\left(\frac{C|_{r=a}}{K_{mg}} - \overline{C_g}\right) \qquad (4)$$

where h_i is coefficient of mass transfer from membrane to stripping gas, K_{mg} is the distribution constant between membrane and stripping gas, concentration in membrane divided by concentration in stripping gas [dimensionless, μg/L : μg/L], and $\overline{C_g}$ is the average bulk concentration in the stripping gas [μg/L]. The bulk concentration in the stripping gas changes along the length of the membrane as it picks up analyte. The average concentration in stripping gas is assumed to be a constant fraction, *f*, of the exit concentration. In other words the concentration profile along the length of the membrane is assumed to have the same shape from start of extraction until steady-state. Flux through the membrane inner surface (mass in) must equal stripping gas exit concentration times flow rate (mass out), which gives

$$AD_m \frac{\partial}{\partial r} C\Big|_{r=a} = Q\frac{\overline{C_g}}{f} \qquad (5)$$

where A is the membrane inner surface area [cm^2], A = 2πaL, L is the length of the membrane, and Q is stripping gas volumetric flow rate [ml/min], assumed constant. (Extraction rate change

is assumed to be slow compared with contact time between membrane and an average element of stripping gas.) The mass transfer coefficient h_i is calculated from the Nusselt number, the same way as h_o, which for flow inside a cylinder is[55]

$$Nu_i = 3.65 + \frac{0.13a\,\mathrm{Re}_d\,Sc}{1+0.04[2a\,\mathrm{Re}_d\,Sc]^{2/3}} \qquad \text{if } \mathrm{Re}_d<2300 \qquad (6)$$

where Re_d and Sc are as defined for eq. (2) above except 'b' is replaced by 'a'. Combining (4), (5) and the relation between h_i and Nu_i gives

$$2aD_m K_{mg}\left(\frac{1}{Nu_i D_g}+\frac{\pi Lf}{Q}\right)\frac{\partial C}{\partial r}-C\big|_{r=a}=0 \qquad (7)$$

Let $k_1 = 2D_m K_g\left(\frac{1}{Nu_i D_g}+\frac{\pi Lf}{Q}\right)$. The parameter k_1 is a measure of resistance to mass transfer at the membrane inner surface, similar to the significance of k_1' at the outer surface.

To estimate 'f' it is determined for the steady state case, let x represent distance along the membrane. At the membrane outer surface r = b the boundary condition is eq.(1). At the membrane inner surface r =a bulk concentration in stripping gas changes with x according to

$$C_g(x) = \int_0^x \frac{2\pi a}{Q} D_m \frac{\partial}{\partial r} C\big|_{r=a}\,dx \qquad (8)$$

so the boundary condition can be written

$$D_m \left.\frac{\partial C}{\partial r}\right|_{r=a} = h_i\left(\frac{C|_{r=a}}{K_g}-\frac{2\pi a D_m}{Q}\int_0^x \frac{\partial C}{\partial r}\,dx\right) \qquad (9)$$

(Diffusion along the axis in membrane and in stripping gas is assumed insignificant.) The steady-state boundary value problem specified by (1), (3) and (9) is solved by applying the Laplace transform in x to obtain a differential equation in one variable, r. This one dimensional

problem is solved.[32] From that result the inverse Laplace solution has the form $C(r,x) = K_{ms}[1 - B(r)e^{-p_0 x}]$ with two poles p=0 and p=p_0,

$$p_0 = \frac{\pi Q^{-1}}{\frac{K_{ms}}{K_{mg} Nu_o D_s} + \frac{1}{Nu_i D_g} + \frac{\ln\phi}{2D_m K_{mg}}} \tag{10}$$

where ϕ=b/a. Substituting this formula for C(r, x) in (8) gives a formula for C_g (x) which is used in $\overline{C}_g = \frac{1}{L}\int_0^L C_g(x)$ to give finally

$$f = \frac{\overline{C}_g}{C_g(L)} = \frac{1}{1 - e^{-p_0 L}} - \frac{1}{p_0 L} \tag{11}$$

independent of the exact expression for B (r). Note 0.5<f<1.

Equations of Diffusion and Extraction Rates

The boundary value problem specified by (1), (3) and (7) is solved in the reference,[32] giving an expression for C(r, t). From this solution the expression for extraction rate can be written down in the dimensionless parameters k'_1, k_1, ϕ and $\Omega = D_m t/a^2$ as

$$G(t) = AD_m \frac{\partial}{\partial r}(r,t)\Big|_{r=a} =$$

$$\frac{A}{a} D_m K_s C_s \{\frac{1}{k_1' + k_1 + \ln\phi} + 2\sum_{n\geq 1} \frac{e^{-\Omega\alpha_n}}{F(\alpha_n)} [k_1'\phi\alpha_n J_1(\phi\alpha_n) - J_0(\phi\alpha_n)][k_1\alpha_n J_1(\alpha_n) + J_0(\alpha_n)]\} \tag{12}$$

Where $\pm\alpha_1$, $\pm\alpha_2$, $\pm\alpha_3$ ... are the roots of

$$[k_1\alpha J_1(\alpha) + J_0(\alpha)][k_1'\phi\alpha Y_1(\phi\alpha) - Y_0(\phi\alpha)] - [k_1\alpha Y_1(\alpha) + Y_0(\alpha)][k_1'\phi\alpha Y_1(\phi\alpha) - J_0(\phi\alpha)] = 0$$

and

$$F(\alpha) = (k_1'^2\phi^2\alpha^2 + 1)[k_1\alpha J_1(\alpha) + J_0(\alpha)]^2 - (k_1^2\alpha^2 + 1)[k_1'\phi\alpha J_1(\phi\alpha) - J_0(\phi\alpha)]^2$$

J_i and Y_i are the Bessel functions of the first and second kind, of order i.

A formula for response time, the time when extraction rate reaches 90% of its steady state, accurate to ±15% for $1.3<\phi<5$ was derived, as explained in the reference [32] using a symbolic algebra program:[57]

$$t_{90\%} = \frac{a2}{2D_m}\frac{(1+\phi^2)\ln\phi - \phi^2 + 1 + (\phi^2 - 1 - 2\ln\phi)k_1 - (\phi^2 - 1 - 2\phi^2\ln\phi)k_1' + 2(\phi^2 - 1)k_1k_1'}{k_1' + k_1 + \ln\phi} \tag{13}$$

If k'_1 and k_1 are not significant, the response time

$$t_{90\%} = \frac{-a^2}{2D_m}(\phi^2 + 1 - \frac{\phi^2 - 1}{\ln\phi}) \cong 0.32\frac{(b-a)^2}{D_m} \tag{14}$$

The formula for steady state extraction rate is seen from (12) to be

$$Ge = \frac{2\pi LD_mK_{ms}C_s}{k_1' + k_1 + \ln\phi} = \frac{\pi LC_s}{\frac{1}{Nu_0D_s} + \frac{K_{mg}}{K_{ms}}(\frac{1}{3.65D_g} + \frac{\pi fL}{Q}) + \frac{\ln\phi}{2D_mK_{ms}}} \tag{15}$$

Concentration in the stripping gas approaches equilibrium if

$$\frac{L}{Q} \rangle \frac{1.6}{\pi}\frac{K_{ms}}{K_{mg}}(\frac{1}{Nu_0D_s} + \frac{\ln\phi}{2K_{ms}D_m} \tag{16}$$

from (8), and under this condition

$$Ge = 0.9C_sQK_{ms}/K_{mg} \qquad \pm 10\% \tag{17}$$

APPENDIX IV. MAPLE PROGRAM FOR AIR MODEL

First, input the parameters:

```
> Digits:=20;
>Kg:=485*.9;Ks:=485;h:=11.25;Dd:=1.91*10^(6);a:=.0305/2;b:=a+.0165;R:=2.5/60;hp:=2.12;
C_Ar:=1;A:=2*Pi*a*4.;theta:=Ks*Dd*A/2/R;
                    Kg := 436.5
                    Ks := 485
                 h := 11.25
               D_d := .19100000000000000000 10^-5
              a := .01525000000000000000
              b := .03175000000000000000
R := .041666666666666666668
hp := 2.12
                   C_Ar := 1
                A := .12200000000000000000 Pi
              theta := .0013561764000000000000 Pi
                    Digits := 20
> k1:=theta; k2:=1.; k3:=0.;
               k1 := .0013561764000000000000 Pi
                    k2 := 1.
                    k3 := 0
> k1p:=.0; k2p:=1.; k3p:=Ks*CAr;
```

k1p := 0

k2p := 1.

k3p := 485

> kappa:=D_d;

kappa := .19100000000000000000 10^{-5}

Next, we must determine the roots of "(5)":

>five:=proc(alph)(k1*alph*BesselJ(1,a*alph)+k2*BesselJ(0,a*alph))*(k1p*alph*BesselY(1,b*al
ph)-k2p*BesselY(0,b*alph))-
(k1*alph*BesselY(1,a*alph)+k2*BesselY(0,a*alph))*(k1p*alph*BesselJ(1,b*alph)-
k2p*BesselJ(0,b*alph)) end;

five :=proc(alph)(k1*alph*BesselJ(1,a*alph)+ k2*BesselJ(0,a*alph))*(
p*alph*BesselY(1,b*alph)-k2p*BesselY(0,b*alph))-(k1*alph*BesselY(1,a*alph)+
k2*BesselY(0,a*alph))*(k1p*alph*BesselJ(1,b*alph)-
k2p*BesselJ(0,b*alph))
end

k := 4

al := array(1 .. 4, [])

Use "plot" to see approximately the first five roots after 0 (note: smallest root may be of the order 0.01 but not equal to 0):

> Digits:=10;plot(five(x),x=0..1000);

Digits := 10

> k:=30;al:=array(1..k);

```
                    k := 30

                al := array(1 .. 30, [])
> Digits:=20;

                    Digits := 20

> froots:= proc (bound,incr,alp,f)  local sgn1,sgn2,arg,temp,term,Nn:sgn1:=csgn(f(0.01*incr)):
term:=1: for arg from incr by incr to 1000*incr while (term<=bound) do sgn2:=csgn(f(arg)): if
sgn2<>sgn1 then alp[term]:=fsolve(f(x),x,(arg-incr)..arg,fulldigits): sgn1:=sgn2: temp:=term+1:
term:=temp: fi: od: Nn := term-1: end;
froots :=
 proc(bound,incr,alp,f)
 local sgn1,sgn2,arg,temp,term,Nn;
    sgn1 := csgn(f(.01*incr));
    term := 1;
    for arg from incr by incr to
       1000*incr while term <= bound
       do
       sgn2 := csgn(f(arg));
       if sgn2 <> sgn1 then
          alp[term] := fsolve(f(x),x,
             arg-incr .. arg,
             fulldigits);
          sgn1 := sgn2;
          temp := term+1;
```

```
        term := temp
      fi
   od;
   Nn := term-1
end
                    Digits := 20
> al[3]:=fsolve(five(x),x=600..850,fulldigits);
              al[3] := 794.93166734701857257


> inc:=30;froots(k,inc,al,five);
                    inc := 30
> evalf(al[10]);
                1817.5084537940576246
> F:=proc(alph) (k1p^2*alph^2+k2p^2)*(k1*alph*BesselJ(1,a*alph)+k2*BesselJ(0,a*alph))^2-
(k1^2*alph^2+k2^2)*(k1p*alph*BesselJ(1,b*alph)-k2p*BesselJ(0,b*alph))^2 end;
F := proc(alph)
      (k1p^2*alph^2+k2p^2)*(
         k1*alph*BesselJ(1,a*alph)+
         k2*BesselJ(0,a*alph))^2-
         (k1^2*alph^2+k2^2)*(
         k1p*alph*BesselJ(1,b*alph)-
         k2p*BesselJ(0,b*alph))^2
   end
```

```
> C:=proc(r,alph) BesselJ(0,r*alph)*(k1*alph*BesselY(1,a*alph)+k2*BesselY(0,a*alph))-
BesselY(0,r*alph)*(k1*alph*BesselJ(1,a*alph)+k2*BesselJ(0,a*alph)) end;

C := proc(r,alph)
      BesselJ(0,r*alph)*(
         k1*alph*BesselY(1,a*alph)+
         k2*BesselY(0,a*alph))-
         BesselY(0,r*alph)*(
         k1*alph*BesselJ(1,a*alph)+
         k2*BesselJ(0,a*alph))
   end

> vv:=proc(r,t) (-a*k3*(k1p-
b*k2p*ln(r/b))+b*k3p*(k1+a*k2*ln(r/a)))/(a*k2*k1p+b*k1*k2p+a*b*k2*k2p*ln(b/a)) -
Pi*Sum(exp(-al[n]^2*kappa*t)*(k1p*al[n]*BesselJ(1,b*al[n])-
k2p*BesselJ(0,b*al[n]))/F(al[n])*C(r,al[n])*(k3*(k1p*al[n]*BesselJ(1,b*al[n])-
k2p*BesselJ(0,b*al[n]))-k3p*(k1*al[n]*BesselJ(1,a*al[n])+k2*BesselJ(0,a*al[n]))),n=1..k) end;
vv :=
proc(r,t)
   (-a*k3*(k1p-b*k2p*ln(r/b))+
   b*k3p*(k1+a*k2*ln(r/a)))/(
   a*k2*k1p+b*k1*k2p+a*b*k2*k2p*ln(b/a)
```

```
  )-Pi*Sum(exp(-al[n]^2*kappa*t)*(
  k1p*al[n]*BesselJ(1,b*al[n])-
  k2p*BesselJ(0,b*al[n]))/F(al[n])*
  C(r,al[n])*(k3*(
  k1p*al[n]*BesselJ(1,b*al[n])-
  k2p*BesselJ(0,b*al[n]))-k3p*(
  k1*al[n]*BesselJ(1,a*al[n])+
  k2*BesselJ(0,a*al[n]))),n = 1 .. k)
end
> tt:=60;plot({vv(r,tt),(k3p*ln(r/a)-vv(a,tt)*ln(r/b))/ln(b/a)},r=a..b);
                        tt := 60
> k:=8;Digits:=10;tt:=75;evalf(vv(a,tt))*2*R/Ks;
                         k := 8
                       Digits := 10
                        tt := 75
                       .02174887080
> "*.95;
                       .02184039153
> plot(vv(a,t)*2*R/Ks,t=0..240);
```

Rate of extraction at inner surface, rr = dvv/dr at r = a.

```
> dC:=proc(alph) -
BesselJ(1,a*alph)*alph*(k1*alph*BesselY(1,a*alph)+k2*BesselY(0,a*alph))+BesselY(1,a*alph
)*alph*(k1*alph*BesselJ(1,a*alph)+k2*BesselJ(0,a*alph)) end;
```

```
dC :=
  proc(alph)
    -BesselJ(1,a*alph)*alph*
      (k1*alph*BesselY(1,a*alph)+k2*BesselY(0,a*alph))+
      BesselY(1,a*alph)*alph*
      (k1*alph*BesselJ(1,a*alph)+k2*BesselJ(0,a*alph))
  end
> rr :=proc(t) (-a*k3*(k1p-
b*k2p/a)+b*k3p*(k1+k2))/(a*k2*k1p+b*k1*k2p+a*b*k2*k2p*ln(b/a)) - Pi*Sum(exp(-
al[n]^2*kappa*t)*(k1p*al[n]*BesselJ(1,b*al[n])-
k2p*BesselJ(0,b*al[n]))/F(al[n])*dC(al[n])*(k3*(k1p*al[n]*BesselJ(1,b*al[n])-
2p*BesselJ(0,b*al[n]))-k3p*(k1*al[n]*BesselJ(1,a*al[n])+k2*BesselJ(0,a*al[n]))),n=1..k) end;
rr :=proc(t)
  (-a*k3*(k1p-b*k2p/a)+b*k3p*(k1+k2))/
  (a*k2*k1p+b*k1*k2p+a*b*k2*k2p*ln(b/a))-Pi*Sum(
  exp(-al[n]^2*kappa*t)*
  (k1p*al[n]*BesselJ(1,b*al[n])-k2p*BesselJ(0,b*al[n]))/
  F(al[n])*dC(al[n])*(
  k3*(k1p*al[n]*BesselJ(1,b*al[n])-k2p*BesselJ(0,b*al[n]))
  -k3p*(k1*al[n]*BesselJ(1,a*al[n])+k2*BesselJ(0,a*al[n]))
  ),n = 1 .. k)
end
> plot(rr(t),t=1..60);
```

APPENDIX V. MAPLE PROGRAM FOR WATER MODEL AND AIR MODEL (WHEN BOUNDARY LAYERS ARE COUNTED)

MAPLE SHEET TO CALCULATE RESPONSE TIME AND STEADY STATE EXTRACTION RATE FROM A MESI SYSTEM MEMBRANE, BASED ON THE THEORY IN "MESI FOR WATER PAPER". JUNE 8, 1997, MARC ADAMS.

VARIABLES:

A - MEMBRANE INNER RADIUS (CM)

B - MEMBRANE OUTER RADIUS (CM)

PHI = B/A

L - MEMBRANE LENGTH (CM)

R - STRIPPING GAS VOLUMETRIC FLOW RATE (CM^3/SEC)

C_S - SAMPLE CONCENTRATION (MASS / CM^3)

U - SAMPLE FLOW SPEED (CM/SEC)

T - AMBIENT TEMPERATURE (K)

N_U - SAMPLE FLUID KINEMATIC VISCOSITY (CM^2/S)

N_U - NUSSELT NUMBER, I - INNER, O - OUTER

R_{ED} - REYNOLDS NUMBER, SC - SCHMIDT NUMBER

K_{MS} - MEMBRANE TO SAMPLE DISTRIBUTION CONSTANT

K_{MG} - MEMBRANE TO STRIPPING GAS DISTRIBUTION CONSTANT

D_S, D_M, D_G - DIFFUSION COEFFICIENT IN THE SAMPLE, MEMBRANE, STRIPPING GAS (CM^2/SEC)

K1P OR K1N - PARAMETER FOR OUTSIDE SURFACE

K1 - PARAMETER FOR INSIDE SURFACE

T90 - RESPONSE TIME (SEC)

GE - STEADY STATE EXTRACTION RATE (MASS / SEC)

THIS WORKSHEET HAS TWO SECTIONS:

1) FORMULAE FOR T90 AND FOR GE.

2) USING THE EXACT MODEL (EQUATION 12 IN REFERNCE 71) TO CALCULATE T90 OR GE OR T1/2.

PARAMETERS OF THE MESI SYSTEM:

> A:=.0305/2;B:=A+.0165;PHI:=B/A;L:=4;R:=2.2/60;C_S:=66;

A := .01525000000

B := .03175000000

PHI := 2.081967213

L := 4

R := .03666666667

C_S := 66

PHYSICO PARAMETERS FOR WATER:

> T:=296;NU:=.1083-.000332*T;U:=55;

T := 296

NU := .010028

U := 55

PHYSICO PARAMETERS FOR AR:

> T:=296;NU:=.15*(T/300)^1.8;U:=1000/60/EVALF(PI*2^2);

T := 296

NU := .1464192171

U := 1.326291192

PARA. FOR TCEY IN WATER:

> KMS:=182;KMG:=443;DS:=.96*10^(-5);DG:=.0875;DM:=1.81*10^(-6);

KMS := 182

KMG := 443

DS := .9600000000 10^{-5}

DG := .0875

DM := .1810000000 10^{-5}

PARA. FOR HEXANE IN WATER:

> KMS:=126;KMG:=224;DS:=.9*10^(-5);DG:=.0732;DM:=2.27*10^(-6);

KMS := 126

KMG := 224

DS := .9000000000 10^{-5}

DG := .0732

DM := .2270000000 10^{-5}

PARAMETERS FOR BENZENE IN AR:

> KMS:=485;KMG:=485;DS:=.093;DG:=0.38;DM;X:=2.12*10^(-6);

KMS := 485

KMG := 485

DS := .093

DG := .38 1090000000 10^{-5}

X := .2120000000 10^{-5}

PARAMETERS FOR BENZENE IN WATER:

> KMS:=136;KMG:=485;DS:=1.09*10^(-5);DG:=0.08;DM:=2.12*10^(-6);

KMS := 136

KMG := 485

DS := .00001090000000

DG := .08

DM := .2120000000 10^{-5}

PARAMETERS FOR TOLUENE IN AR:

> KMS:=1872;KMG:=1872;DS:=.085;DG:=0.38*.085/.093;DM:=1.59*10^(-6);

KMS := 1872

KMG := 1872

DS := .085

DG := .3473118280

DM := .1590000000 10^{-5}

PARAMETERS FOR TOLUENE IN WATER:

> KMS:=346;KMG:=1872;DS:=.95*10^(-5);DG:=0.38*.085/.093;DM:=1.59*10^(-6);

KMS := 346

KMG := 1872

DS := .9500000000 10^{-5}

DG := .3473118280

DM := .1590000000 10^{-5}

PARAMETERS FOR ETHYLBENZENE IN AR:

> KMS:=3380;KMG:=3380;DS:=.0755;DG:=0.38*.0755/.093;DM:=1.09*10^(-6);

KMS := 3380

KMG := 3380

DS := .0755

DG := .3084946237

DM := .1090000000 10^{-5}

PARAMETERS FOR ETHYLBENZENE IN WATER:

KMS:=847;KMG:=3380;DS:=.9*10^(-5);DG:=0.38*.0755/.093;DM:=1.09*10^(-6);

KMS := 847

KMG := 3380

DS := .9000000000 10^{-5}

DG := .3084946237

DM := .1090000000 10^{-5}

PARAMETERS FOR TCEY IN AR:

> KMS:=443;KMG:=443;DS:=.0755;DG:=0.38*.0755/.093;DM:=1.81*10^(-6);

KMS := 443

KMG := 443

DS := .0755

DG := .3084946237

DM := .1810000000 10^{-5}

CALCULATIONS START HERE:

FUNCTIONS:

T90 - ESTIMATES THE RESPONSE TIME, SEC

GE - GIVES THE STEADY STATE EXTRACTION RATE (MASS/SEC)

FIVE - THE FUNCTION FOR THE ROOTS USED IN THE SERIES FOR G(T)

F - FUNCTION PART OF EXPRESSION FOR G(T). (SEE PAPER)

G(T) - THE EXTRACTION RATE AS A FUNCTION OF TIME

TII - FIND THE RESPONSE TIME

CALCULATE DIMENSIONLESS FLUID PARAMETERS FOR FLUID AND ANALYTE:

> T:=296;RED:=2.*U*B/NU;SC:=NU/DS;NUO:=.3+.62*RED^.5*SC^.33/(1+(.4/SC)^.66)^.25;

T := 296

RED := .5751942428

SC := 1.722579025

NUO := .8189807674

PARAMETERS FOR STRIPPING GAS:

> NUI:=3.65;

NUI := 3.65

NOW CALCULATE THE MODEL PARAMETERES AND PREDICTIONS:

>K1P:=2*KMS*DM/NUO/DS;K1A:=2*KMG*DM/NUI/DG;K1B:=EVALF(2*KMG*DM*PI*

L/R);P0L:=K1B/(K1P+K1A+LN(PHI));F:=EVALF(1/(1-EXP(-P0L))-

1/P0L);K1:=K1A+K1B*F;

K1P := .08551461318

K1A := .004695918232

K1B := 2.040193681

P0L := 2.477395062

F := .6880075686

K1 := 1.408364612

```
PREDICT THE RESPONSE TIME:
> T90:=PROC (PHIS, K1M, K1N) OPTIONS OPERATOR, ARROW;
A^2/DM*(2*LN(PHIS)*K1N*PHI^2-2*LN(PHIS)*K1M+LN(PHIS)+LN(PHIS)*PHIS^2-
K1N*PHIS^2+PHIS^2*K1-PHIS^2+2*PHIS^2*K1M*K1N+K1N-K1M+1-
2*K1M*K1N)/(K1N+K1M+LN(PHIS))/2. END;
> EVALF(T90(PHI,K1,K1P));
T90 := (PHIS, K1M, K1N) -> .5000000000 A  (2 LN(PHIS) K1N PHI
   - 2 LN(PHIS) K1M + LN(PHIS) + LN(PHIS) PHIS  - K1N PHIS
   + PHIS  K1 - PHIS  + 2 PHIS  K1M K1N + K1N - K1M + 1 - 2 K1M K1N
  )/(DM (K1N + K1M + LN(PHIS)))

PREDICT THE STEADY STATE EXTRACTION RATE:
> GE:=EVALF(2*PI*L*DM*KMS*CS/(K1P+K1+LN(PHI)));
                GE := 2.216812792
THE EXACT MODEL CAN BE USED TO PREDICT EXTRACTION RATE VS TIME:
> DIGITS:=10;ALIAS(J=BESSELJ,Y=BESSELY);
                  DIGITS := 10
> FIVE:=PROC(ALPH)  GLOBAL PHI,K1,K1P;
(K1*ALPH*J(1,ALPH)+J(0,ALPH))*(K1P*PHI*ALPH*Y(1,PHI*ALPH)-Y(0,PHI*ALPH))-
(K1*ALPH*Y(1,ALPH)+Y(0,ALPH))*(K1P*PHI*ALPH*J(1,PHI*ALPH)-J(0,PHI*ALPH))
END;
FIVE := PROC(ALPH)
GLOBAL PHI, K1, K1P;
```

```
  (K1*ALPH*J(1, ALPH) + J(0, ALPH))*
  (K1P*PHI*ALPH*Y(1, PHI*ALPH) - Y(0, PHI*ALPH)) -
  (K1*ALPH*Y(1, ALPH) + Y(0, ALPH))*
  (K1P*PHI*ALPH*J(1, PHI*ALPH) - J(0, PHI*ALPH))
END

> FROOTS:= PROC (BOUND,INCR,ALP,F)  LOCAL
> SGN1,SGN2,ARG,TEMP,TERM,NN:SGN1:=CSGN(F(0.01*INCR)): TERM:=1: FOR ARG
> FROM INCR BY INCR TO 1000*INCR WHILE (TERM<=BOUND) DO
> SGN2:=CSGN(F(ARG)): IF SGN2<>SGN1 THEN
> ALP[TERM]:=FSOLVE(EVALF(F(XYZ)),XYZ,(ARG-INCR)..ARG,FULLDIGITS):
> SGN1:=SGN2: TEMP:=TERM+1:  TERM:=TEMP: FI: OD: NN := TERM-1: END;

FROOTS := PROC(BOUND, INCR, ALP, F)
LOCAL SGN1, SGN2, ARG, TEMP, TERM, NN;
   SGN1 := CSGN(F(.01*INCR));
   TERM := 1;
   FOR ARG FROM INCR BY INCR TO 1000*INCR WHILE TERM <= BOUND DO
      SGN2 := CSGN(F(ARG));
      IF SGN2 <> SGN1 THEN
         ALP[TERM] := FSOLVE(EVALF(F(XYZ)), XYZ,
         ARG - INCR .. ARG, FULLDIGITS);
         SGN1 := SGN2;
```

```
        TEMP := TERM + 1;
        TERM := TEMP
END

> F:=PROC(ALPH)
> (K1P^2*PHI^2*ALPH^2+1)*(K1*ALPH*J(1,ALPH)+J(0,ALPH))^2-
(K1^2*ALPH^2+1)*(K1P*PHI*ALPH*J(1,PHI*ALPH)-J(0,PHI*ALPH))^2 END;

F := PROC(ALPH)
   (K1P^2*PHI^2*ALPH^2 + 1)*(K1*ALPH*J(1, ALPH) + J(0, ALPH))^2
    - (K1^2*ALPH^2 + 1)*
   (K1P*PHI*ALPH*J(1, PHI*ALPH) - J(0, PHI*ALPH))^2
END

> G:=(T) -> 2*PI*L*DM*KMS*CS*(1./(K1P+K1+LN(PHI)) - 2*SUM(EXP(-
AL[N]^2*T)*(K1P*PHI*AL[N]*J(1,PHI*AL[N])-
J(0,PHI*AL[N]))*(K1*AL[N]*J(1,AL[N])+J(0,AL[N]))/F(AL[N]),N=1..K));
EXP(-AL[N]  T) (K1P PHI AL[N] J(1, PHI AL[N]) - J(0, PHI AL[N]))
(K1 AL[N] J(1, AL[N]) + J(0, AL[N]))/F(AL[>
K:=20;AL:=ARRAY(1..K);FROOTS(K,INC,AL,FIVE);
> T:=0.0396;EVALF(G(T*DM/A^2))/GE;
> PLOT(EVALF(G(TS*DM/A^2))/GE,TS=0..300)
```

GLOSSARY

a membrane inner radius [cm]

b membrane outer radius [cm]

d membrane wall thickness

f ratio of average concentration to exit concentration in stripping gas [dimensionless]

h_o, h_i mass transfer coefficients at the membrane outer and inner surfaces, respectively [kg s^{-1} m^{-2}]

k'_1 $K_{ms}D_m/bh_o$ [dimensionless]. This parameter is a measure of the resistance to mass transfer at the membrane outer surface.

k_1 [dimensionless]. This parameter is a measure of the resistance to mass transfer at the membrane inner surface.

r radius since the membrane axis [cm]

t time [s]

$t_{90\%}$ response time, t, at which extraction rate reaches 90% of its steady state value [sec]. This is also the time from any change in C_s until 90% of the resulting change in steady state extraction rate.

u sample fluid velocity [cm s^{-1}]

x distance along the length of the membrane [cm]. x = 0 at the point where stripping gas enters the membrane, and x = L at the exit.

A membrane inner surface area [cm^2], $A = 2\pi aL$.

B(r) a function of r in the expression for C(r,x), not given explicitly because it cancels out.

C or C(r,t) analyte concentration in the membrane, a function of r and of t [μg L^{-1}]

C_s analyte concentration in the bulk sample [μg L^{-1}]

$C_g(x)$ analyte bulk concentration in the stripping gas as a function of x [$\mu g\ L^{-1}$]

Average concentration in stripping gas.

D diffusion coefficient [$cm^2\ s^{-1}$]

D_s analyte's diffusion coefficient in the sample [$cm^2\ s^{-1}$]

D_m analyte's diffusion coefficient in the membrane [$cm^2\ s^{-1}$]

D_g analyte's diffusion coefficient in the stripping gas [$cm^2\ s^{-1}$]

E_d analyte's apparent activation energy for diffusion in a polymer

G(t) overall extraction rate of the MESI membrane and stripping gas [$ng\ s^{-1}$]

G_e overall steady-state extraction rate [$ng\ s^{-1}$]

G extraction rate.

G_{ss} extraction rate at steady-state permeation.

ΔH analyte's heat of sorption from sample to membrane

J_i , Y_i Bessel functions of the first and second kind, of order i.

K_g: Partition coefficient between membrane and carrier gas

K_{ms} analyte partition coefficient between membrane and sample, concentration in membrane divided by concentration in sample at the interface [dimensionless, $\mu g\ L^{-1}$: $\mu g\ L^{-1}$]

K_{mg} analyte partition coefficient between membrane and stripping gas, concentration in membrane divided by concentration in stripping gas [dimensionless, $\mu g\ L^{-1}$: $\mu g\ L^{-1}$]

K_s Partition coefficient between membrane and air

L length of the membrane [cm]

Nu_o, Nu_i Nusselt numbers at the outer and inner membrane surfaces, respectively [dimensionless]

P_o pole in Laplace transform

R gas constant

Q stripping gas volumetric flow rate [mL min^{-1}]

R_{ed} Reynolds number of a fluid, defined Red = ud/ν where d is diameter of the membrane outer or inner surface depending on context [dimensionless]

S_c Schmidt number of a fluid, defined Sc = ν/D_s or ν/D_g [dimensionless]

T absolute temperature in degrees Kelvin

ν fluid kinematic viscosity [cm^2 s^{-1}]

ϕ ratio of membrane's outer to inner radius, = b/a [dimensionless]

Y Bessel function of the second kind.

Z Extraction amount.

Ω = $D_m t/a^2$, dimensionless time parameter [dimensionless]

Roots in the equations.

θ =$ADfK_s/Q$.